GLUTAMINE AND GLUTAMATE LIMIT THE SHORTENING OF CARDIAC ACTION POTENTIAL DURING AND AFTER ISCHEMIA AND ANOXIA

By

Kenneth James Drake

Dissertation

Submitted to the Faculty of the

Graduate School of Vanderbilt University

in partial fulfillment of the requirements

for the degree of

DOCTOR OF PHILOSOPHY

in

Molecular Physiology and Biophysics

December, 2015

Nashville, Tennessee

Approved:	Date:
Tony Weil, Committee Chair _____	_____
Owen McGuinness _____	_____
John McLean _____	_____
David Wasserman _____	_____
Jamey Young _____	_____

For my daughters Rosalie and Evangeline

You are the laughter and light of my world.

For my wife Martha…

Forever and a day.

ACKNOWLEDGEMENTS

This work would not have been possible without the financial support of the National Institutes of Health, Grant HL58241-11 through the American Recovery and Reinvestment Act of 2009, the Defense Threat Reduction Agency, Grant HDTRA1-09-1-0013, and the Vanderbilt Institute for Integrative Biosystems Research and Education.

First of all, I must thank my advisor Dr. John P. Wikswo. He has pushed me to think about everything from more than my own perspective, guided me in my wandering journey through graduate school and supported me in a research lab unlike any other. Together with my co-investigator Dr. Veniamin Sidorov we have sought to unify disparate fields and understand phenomena that others have taken for granted. Dr. Sidorov's patient training and expertise enabled me to design and execute my experiments quickly and efficiently once I started on this project.

I would also like to acknowledge Dr. Dmitry Markov and our failed backscatter interferometry project. The two years spent on this project bore no fruit but they honed my ability to forge ahead with tantalizing data and focus on the details of the experiment. There is nothing like a universal detector to show you how much of the universe is bent on confounding your data.

Our lab's manuscript editor Allison Price is an unsung hero in our group, tirelessly editing documents, tracking enormous grant applications and managing

complicated manuscript submissions with ease and a smile. I truly have no idea what we would do without her.

I am grateful to the members of my Dissertation Committee, who have provided extensive guidance in my studies and invaluable insights that have helped me develop my thesis beyond what I thought possible. I would especially like to thank Dr. Tony Weil, the chairman of my committee, without whom I would not have completed my benchmarks or recorded our meetings half as well as I did (which was still only half as well as I should have done).

I am eternally grateful for the enormous patience and support of my family. My parents somehow managed to help me survive to adulthood despite my own best efforts, and my wife and parents by marriage have taken up this heavy burden. Thank you all for helping me get to where I am today.

There are no words to express how much I owe my wife, Martha. She has always been my rock; through the trials of grad school, the highs and lows of parenthood and my own personal struggles she has been the light that led me through. Without her I would probably not have even finished community college. She makes me strive to be the man I ought to be and I do it just to see her smile.

TABLE OF CONTENTS

Page
DEDICATION ii

ACKNOWLEDGEMENTS iii

TABLE OF CONTENTS v

LIST OF TABLES vii

LIST OF FIGURES viii

LIST OF ABBREVIATIONS x

CHAPTERS

I. OVERVIEW OF CARDIAC AMINO ACID METABOLISM 1
Introduction 1
Amino Acid Metabolism in the Heart 6
Amino Acids as Protein Precursors 18
Amino Acid Detection Methods 20
Current Medical Interventions 21
Conclusion 22

II. MATERIALS AND METHODS 25
Introduction 25
Animal Care and Surgery 25
Experimental Preparation 26
Study Protocol 29
Anoxia 31
Ischemia 32
APD Measurement Techniques 33
MAP Probe 33
Optical Fluorescence Detection 34
APD Analysis 35
Anoxia 36
Ischemia 36
Isoprostane & Isofuran Assays 40
Biostatistical Analysis 44

III. CARDIAC ANOXIA AND AMINO ACIDS 46
Introduction 46
Preliminary Experiments 48
Results 53

Discussion 58
Amino Acids 58
Anoxia 59
Statistics 62
Mechanisms 64

IV. CARDIAC ISCHEMIA AND AMINO ACIDS 68
Introduction 68
Results 70
Action Potential Duration 71
APD Difference 76
Action Potential Slope 81
Isoprostanes and Isofurans 84
Discussion 87

V. SUMMARY AND FUTURE DIRECTIONS 89
Summary 89
Future Directions 91

APPENDIX 99
A. Biometrics Paper and Supplement 99

REFERENCES 112

LIST OF TABLES

Table Page

1-1. Amino acids and their roles in cardiac metabolism 8

3-1. Comparison of raw data and model-fitted values ……..…..... 64

4-1. Mean values with 95% confidence intervals for model-fitted data …… 73

4-2. Differences between model-fitted groups …….. 78

5-1. List of electron transport inhibitors and their mechanisms of action ……..…. 93

LIST OF FIGURES

Figure Page

1-1. Metabolite supply and function in the heart …..... 2

1-2. Amino acids and the TCA cycle 5

2-1. Heart stabilization and ECG framework ……..……..…….…….…… 27

2-2. Anoxia Langendorff perfusion apparatus ……..……..……..…… 28

2-3. Ischemia Langendorff perfusion apparatus ……..…..……. 30

2-4. Timeline of an anoxia experiment ……..……..……..…..…… 32

2-5. Timeline of an ischemia experiment ……..……...……..…… 32

2-6. Map probe illustration ……..……..……... 34

2-7. MAP probe APD calculation ……..……..……..……..…… 36

2-8. A “Gus2” data display ……..…….……..……..……..……. 37

2-9. Optical APD calculation ……... 38

2-10. Motion and trend compensation in APDClicker …….. 38

2-11. Comparison of right and left ventricle for ischemic imaging ……..…….. 39

2-12. Identical points on the surface during perfusion and ischemia ……..…... 40

2-13. Isoprostane quantification ……..……..…… 43

3-1. Preliminary studies of various durations of anoxia challenge ……...…..... 49

3-2. APD after a single anoxia ……..……..……..……..……. 50

3-3. Initial anoxia challenges decrease the effects of subsequent challenges .. 51

3-4. Hearts perfused with enriched media tolerate longer periods of anoxia …. 52

3-5. APD stability during long recovery phase after single anoxia ……..……. 53

3-6. A typical double anoxia experiment ……..……..……..……..…. 55

3-7. APD change in response to two sequential insults of anoxia ..……..…... 56

3-8. TCA cycle GTP production ..……..……..……...……..…… 65

3-9. Glutathione production from amino acid precursors ..……..…….. 67

4-1. Model-fitted mean for APD_{50} for each experimental condition 74
4-2. Model-fitted mean for APD_{70} for each experimental condition 75
4-3. Model-fitted mean for APD_{90} for each experimental condition 76
4-4. Difference between AA-/AOA- and AA+/AOA-hearts 79
4-5. Difference between AA+/AOA- and AA+/AOA+ hearts 80
4-6. Difference between AA-/AOA- and AA-/AOA+ hearts 81
4-7. Difference between AA-/AOA+ and AA+/AOA+ hearts 82
4-8. Comparison of strong and weak action potentials 83
4-9. Slopes of the AP at the end of each stage of the experiment 84
4-10. Slopes of the AP at the end of each reperfusion period 85
4-11. Initial results from the isoprostane analysis 86
4-12. Complete isoprostane dataset 87
5-1. Electron transport chain (ETC) and oxidative phosphorylation 94

LIST OF ABBREVIATIONS

AA – Amino Acid

ACN – Acetonitrile

AOA – Aminooxyacetic Acid

AP – Action Potential

APD – Action Potential Duration

BCAA – Branched Chain Amino Acids

BHT – Butylated Hydroxytoluene

CHF – Congestive Heart Failure

CI – Confidence Interval

DIPE – Diisopropylethylamine

DME – Dimethylformamide

Gln – Glutamine

Glu – Glutamate

HF – Heart Failure

LA – Langendorff Apparatus

LV – Left Ventricle

MAP – Monophasic Action Potential

MI – Myocardial Infarction

NIH – National Institutes of Health

PET – Positron Emission Tomography

PFBB – Pentafluorobenzyl Bromide

ROS – Reactive Oxygen Species

RV – Right Ventricle

TLC – Thin-Layer Chromatography

CHAPTER I

OVERVIEW OF CARDIAC AMINO ACID METABOLISM

Published in Experimental Biology and Medicine[1]

Exp Biol Med. 2012 Dec;237(12):1369-78.

Introduction

The heart is a highly active organ that consumes 10% of the body's total oxygen uptake and produces upwards of 35 kg of ATP every day.[2] This high rate of energy flux is required to accomplish the monumental task of pumping over 6500 liters of blood per day at a relatively constant pressure and flow rate in the average human heart. This extraordinary amount of work requires a constant supply of metabolic substrates and oxygen. (Figure 1-1)

An understanding of metabolism is essential for any study of the heart. Metabolism is the fundamental system that governs the entire organ's behavior and it ties together all fields of study, including molecular physiology, electrophysiology, toxicology and clinical cardiology. All cardiac behaviors are highly ATP-dependent and, without ATP, the heart will cease to function in a matter of minutes. In many types of heart disease and dysfunction, metabolism is the first area affected, which can then lead to channelopathies, ion imbalance, decreased contractile function, increased free radical production and cardiac death. Amino acids play a central role in cardiac metabolism, but their

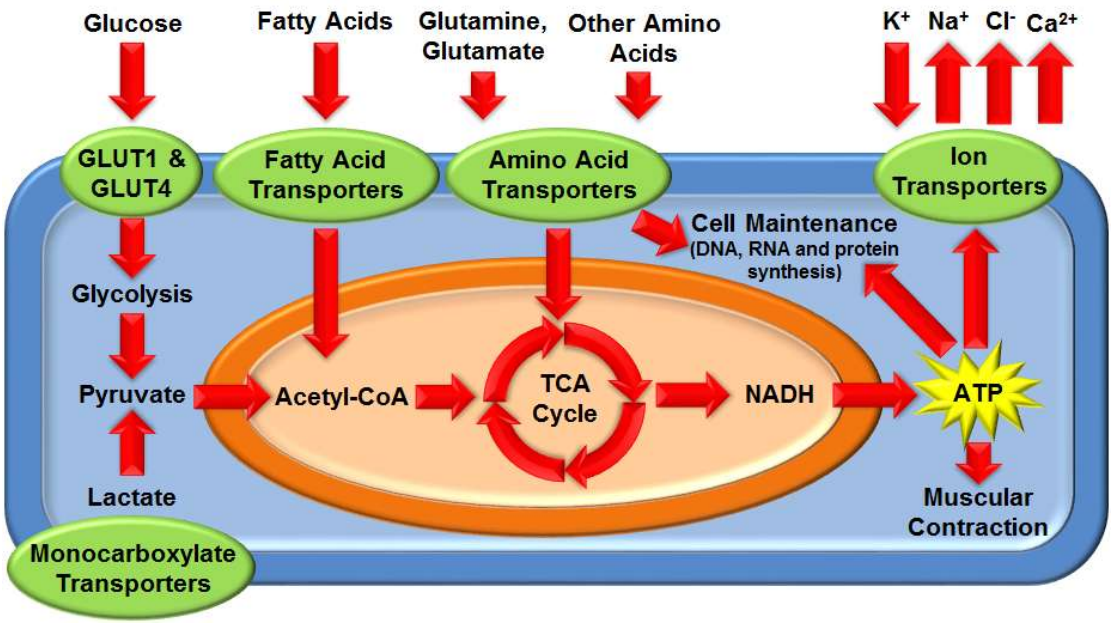

Figure 1-1. Metabolite supply and function in the heart. The heart is capable of utilizing a wide variety of substrates to supply its vast energy needs.

cardioprotective roles as a source of acetyl-CoA and as a substrate for anaplerotic reactions during cardiac ischemia, their ability to contribute to NADH and $FADH_2$ production after reoxygenation, and the conversion of glutamine and glutamate to free radical scavengers may not be fully appreciated.

Fortunately, the heart is also quite resilient, being able to maintain contractile function even under ischemic and anoxic conditions. It has been shown that an increase in non-oxidative ATP production in the ischemic and reperfused heart is associated with decreased cell death and increased functional recovery both *in vivo* and in culture, though the mechanism is not entirely clear.[3-8] In this light, it is important to recognize the heart as a metabolic

omnivore; it is capable of utilizing glucose, lactate, fatty acids, ketone bodies and certain amino acids as metabolic substrates.[4, 9-13]

This ability is especially important under conditions of prolonged stress or ischemia. Deprived of fatty acid oxidation by the loss of their oxygen supply, cardiomyocytes must derive energy from other molecules including amino acids. It is well known that the heart's primary metabolic substrates under normal conditions are fatty acids and lactate, but under conditions unfavorable for oxidation, *i.e.*, ischemia, anoxia and many types of cardiomyopathy, fatty acid oxidation is inhibited and the heart preferentially performs glycolysis and substrate-level phosphorylation.[14, 15]

Amino acids are now becoming more widely appreciated as cardioprotective substrates, as evidenced by the recent increase in excellent review articles detailing the importance of cardiac amino acid metabolism.[16, 17] Glucose, fatty acids and other substrates require oxygen for full energy yield and produce significant levels of acidic by-products.[14] Amino acids are of particular interest in this regard due to their potential for non-oxidative metabolism and their low contribution to cellular acidification. It may be possible to prolong cellular function during – and improve recovery after – anoxia by supplementing cells with glutamate and glutamine due to the ease with which these particular amino acids can be converted to α-ketoglutarate, a TCA cycle intermediate.[18-21] Other amino acids, such as asparagine and aspartate, may also be important metabolic indicators due to their ability to remove amine groups and excess TCA cycle intermediates downstream from the conversion to succinate. The ability to

produce ATP directly from glutamine and glutamate through substrate-level phosphorylation makes these amino acids important for ischemic and hypertrophied hearts as they begin to suffer loss of function and increasing metabolic damage from free radicals and low pH. It should be noted, however, that glutamate and glutamine can provide only a small amount of ATP through this mechanism and that the reducing environment of the ischemic heart can inhibit these reactions. Each molecule of glutamate or glutamine can produce one GTP and one NADH molecule in their conversion to succinate. This is, however, an anaerobic process, does not contribute to acidification and may serve to maintain the levels of NADH and TCA cycle intermediates through an ischemic event, keeping the metabolic machinery primed to begin oxidative phosphorylation as soon as oxygen returns.

Since amino acids are synthesized in a wide variety of pathways and reactions, some amino acids are more readily converted to metabolic intermediates than others. This is especially true in the heart, as the heart is completely unable to metabolize the aromatic amino acids, whereas alanine is synthesized and secreted in abundance under even the most favorable conditions. Other amino acids, like glutamate, glutamine, aspartate, asparagine and the branched chain amino acids (BCAAs), have been shown to be preferentially used as metabolic and anaplerotic substrates in the TCA cycle during anoxia and ischemia.[22-24]

Although it is well known that the heart is capable of metabolizing a wide variety of substrates (Figure 1-2), the heart's substrate preference under

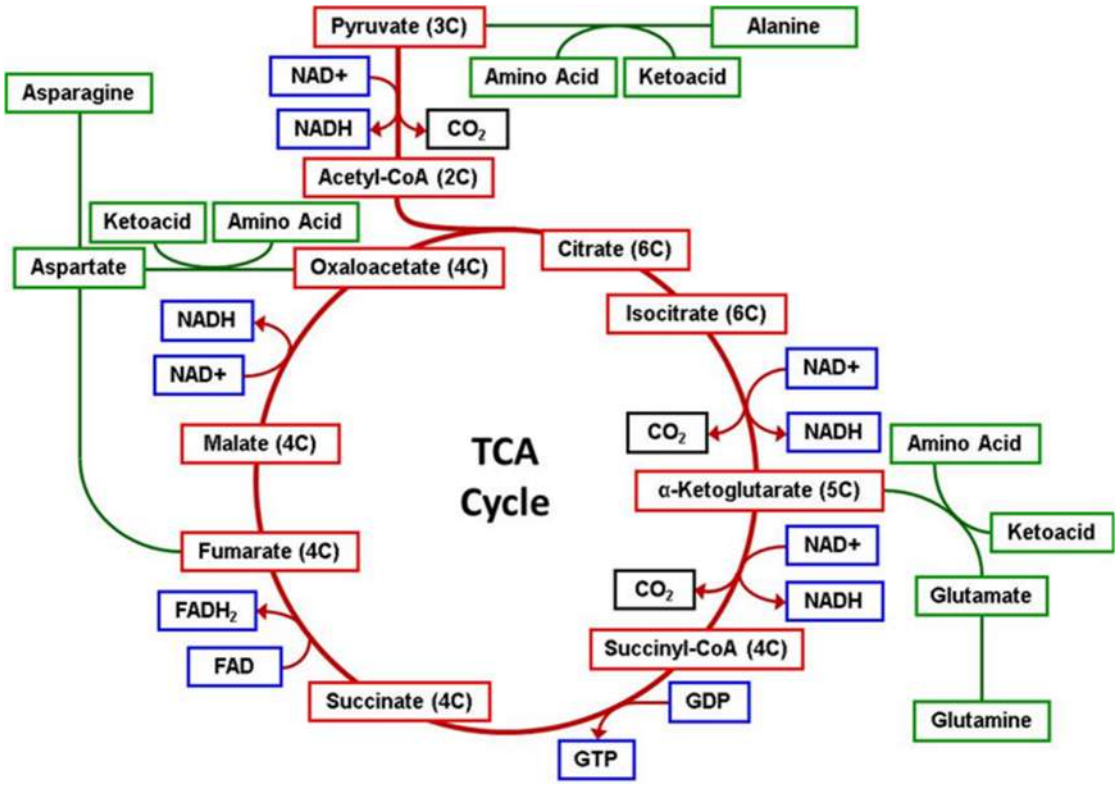

Figure 1-2. Amino acids and the TCA cycle. The amino acid conversions are all reversible and hence are not drawn with arrows. In the glutamate, alanine and aspartate transamination reactions, any amino acid can be used as an amine donor, converting it to its respective ketoacid.

anaerobic conditions is not well understood. Anoxic and ischemic tissues suffer from several issues of supply and demand: 1) inadequate substrate supply, 2) unmet energetic demands, 3) excess acid and reactive oxygen species (ROS) production and 4) inadequate buffering capacity for these metabolic by-products.

Without oxygen, the heart cannot break down fatty acids and ketone bodies into acetyl-CoA. This becomes especially important during acute ischemia, as a lower pH also inhibits glycolysis, forcing the heart to utilize metabolic substrates that do not require oxidation and do not require glycolytic conversion, which

contributes to increased acidification. Certain amino acids could serve in this capacity.[13]

It is important to note that while amino acid metabolism may have several important functions and provides a measure of protection against ischemia and anoxia, it is not capable of sustaining the heart's extraordinary energy demands for extended periods. Amino acids should be viewed as an adjuvant for standard therapies in that they will extend the length of time between the onset of ischemia and the point of irreversible cardiac damage. In the case of cardiac ischemia, ROS production and metabolic demands will far outstrip the supply of antioxidants and metabolic substrates, but even minor increases in these stores should improve the function and recovery of the tissues over unsupplemented hearts.

Amino Acid Metabolism in the Heart

Amino acids seem to be especially well suited for use as metabolic substrates in the absence of adequate tissue perfusion. Glutamate and glutamine are notable due to their ready conversion to α-ketoglutarate, which not only maintains the levels of TCA cycle intermediates, but also provides cellular energy through substrate-level phosphorylation during the conversion to succinate. This is an oxygen-free metabolic conversion, with no acidic or reactive by-products. Indeed, changes in amino acid flux have been seen at rest as well as during ischemia, indicating that repeated bouts of acute ischemia induce biochemical changes that enhance the heart's ability to utilize these alternative substrates.[22]

Peuhkurinen *et al.* specifically indicates that chronic ischemia results in increased glutamate uptake and alanine release.[25] Nishimura *et al.* demonstrated the heart's ability to utilize valine as an alternative to glucose in order to maintain action potential duration (APD).[4] Studies conducted by Schwartz *et al.* indicated that BCAAs are metabolized by the myocardium even during normal cardiac function,[23] though this has not been seen in all studies.[22, 24] The heart is unable to produce the aromatic amino acids (phenylalanine, tyrosine and tryptophan) so uptake of other amino acids without commensurate uptake of aromatic amino acids indicates that the amino acids are not being used for protein synthesis.[2, 9-11, 26] Indeed, amino acids are still consumed even when there is no net protein synthesis or when protein is being degraded, indicating that the amino acids are being metabolized.[25-27] Glutamine supplementation leads to rapid glutamine uptake and increased levels of intracellular glutamate due to high levels of glutaminase activity in the heart.[18] Cardiac ischemia and cell damage therefore are expected to be accompanied by altered amino acid flux during and after ischemic episodes.

Amino acids can be readily metabolized into TCA cycle intermediates; however, not all amino acids are metabolized equally in the heart. There are several different processes by which amino acids can be used to supply cardiomyocytes with energy (Table 1-1):

1. Glutamate and α-ketoglutarate are readily interconvertible via a transamination reaction. This increase in TCA cycle intermediates is called anaplerosis and contributes to the maintenance of oxidative

Table 1-1. Amino acids and their roles in cardiac metabolism.

Amino Acid	Plasma Conc. (μmol/L)	Metabolic Role in the Heart
Alanine	230–510	Alanine is interchangeable with pyruvate via transamination.
Arginine	13–64	Arginine plays an important role in nitrogen balance. In the urea cycle, the enzyme arginase hydrolyzes the guanidinium group to yield urea and the L-amino acid ornithine.
Asparagine	45–130	The amide in asparagine is easily hydrolyzed, converting asparagine to aspartate.
Aspartate	0–6	Aspartic acid and oxaloacetate are interconvertible by a simple transamination reaction, just as alanine and pyruvate are interconvertible.
Cysteine	30–65	Cysteine can react with itself to form an oxidized dimer by formation of a disulfide bond. The environment within a cell is too strongly reducing for disulfides to form, but in the extracellular environment, disulfides can form and play a key role in stabilizing many such proteins, such as the digestive enzymes of the small intestine. This may affect amino acid measurements if not kept in a reducing environment.
Glutamate	18–98	Glutamic acid and α-ketoglutarate are interconvertible by transamination. Glutamic acid can therefore enter the Krebs cycle for energy metabolism, and be converted to glutamine, a crucial molecule in nitrogen metabolism. It is also readily converted to proline.
Glutamine	390–650	Glutamine is the amide of glutamic acid, and is uncharged under all biological conditions. It is rapidly taken up in the heart and converted to glutamate.
Glycine	170–330	Glycine is the smallest amino acid, and it acts as a precursor in many synthetic pathways.
Histidine	26–120	Histidine is probably not actively metabolized by the working heart, but little is known about its role in the heart.
Isoleucine	42–100	Isoleucine is one of the three amino acids having branched hydrocarbon side chains. It is usually interchangeable with leucine and occasionally with valine in proteins.
Leucine	66–170	Leucine is one of the three amino acids having branched hydrocarbon side chains. It has one additional methylene group in its side chain compared with valine.
Lysine	150–220	The lysine amino group is highly reactive and often participates in enzymatic reactions.
Methionine	16–30	Methionine as the free amino acid plays several important roles in metabolism. It can react to form *S*-adenosyl-L-methionine (SAM), which serves as a methyl donor in reactions. Unlike cysteine, the sulfur of methionine is not highly nucleophilic, although it will react with some electrophilic centers. It is generally not a participant in the covalent chemistry that occurs in the active centers of enzymes.
Phenylalanine	41–68	Phenylalanine is quite hydrophobic and even the free amino acid is not very soluble in water. This is one of the amino acids that is not metabolized by the heart, and is therefore a good marker for protein flux.
Proline	110–360	Proline is technically an imino acid; nonetheless, it is called an amino acid. It is unknown what role it may play in cardiac metabolism.
Serine	56–140	Serine differs from alanine in that one of the methylenic hydrogens is replaced by a hydroxyl group.
Taurine	45–130	Taurine is a very important amino acid for the heart. It has been shown to exert cardioprotective effects by reducing the severity and rate of arrhythmias and improving contractile function.
Threonine	92–240	Threonine is another hydroxyl-containing amino acid. It differs from serine by having a methyl substitution in place of one of the hydrogens on the β carbon, and it differs from valine by replacement of a methyl substitution with a hydroxyl group. Note that both the α and β carbons of threonine are optically active, which may affect detection.
Tryptophan		Tryptophan, an essential amino acid, is the largest of the amino acids. The indole functional group absorbs strongly in the near ultraviolet part of the spectrum. This is one of the amino acids that is not metabolized by the heart, and is therefore a good marker for protein flux.
Tyrosine	45–74	While tyrosine is hydrophobic, it is significantly more soluble than phenylalanine. This is one of the amino acids that is not metabolized by the heart, and is therefore a good marker for protein flux.
Valine	150–310	Valine differs from threonine by replacement of the hydroxyl group with a methyl substitution. Valine is often referred to as one of the amino acids with hydrocarbon side chains, or as a branched chain amino acid. Note that valine and threonine are of roughly the same shape and volume. It is difficult even in a high resolution structure of a protein to distinguish valine from threonine.

capacity. The α-ketoglutarate can then be processed through the TCA cycle to yield NADH and GTP. Glutamine can be converted to glutamate, or glutamate can be amidated in order to transport amine groups out of the cell. Glutamate, however, is also a neurotransmitter and may interfere with normal function of the nervous system, causing unintended side effects. Glutamine does not suffer from this shortfall and can be supplemented at very high levels relative to glutamate. [28]

2. Asparagine can serve as a means of exporting nitrogen from the cell, or it can be converted to aspartate. Aspartate can be transaminated to oxaloacetate, a crucial regulator of levels of TCA cycle intermediates. This reaction is critical, as it allows aspartate and asparagine stores to serve as sinks for excess oxaloacetate produced from supplemented α-ketoglutarate precursors.
3. Alanine can also be transaminated to become pyruvate. Pyruvate oxidation produces three molecules of NADH and one of GTP. However, alanine is usually transported out of the myocardium to remove amine groups from the working cell.
4. Many amino acids can be catabolized by the heart, through many different pathways, and the energy recovery from each will vary. [24, 25, 29, 30] The BCAAs, for example, can be converted to acetyl-CoA, pyruvate or succinyl-CoA through somewhat lengthy conversion processes, or transaminated with 2-oxoglutarate to form their respective oxoacids and glutamate.[25] This makes their involvement in metabolism difficult to quantify. A recent review by Huang *et al.* explored the important role of BCAAs in the failing heart.[16]

In the fully functional heart, amino acid metabolism makes up a very small percentage of cardiac ATP production, but as the heart becomes oxygen-limited, amino acids become more important as a fuel source. [9, 10, 21, 30] Without oxygen, the fatty acids cannot be broken down into acetyl-CoA.[14, 31] There is also a decrease in fatty acid consumption and an increase in glycolysis in hypertrophied

hearts, despite sufficient oxygen.[13, 32, 33] Glucose and glycolysis become the primary means of producing ATP, but this yields far less energy per molecule and produces two protons per molecule of glucose consumed.[10, 13, 34, 35] This energy deficit and acidification increase become especially important during acute ischemia, as a lower pH inhibits glycolysis.[2, 13] The heart is eventually unable to produce sufficient ATP through glycolysis, and will out of necessity turn to anaerobic, non-glycolytic fuels, such as amino acids. It is unlikely that these fuels will be able to meet the cardiac metabolic demand for more than a brief interval, but any increase in function is associated with lower mortality.

Amino acids are of particular interest as metabolites in the ischemic, diseased or hypertrophied heart for many reasons. They are plentiful in the cell, though most are bound in proteins and unavailable for immediate metabolism. This is particularly true during acute ischemia as proteolysis is decreased.[2, 25] The limited availability of myocardial proteins and the potential loss of function and increasing metabolic damage from free radicals and low pH create an important role for the provision of a blood-borne amino acid supply as a potential substrate for ATP formation in ischemic and hypertrophied hearts. It may be possible to improve recovery and maintain function by gaining a more thorough understanding of the role amino acids play in ischemia and hypertrophy.

Cardiac ischemia, typically the result of the partial or complete occlusion of a coronary artery, is manifested as a fall in intracellular levels of ATP, glycogen, glutamate and aspartate and increased lactate production and alanine-to-glutamate ratios. It has been proposed that supplementation with exogenous

glutamine, glutamate and aspartate may enhance cardiac metabolism when administered in the reperfusate after removal of coronary blockages.[18-21, 36] Amino acid supplementation may contribute to cardioprotection in several ways : 1) anaplerosis of TCA intermediates, 2) elimination of inhibition of succinate-CoA reductase by oxaloacetate and increased substrate-level phosphorylation, 3) providing high levels of NADH and NADPH for rapid oxidation once oxygen returns and 4) the production of reduced glutathione, an antioxidant that can protect the heart from free radical damage.[18, 37]

In a study by Julia *et al*., immature dog hearts were found to be more tolerant of ischemic conditions than mature hearts and also to contain higher intrinsic levels of glutamate.[30] Other studies have shown that elevated levels of intracellular glutamate are at least partially responsible for the heart's resistance to ischemic damage.[18-20] Blockage of glutamate transamination using aminooxyacetic acid (AOA) inhibits glutamate and aspartate utilization and reduces the heart's ability to recover from ischemic episodes. Specifically, the blockage of glutamate transamination in tissue homogenates resulted in an immediate decrease in lactate, alanine and succinate production, all of which should be produced by tissue homogenates. In the absence of AOA, the hearts were able to withstand 45 minutes of global ischemia, requiring no external stimuli to resume normal function and showing little or no ill effect from the prolonged insult. Administration of AOA, however, resulted in severe loss of function after the same period. It also resulted in much less lactate, alanine and succinate production, and much lower glutamate conversion.[30] These results

demonstrate that cardiac function and long-term recovery require glutamate and aspartate transamination, while blockage of transamination results in decreased recovery and increased mortality.[30] Cardiac transaminases are so prevalent, in fact, that their presence in the blood was diagnostic for heart damage for many years before troponin and creatine kinase tests.

Glutamate and aspartate have very large muscle/plasma ratios, indicating that they are taken up into cells with high affinity. However, during ischemia the large concentration gradient leads to their release during ischemia[25, 36] because of the loss of transporter function that normally maintains the gradient. Cardiac cells supplemented with excess glutamate show significantly increased NADH/NAD+ ratios and ATP levels *in vitro*. A fall in intracellular glutamate is associated with increased alanine production and decreased ATP concentrations after at least 10 minutes of ischemia.[25, 37] Glutamate loading also improves the cells' contractile activity and Ca^{2+} homeostasis after chemical hypoxia.[36, 37] Increased intracellular glutamate stores are correlated with improved metabolic recovery, increased cardiac output and elevated glutathione levels after an ischemic episode.[18-20]

Ischemia significantly reduces the stores of tissue glutamate, ATP and glutathione while increasing lactate levels.[18] In response to ischemia, the heart will significantly enhance alanine production and glutamate consumption, though these effects become significant only when the partial pressure of oxygen in the tissue falls to 5% of normal levels. While the uptake of glutamate does not directly correlate with alanine production and release, it is a contributor under

reduced oxygen conditions.[24] Though glutamate is taken up by the heart, intracellular stores of the amino acid are readily transaminated with aspartate and alanine, allowing a greater storage and flux capacity than might otherwise be expected.[25] Glutamate and glutamine may also work as reservoirs to protect against post-ischemic reduction in cardiac output by maintaining metabolic intermediates.[29] Glutamate and glutamine are readily interconvertible in the heart and may serve as a means of controlling levels of TCA cycle intermediates via conversion of glutamate to α-ketoglutarate.[20]

Glutamine supplementation prior to an ischemic event improves cardiac function and reduces free radical damage by improving ATP production and content, oxidative capacity and glutathione content.[18, 20, 21] Studies have shown that glutamine supplementation significantly increases glutathione and reduces cardiac damage from surgery, toxins and presumably from transient ischemia as well.[38, 39] Glutamine does not appear to activate heat shock proteins but it does increase myocardial COX-2 levels, which are associated with decreased infarct sizes and reduced ROS damage during reperfusion and subsequent ischemia.[40]

Despite the evidence supporting the role of glutamate in the ischemic heart, it may not be clinically feasible to supply intravenous glutamate due to possible neural and cardiac toxicity at high plasma concentrations (20-70 mM).[18] A single dose of oral or intravenous glutamine was shown to improve tissue glutamate levels without the need for high levels of glutamate in the plasma.[18, 19] This is due to the presence of high-affinity transporters for glutamine in the heart, and a high level of glutaminase activity allowing the heart to rapidly convert

circulating glutamine into intracellular glutamate stores. The improved cardiac performance from glutamine has been seen with circulating glutamine levels as low as 1.25 mM, a level easily achieved by an oral dose of glutamine.[18, 19] Intracellular glutamate protects against loss of TCA cycle intermediates and improves post-ischemic oxidative metabolism, which may help to explain the increased ATP content in the glutamine-treated hearts. Glutamine supplementation increased post-ischemic phosphocreatine and NAD+/NADH content after ischemia and reperfusion while decreasing lactate production. Glutamine's protective effects have been seen even when administered 18 hours before ischemia, though the effects are greater when administered 4 hours before ischemia.[18, 19] This has important clinical implications as it has allowed cardiac surgeons to easily and reliably administer prophylactic glutamine treatments before surgeries.

Glutamine cardioprotection is also associated with increased levels of UDP-GlcNAc and protein O-GlcNAc, nucleoplasmic proteins which have been shown to protect against ischemic injury and other damaging events.[21] Blockage with azaserine and alloxan of the pathways that lead to the formation of these molecules eliminates the protection afforded by glutamine supplementation. Glutamine alone increased ATP levels three-fold after ischemia and reperfusion compared to controls, but the addition of azaserine and alloxan reversed this effect.[21]

Conflicting reports about whether amino acid supplementation is actually cardioprotective may be attributed to the effects of differing K^+, Na^+ and H^+

gradients, which may vary widely across experimental preparations.[36, 37] Inclusion of aspartate, glutamate and glutamine in animal heart perfusates and cardioplegic solutions improves metabolic and functional recovery and elevates high-energy phosphate levels post-ischemia, and they have been used experimentally in cardioplegic solutions with good results.[18, 19, 28, 41] Questions regarding the efficacy of these amino acids may arise from xenotypic differences, protocol incompatibility or the use of free acids vs. amino acid salts.[36]

Another assumption is that perfused amino acids are readily available for intracellular functions, without regard to transporter activity. Glutamate has a very high rate of uptake in isolated cells, and this uptake is enhanced by anoxia. The cells are also able to establish intracellular glutamate stores against very high gradients.[42] Rennie *et al.* explored the role of glutamine transporters in both cardiac and skeletal muscle and showed the beneficial effects of glutamine supplementation and possible mechanisms of glutamine uptake stimulation.[12] A more general view of amino acid transporters and their distribution was taken by Malandro and Kilberg.[43]

Despite an abundance of evidence showing that amino acid supplementation improved myocardial protection during ischemia and surgery, relatively little is known about endogenous amino acid metabolism or the exact mechanism of the cardioprotective effect. While the use of amino acid supplementation for cardioprotection has been explored, there are few studies addressing electrophysiological changes concomitant with the supplementation.

Data from human subjects with exercise-induced ischemia showed that these patients release significantly more alanine during cardiac ischemia and take up more glutamate than non-ischemic subjects.[22] This has been seen in other model systems as well, indicating that this is a conserved process.[25] Changes in amino acid flux were seen not only during acute ischemic episodes, but for many days after the episode, indicating that bouts of acute ischemia induce biochemical changes that enhance the heart's ability to utilize alternative substrates.

Alanine is produced and secreted by the heart under almost all conditions, including hypoxia and ischemia. This has been demonstrated in patients with chronic ischemic heart disease[25] and exercise-induced ischemia,[22] as well as in hypoxic[24] and ischemic[36] heart tissues and insulin-clamped working hearts.[23] Large amounts of alanine can be found in hypoxic tissues, including the tissues of diving mammals and hypoxic skeletal muscle, especially in chronic ischemic heart disease. Taegtmeyer showed that alanine production was not significantly enhanced until the concentration of oxygen was decreased to less than 5%.[24] In another study, glutamate supplementation had a negligible effect on papillary muscle alanine production in the presence of glucose in both aerobic and anaerobic conditions, and glutamate consumption was not enhanced until the oxygen concentration of the buffer was reduced to 5%.[24, 37] L-cycloserine, an inhibitor of alanine aminotransferase, markedly decreased intracellular alanine and increased glutamate levels, even above baseline levels, showing that glutamate is not directly responsible for all of the observed alanine production,

although it is a contributor. This also indicates that alanine production is most likely due to glutamate/pyruvate transamination, but acute alanine production may not necessarily reflect the rate of glycolytic pyruvate production, since ischemia could be causing the release of intracellular stores of alanine.[24, 30]

Pyruvate levels in the cell decrease by 50% during ischemia, and lactate levels in the surrounding media increase 27-fold after 20 minutes of ischemia.[25] Another study showed that increasing the levels of pyruvate in the media results in increased alanine production in both aerobic and anaerobic cells, indicating that substrates are the limiting factor in alanine production and supporting the idea that alanine is produced via transamination of pyruvate.[30] In glucose-free media, lactate and alanine production is increased compared to normal media, and inhibition of glycolysis suppresses this production significantly.[24] Ammonia is also produced by the deamination and deamidation of amino acids, and has been measured at 5.5 times normal levels during ischemia.[25]

Though the addition of amino acids may improve metabolic function, it does not increase protein synthesis until amino acids are present at 5 times normal physiologic concentrations. Glycine, alanine and glutamate showed net myocardial release under non-ischemic insulin-supplemented conditions. The BCAAs leucine and isoleucine were taken up by the heart in a concentration-dependent manner. No other amino acids showed significant uptake or release with or without insulin supplementation.[23] It had been previously demonstrated that glutamine and asparagine were released and leucine and isoleucine were consumed in humans, though Schwartz *et al.* improved glutamine detection

methodology and revealed a higher rate of glutamine uptake than had been seen in earlier studies. Despite these findings, BCAA supplementation has shown negligible uptake or improved performance in subsequent studies of ischemia. [24, 25, 36]

Any increased uptake of BCAAs likely results in a corresponding increase in their metabolism, since net protein synthesis is negligible over the course of an ischemic episode, and cellular concentrations would have been 2-4 times higher than the arterial concentration were they not metabolized. However, conversion to ketoacids or oxidation necessitates removal of amine groups from the BCAAs with no commensurate increase in alanine or glutamate, so it is unclear exactly how they are metabolized. Since these amino acids have several pathways through which they can be converted, the nitrogen may be lost through any number of metabolites which were not measured.[23]

Amino Acids as Protein Precursors

In the healthy heart, the aromatic amino acids (phenylalanine, tryptophan and tyrosine) are not metabolized.[27] This makes these amino acids useful markers for protein turnover experiments, as any aromatic amino acid released from the heart must have come from proteolysis, and any aromatic amino acids taken up by the heart are almost certainly being incorporated into nascent protein.[26] Protein turnover, however, is a balance between degradation and synthesis, so a zero net aromatic amino acid flux does not necessarily indicate a

lack of protein turnover, but rather a balance between proteolysis and protein synthesis.

Studies of phenylalanine incorporation have shown that elevated levels of amino acids lead to greater protein synthesis.[27] The human heart contains 284±17 μmoles of phenylalanine per gram, and Morgan *et al.* saw that 1.24 μmoles were incorporated in 90 minutes, indicating 14.3 days for complete protein turnover *in vitro*. *In vivo* turnover may be faster, since incorporation rates are lower *in vitro* than *in vivo*. The elevated rates of incorporation were not due to increased ATP levels, as an aggregation of ribosomes was seen, but there was no commensurate rise in the ATP/p-creatine ratio.[27]

Another corollary between amino acid metabolism and ischemia is that long-term ischemia/damage is expected to result in increased proteolysis and contribute to the decline in long-term cardiac function after ischemia, though it should be noted that proteolysis decreases during acute ischemic episodes to 12% of normal.[25] In the presence of puromycin (a protein synthesis inhibitor), tyrosine was produced by cells under aerobic and anoxic conditions equally in the presence of 5 mM glucose. Alanine production was not affected by these conditions. Under anoxic conditions without puromycin, twice as much tyrosine was produced as under aerobic conditions, indicating an increase in the rate of proteolytic aromatic amino acid production.[24] This means that protein degradation during oxygen deprivation should be manifested as an increase in the rate of aromatic amino acid release from the myocardium.

In an interesting study by Razeghi *et al*., a heterotopic anastomized heart model was used to simulate cardiac atrophy.[44] The heart was removed from one rat and placed in another rat to create a cardiac bypass to decrease the load on the main heart, resulting in atrophy. Results showed proteolysis and protein synthesis occurring simultaneously in atrophic remodeling, rapidly in the first two days, peaking between 2-4 days and slowing considerably by 28 days. This demonstrates that remodeling requires activation of both degradative and synthetic pathways, but that the difference between the two would be manifested in an altered flux of the aromatic amino acids. These results can be extended to chronic ischemia, hypertrophy and several other conditions as there is increased protein synthesis, but also increased protein turnover, in long-term cardiac diseases.[34]

Amino Acid Detection Methods

Amino acid monitoring in the heart has historically been done by measuring the difference in amino acid concentrations between coronary arterial input and coronary venous output across the whole heart. This, of course, is insufficiently precise for current studies, and many methods are now in use for precisely quantifying the amino acid flux in the myocardium, as well as identifying the metabolic fates of the molecules.

The most accurate and widely used amino acid monitoring technique is the radiolabeled tracer study.[42, 45, 46] These labels can be detected with positron emission tomography (PET) for imaging amino acid accumulation in the tissues

as well as quantifying media depletion in a culture setting. Similarly, NMR studies detect the labels and can track the labeled carbon or nitrogen through its many conversions to determine how the amino acid was metabolized.[47] Mass spectrometry is also a common method of quantifying amino acid flux, as it is highly sensitive to even small changes in concentration and is capable of very rapid processing of large numbers of samples.[48] It has the additional benefit of being highly adaptable to pre-separation protocols like gas chromatography and ion mobility mass spectrometry.[49-53]

Unfortunately, once amino acids enter the TCA cycle carbon labeling becomes much more difficult to track, as the carbons are fungible. The appearance of labeled CO_2 is highly indicative of amino acid oxidation, but it does not necessarily mean that the entire amino acid has been oxidized or that the conversion was direct, since there are many paths that feed into and out of the TCA cycle. Nitrogen labeling is reliable insofar as oxidized amino acids must release NH_3, but there are many ammonia acceptors within the cell. Often the amine is transferred to pyruvate to form alanine or α-ketoglutarate to form glutamate and glutamine, but this is not always the case.[45]

Current Medical Interventions

Heart failure is caused by an imbalance in supply and demand, and often the deficit is in oxygen supply. Interventions that shift metabolism away from fatty acids to substrates with greater ATP produced/O_2 consumed ratios will have anti-anginal effects. Current medical treatments focus primarily on increasing cardiac

output and decreasing afterload, but few treatments attempt to rectify the underlying metabolic dysfunction of the failing or ischemic heart. Medications focus on lowering blood pressure, fluid retention and cardiac work to relieve symptoms of acute and chronic heart failure while the accompanying alterations in cardiac metabolism are left untreated. A few drugs for treatment of the metabolic disease state – for example, trimetazidine – have been developed recently to treat the underlying metabolic disease state instead of just the symptoms and have shown promise.[54, 55] We need to continue learning more about cardiac metabolism if we wish to effectively treat the underlying metabolic derangement. We must understand in detail how changes in metabolic substrate affect electrophysiology, and we need to find new ways to optimize the heart's fuel usage and minimize the damage incurred by transient ischemia if we want to turn the tide in the battle against heart disease.

Conclusion

The fact that amino acids are not only protein precursors but can also be metabolites, neurotransmitters and antioxidants makes them ideal candidates for determination of underlying cellular functioning in the age of metabolomics. It is already clear that uptake and release of certain amino acids can give a great deal of information about intracellular processes. Even without looking inside the cell, it is recognized that if tyrosine, phenylalanine or tryptophan show net uptake by cardiomyocytes over a period of days or weeks, then they are being incorporated into new proteins. This would indicate not simply protein turnover,

but an increase in the total protein pool. Such information can be used to determine the effects of pharmacologic agents or other interventions that perturb normal cell function.

Computational models of cardiac myocyte excitation are beginning to include contraction and energy metabolism.[56-58] However, we believe that these models need also to include amino acid pathways and fluxes to accurately model the metabolic events that accompany both chronic and acute ischemia and other diseased states of the heart. Such models would also benefit from the inclusion of models of intracellular pH regulation, as it is associated with ischemia and affects many metabolic reactions.

The versatility of amino acids makes them ubiquitous across all cells and tissues. If alterations in amino acid flux can be linked to abnormal cell behavior, tools to monitor amino acid flux could serve to evaluate tissue viability. If, for example, a donor heart could be transported with an amino acid detector, its health could be monitored in transit, and transplant surgeons would have a better understanding of its viability and more information about its expected longevity once it is implanted. If the heart displays characteristics associated with starvation or stress, then special interventions may be needed to improve its condition *before* it is implanted. This scenario is still not possible, but with advances in metabolic monitoring, it becomes a very real possibility in the not-too-distant future.

In summary, we have reviewed the import of the role of amino acid metabolism in the normal and failing heart. Our review of the literature would

suggest that additional research is required to understand how amino acid supplementation affects not only the metabolic but also the mechanical and electrical performance of the heart. It is hoped that this review clearly illustrates the need to unite the disparate fields of electrophysiology and metabolism to understand the complex interplay between action potential and metabolic flux.

CHAPTER II

MATERIALS AND METHODS

Introduction

Since there is a great deal of overlap in the materials and methods used throughout my experiments, I have chosen to describe them in a dedicated chapter of this thesis to save time and space. This will also facilitate discussion of the distinctions between methodologies as they can be discussed together in one section instead of across separate chapters.

Animal Care and Surgery

All experiments conformed to the Guide for the Care and Use of Laboratory Animals published by the U.S. National Institutes of Health (NIH) and were approved in advance by the Vanderbilt Institutional Animal Care and Use Committee. Animals were housed for between 1 and 14 days in the Vanderbilt Division of Animal Care. They were given food and water *ad libitum*.

New Zealand white rabbits of either sex weighing 2.7 to 3.1 kg were used in the experiments. On the day of the experiment, animals were randomly assigned to either the control or experimental groups using a coin toss decision. Before surgery, the animals were preanesthetized with ketamine (50 mg/kg), heparinized (1,000 units) and anesthetized with sodium pentobarbital (60 mg/kg) via a left ear vein.

Upon failure to respond to the paw pinch and eye reflex tests, the animals' chests were opened by midsternal incision and radical medial thoracotomy. The hearts were quickly removed from the chest and the aorta cannulated on a temporary Langendorff apparatus (LA) located above a sink immediately adjacent to the surgical table.

Experimental Preparation

On the temporary LA the aorta was sutured tightly to a cannula mounted in a square plexiglass frame (Figure 2-1). The LA perfuses the coronary arteries with oxygenated Tyrode's solution of the following composition (mM): 133 NaCl, 4 KCl, 2 $CaCl_2$, 1 $MgCl_2$, 1.5 NaH_2PO_4, 20 $NaHCO_3$, and 10 D-glucose, buffered with 95% O_2 and 5% CO_2 (pH = 7.35 at 37°C). Hearts assigned to the amino acid supplemented group received the Tyrode's solution supplemented with 2.5 mM glutamine and 150 μM glutamate. Hearts assigned to the aminooxyacetate (AOA) treated groups received 1.0 mM AOA.

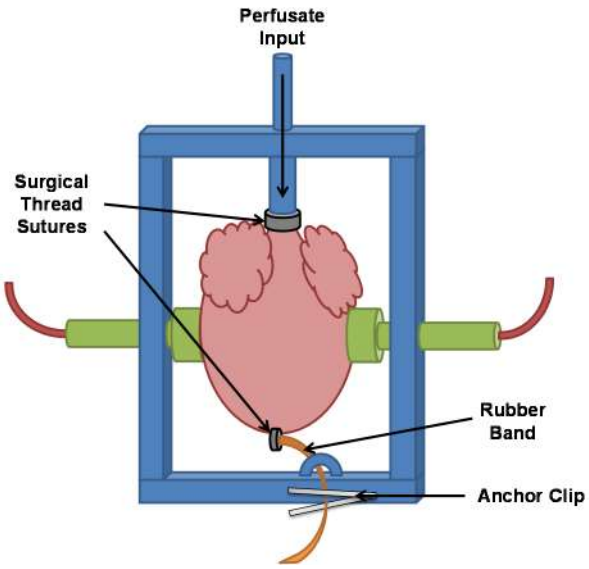

Figure 2-1. Heart stabilization and ECG frame. A rectangular plexiglass frame allowed for flexible anchoring of the heart to reduce movement. A rubber band is sutured to the apex of the heart and gently anchored to the bottom of the frame to reduce motion and counter the natural buoyancy of the heart.

A small suture was placed very shallowly in the apex of the heart. This suture was tied loosely but firmly so as to not cause localized ischemia but remain secure. In the apical suture a 1-2" length of rubber band was tied. This was threaded through a hole in the plexiglass framework below the heart and pulled just tight enough to remove all slack from the band. The band's tension was maintained by means of a clip on the framework. This apical tension reduced motion of the heart and prevented it from floating when placed in a media bath. For experiments involving ischemia, a small puncture was made in the bottom of the left ventricle (LV) near the apical suture using small surgical scissors to breach the epicardium and a 12 gauge needle to puncture the endocardium. The needle remained in the LV to act as a shunt in case of aortic

valve regurgitation and LV inflation. This was not necessary during anoxia experiments since perfusion pressure remains constant, whereas ischemia experiments require pumps to turn on and off, leading to possible spikes in perfusion pressure.

Once the sutures and shunt were properly placed the plexiglass framework and cannulated heart were quickly moved to a permanent LA (Figure 2-2) located in a Faraday shield maintained at 37 ± 0.5°C by a precision heater controller (Air-Therm, World Precision Instruments, Sarasota, FL). The

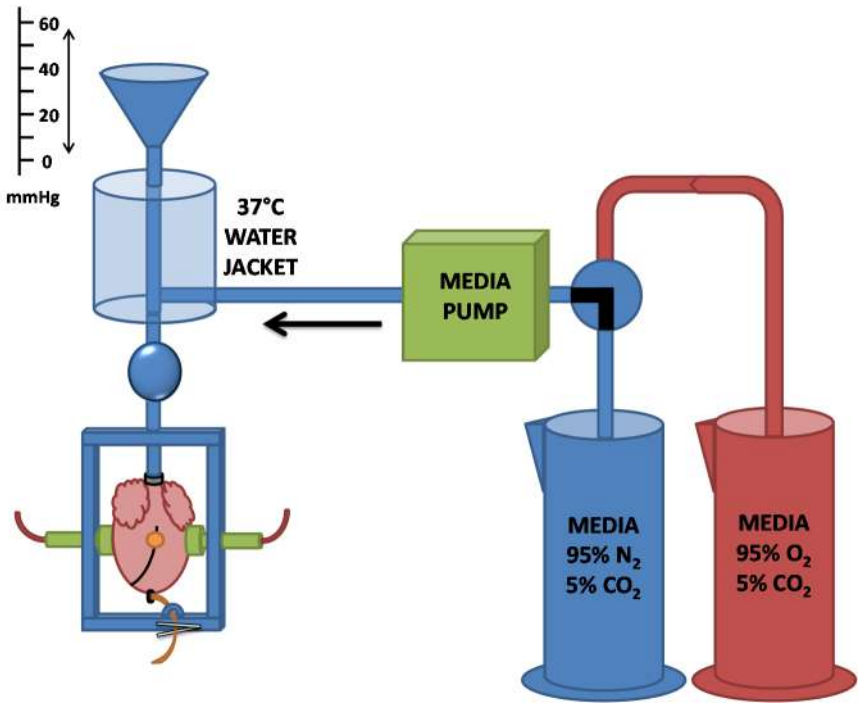

Figure 2-2. Anoxia Langendorff perfusion apparatus. Two graduated cylinders were filled with media, one oxygenated and the other deoxygenated. Anoxia and recovery were caused by switching from one media source to the other. The MAP probe (orange circle) was placed on the septum (curved black line on the heart).

permanent LA had increased experimental capacity as well as superior thermal and media handling capabilities. The coronary perfusion pressure was adjusted to 50 mmHg and the flow rate was 44 – 49 ml/min. To ensure that all hearts were performing equal amounts of work we applied an external pacing electrode, and the pacing stimulation was maintained at a cycle length of 300 ms delivered via a bipolar glass-coated platinum electrode (0.25 mm wire diameter; 1 mm electrode separation) located on the anterior surface of the right ventricle near the septum. The stimulus was 4 ms in duration for anoxia experiments and 10 ms for ischemia experiments, and the amplitudes were adjusted to between 2-10 mA depending on the excitation threshold of the heart throughout the experiment.

Anoxia experiments were conducted without immersing the heart in a media bath since the constant flow of perfusate adequately heats the heart and prevents dessication (Figure 2-2). For ischemia experiments, however, cessation of flow raises the possibility of cardiac hypothermia and dessication so a media bath is required (Figure 2-3). The media bath's temperature and circulation are maintained by a separate media source and external circulatory pump.

Study Protocol

The standard method of experimental design for cardiac experiments began with unknown intervention duration and unknown recovery duration for a drug treatment with unknown dosage. We began by challenging hearts with increasing intensity or duration of the challenge to adequately tax the heart without causing irreversible damage. We wanted to see reduced performance

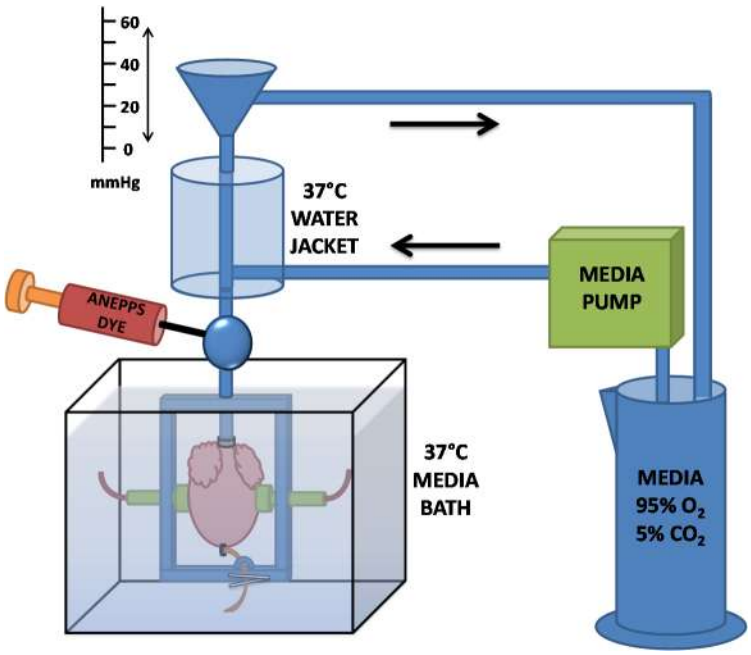

Figure 2-3. Ischemia Langendorff perfusion apparatus. A single media source was continuously bubbled with oxygen, and ischemia was induced by stopping the pump and clamping the line above the water jacket to eliminate perfusion normally driven by the head pressure of the water column. Voltage-sensitive dye was added to the perfusate via a bubble trap located above the heart. The media bath was heated by continuously circulating the media through an external heater (not shown).

that resulted in moderately depressed long-term performance in the untreated group. This is a difficult problem since the heart is a resilient organ with a variety of compensatory mechanisms to maintain cardiac output. Many challenges result in acute loss of function with complete recovery almost immediately. On the other hand, an over-taxing challenge results in irreparable declines in cardiac function resulting in cardiac death. There is also the issue of cardiac preconditioning where an initial challenge prepares the heart for subsequent

challenges and increases its tolerance. This may result in a given challenge being mislabeled as lethal or non-lethal simply due to its order in the experiment.

Once a satisfactory treatment dosage is established, we need to test the effective concentration of a drug or metabolite. The heart will theoretically reach a toxicity threshold and cardiac function will suffer. This decrease in function may or may not be the result of the treatment since the heart may be responding to external factors such as the duration of the surgery or the amount of time the heart has been hanging. We may also have been far below or above the treatment threshold, necessitating further experiments to test this possibility.

Duration of recovery is somewhat easier to determine since there is no limit to how long the heart can be allowed to recover. We simply monitor recovery and find the point at which the heart reaches a new steady state (+/- 5%) for about 5 minutes.

Anoxia

The timeline of the anoxia experiments is shown in Figure 2-4. Hearts were placed on the LA and allowed to acclimate to perfusion and pacing for 30-40 minutes. Once the hearts were stable, baseline APD measurements were taken every 4 minutes for 20 minutes. The heart was then switched from O_2-bubbled media to N2-bubbled media. Measurements were taken every minute for the 6-minute anoxic episode. After 6 minutes the hearts were returned to oxygenated media for 20 minutes, with measurements taken every minute for 6

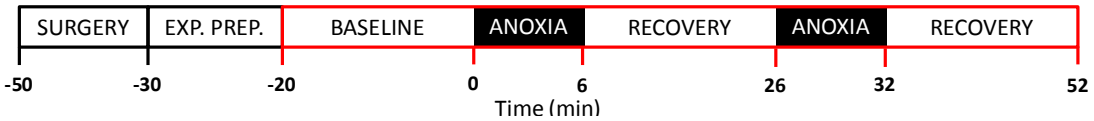

Figure 2-4. Timeline of an anoxia experiment. Anoxia episodes lasted for 6 minutes each, and the baseline and recovery periods were 20 minutes each.

minutes, every 2 minutes for the next 6 minutes and then at 15 minutes and 20 minutes post-anoxia. The anoxia and recovery cycle was then repeated.

Ischemia

The timeline of the ischemia experiments was similar to that of the anoxia with a few crucial differences (Figure 2-5). We used three consecutive challenges instead of two and extended the insult from 6 minutes to 10. We also added a shunt to the LV to reduce ventricular hyperinflation and maintained the hearts in a media bath to maintain temperature and hydration throughout the experiment.

Ischemia was induced by turning off the perfusion pump and clamping the perfusate line that maintains perfusion pressure. The head pressure line must be clamped to eliminate perfusion from the pressure of the water column. Flow is

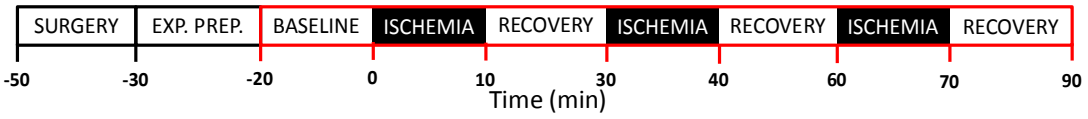

Figure 2-5. Timeline of an ischemia experiment. Ischemic episodes lasted for 10 minutes each, and the baseline and recovery periods were 20 minutes each.

returned by removing the clamp and turning the pump on at very low speed for 30 seconds before returning to operating speed. This low initial flow rate eliminates pressure transients on pump startup that can overpressurize the LV and potentially damage the aortic valve.

After the experiments, the hearts were frozen at -80°C within 5 minutes of the end of the experiment. The frozen hearts were then sent to the Vanderbilt laboratory of Dr. Jackson Roberts for isoprostane and isoketal analysis.

APD Measurement Techniques

MAP Probe

A monophasic action potential (MAP) was recorded using a commercially available standard MAP catheter (1675P, EP Technologies) (Figure 2-6). While MAP is an extracellularly recorded wave form, it closely reproduces the course of the repolarization phase of the transmembrane action potential and has been broadly utilized in both clinical and experimental conditions to obtain stable recordings to monitor APD [59-62]. The MAP probe was positioned on the epicardium close to the septum on the anterior side of the heart and held perpendicular to the surface. The signals were amplified with a differential amplifier (DP-301; Warner Instruments, LLC, Hamden, CT) and then visualized and recorded at 25 kHz with a digital oscilloscope (TDS5034B; Tektronix, Beaverton, OR).

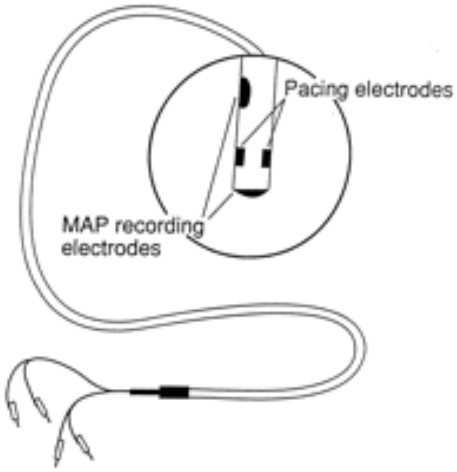

Figure 2-6. MAP Probe Illustration. The MAP probe measures the transmembrane potential of ~5 mm^2 of the epicardium by pressing an electrode against the epicardium and comparing it to a reference electrode. The pacing electrodes were not used in these experiments. Image from Franz MR. Cardiovasc Res (1999) 41 (1): 25-40.

Optical Fluorescence Detection

For the ischemia experiments we adopted an optical voltage detection method that was already in use in the lab.[63, 64] This decision was made for several reasons:

1) The need to keep the heart warm in a media bath made the MAP probe unfeasible due to space constraints in the bath.
2) The MAP probe was prone to signal decay due to localized ischemia from the pressure of the probe and movement of the probe on the surface of the beating heart.

3) Use of the MAP probe restricts data acquisition to a single location directly under the probe. If the location proves substandard during data analysis, there is no way to choose a new point.

For ischemia experiments the hearts were stained with a voltage-sensitive dye called di-4-ANEPPS (Invitrogen Co, Carlsbad, CA, USA) stock solution (0.5 mg/ml dimethyl sulfoxide) administered via a bubble trap above the aorta and allowed to equilibrate for 5 minutes.

The anterior LV was illuminated by 532 nm laser light (Verdi, Coherent, Santa Clara, CA, USA). The emitted light passed through a cutoff filter (no. 25 Red, 607 nm, Tiffen, Hauppauge, NY, USA) and was imaged with a CCD camera (Model CA D1-0128T, Dalsa, Waterloo, ON, Canada) with spatial and temporal resolution of 128 ×128 pixels and 500-1000 frames s^{-1}. Custom-developed data acquisition software using LabVIEW (National Instruments, Austin, TX, USA) and MATLAB was used to record and analyze the data.

Action Potential Duration Analysis

There are two types of APD data collected in these experiments: MAP probe data collected on an oscilloscope for anoxia experiments and optical data collected on a PC for ischemia experiments. Both types of data are processed using MATLAB software and plotted in Microsoft Excel spreadsheets, but the algorithms used to identify and define APD are different for each type of data.

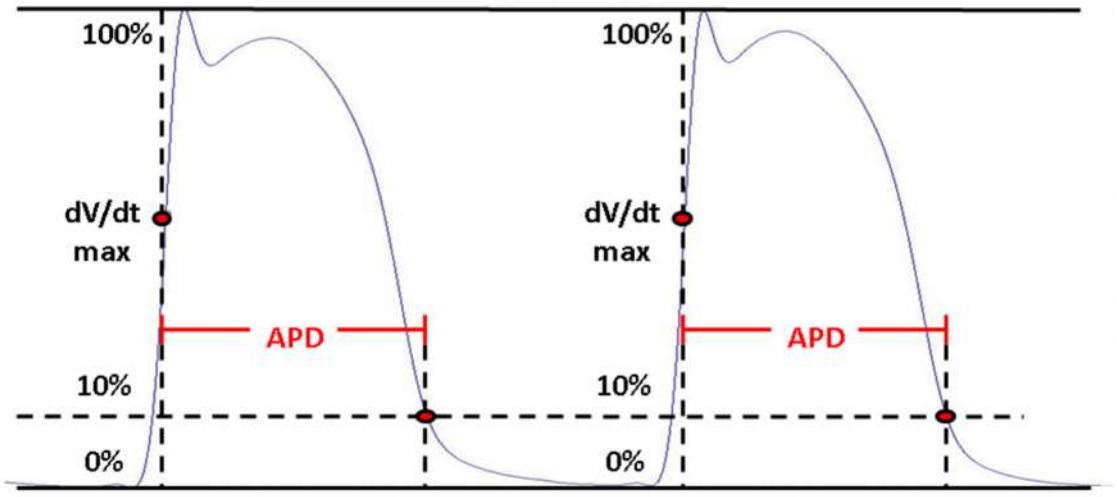

Figure 2-7. MAP probe APD calculation. Action potential duration was calculated from the point of maximal rate of depolarization (dV/dt max) to the point when the potential was 10% of the maximum action potential amplitude (APD_{90}). Each measurement consisted of 6-8 sequential action potentials, and the results were averaged for each measurement with a single baseline and maximum amplitude used for all AP's in the measurement as shown here.

Anoxia

The MAP data were analyzed using MATLAB software to measure APD. APD was calculated by finding dV/dt_{max} and measuring the length of time for the action potential to return to 90% (APD_{90}) repolarization (Figure 2-7). Each time point is the average APD of 6-8 sequential action potentials taken in series.

Ischemia

In MATLAB the optical data are analyzed using algorithms written by Raghav Venkataraman, a former graduate student in the lab of our collaborator Franz Baudenbacher, and various lab personnel. The data are visualized using

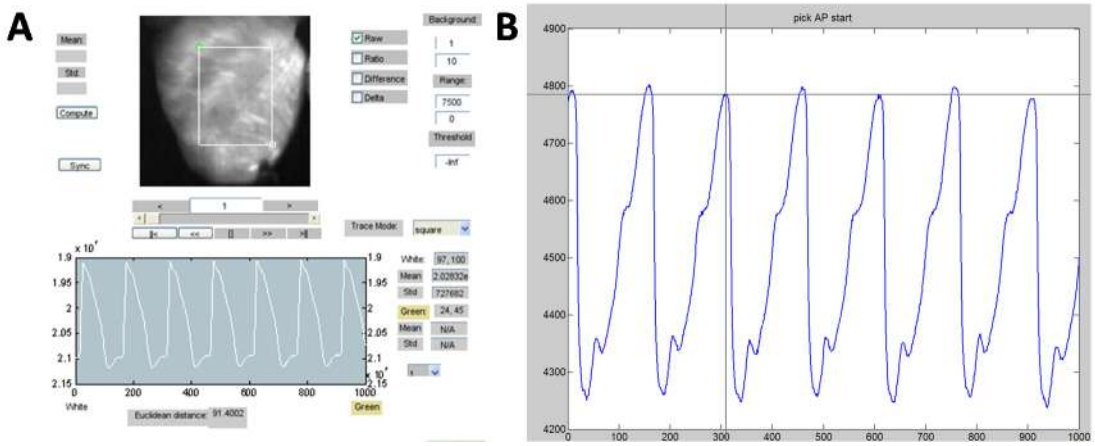

Figure 2-8. A. Data display of the “Gus2” analysis software showing action potentials averaged over a selected area of the heart B. “APDClicker” action potential plotter showing fluorescence intensity over time.

an algorithm titled “Gus2” written by Gustavo Rohde, a former Vanderbilt undergraduate and graduate student. The data was then analyzed by another algorithm called “APDClicker” written by Raghav Venkataraman, another former Vanderbilt graduate student (Figure 2-8). APDClicker allows the user to choose any pixel on the 128x128 pixel image to analyze. This algorithm then calculates baseline voltage, dV/dt_{max} and APD_{50}, APD_{70} and APD_{90} for each action potential independently in the 5x5 pixel area around the selected point (Figure 2-9). Independent AP calculation is important as it reduces the impact of signal drift, alternans and inter-beat variability (Figure 2-10). APDClicker data are then exported to Microsoft Excel for further statistical analysis and modeling.The selection of the proper location for APD analysis requires minimal motion artifacts for proper APD calculation. The region chosen for our experiments was on the

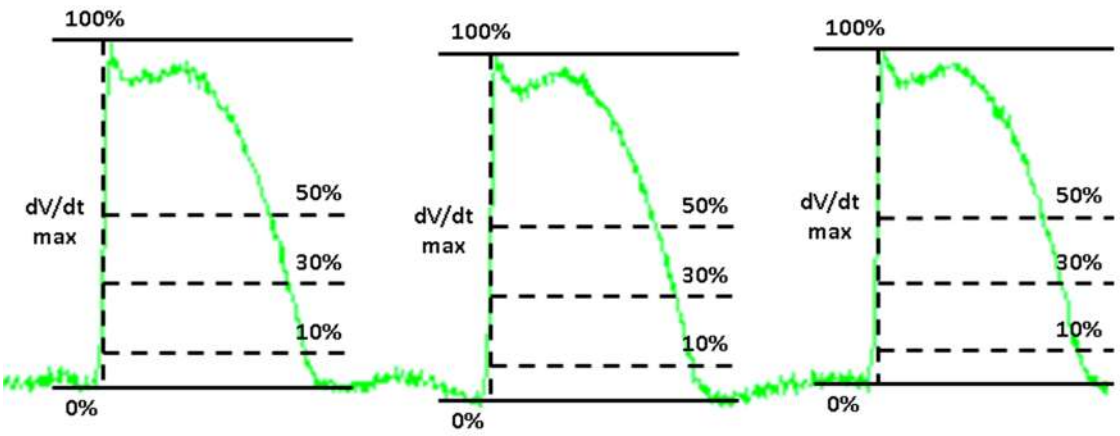

Figure 2-9. Optical APD calculation. APD was calculated from the point of maximal rate of depolarization (dV/dt max) to three points of the restitution curve: 50% (APD_{50}), 30% (APD_{70}), and 10% (APD_{90}) of the maximum AP amplitude. Each measurement consisted of 6-8 sequential action potentials and the results were averaged for each measurement. This figure shows only three action potentials for illustrative purposes and simplicity.

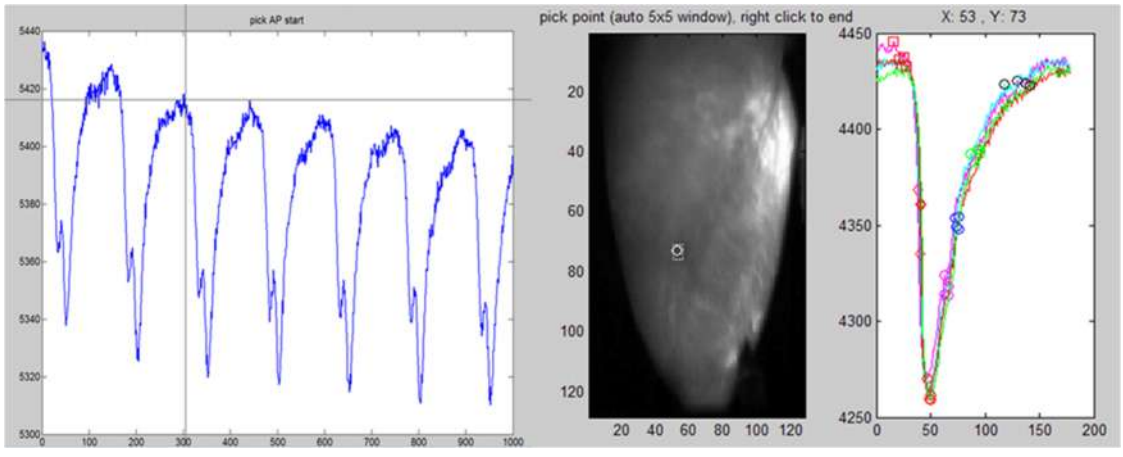

Figure 2-10. Motion and trend compensation in the “APDClicker” software. This trace had a slow baseline drift that does not appear in the final data due to independent baseline correction for each AP.

epicardium closest to the septum of the heart approximately halfway between the apex and the atria (Figure 2-11). The septum was chosen due to its relative stability (compared to the LV's motion) and its high level of activity and response to challenge (compared to the RV's quiescence and resilience). The center of the septum was chosen as a compromise between the pendulum-like motion of the apex and the complex anatomy around the top of the heart. This area in the center of the heart is also held steady by light pressure against the front wall of the media bath, further reducing motion artifacts in the region. These parameters limit the region of interest to an area approximately 20x40 pixels. The user then

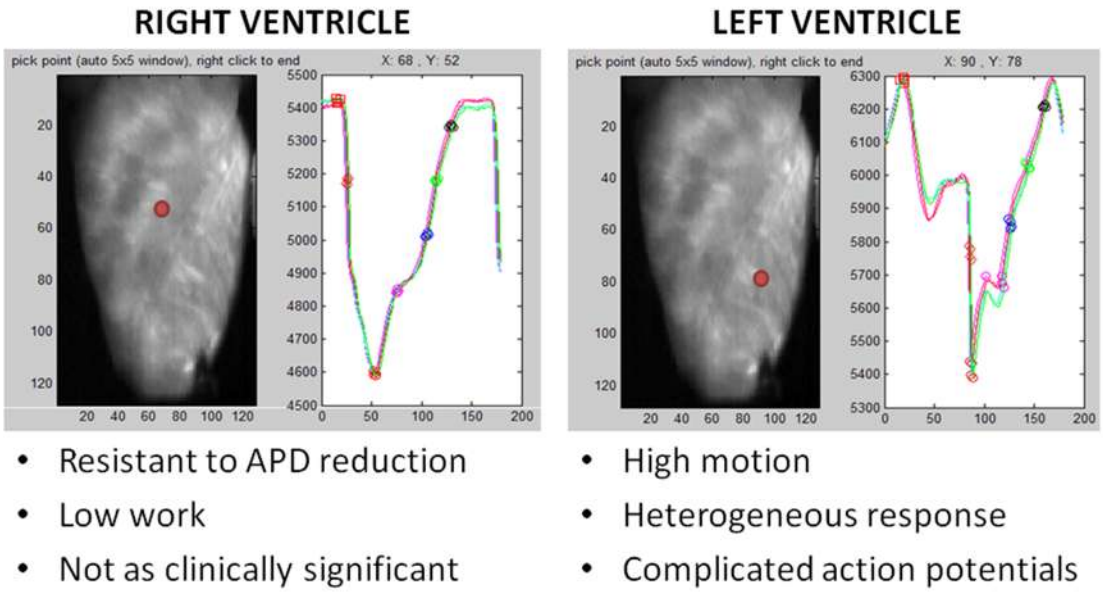

Figure 2-11. Comparison of the right and left ventricle for ischemic imaging. The red circle indicates the location of the MAP probe on the surface of the heart adjacent to the septum. Selection of a point on the surface averages the fluorescence of a 5x5 pixel area and displays the intensity over time.

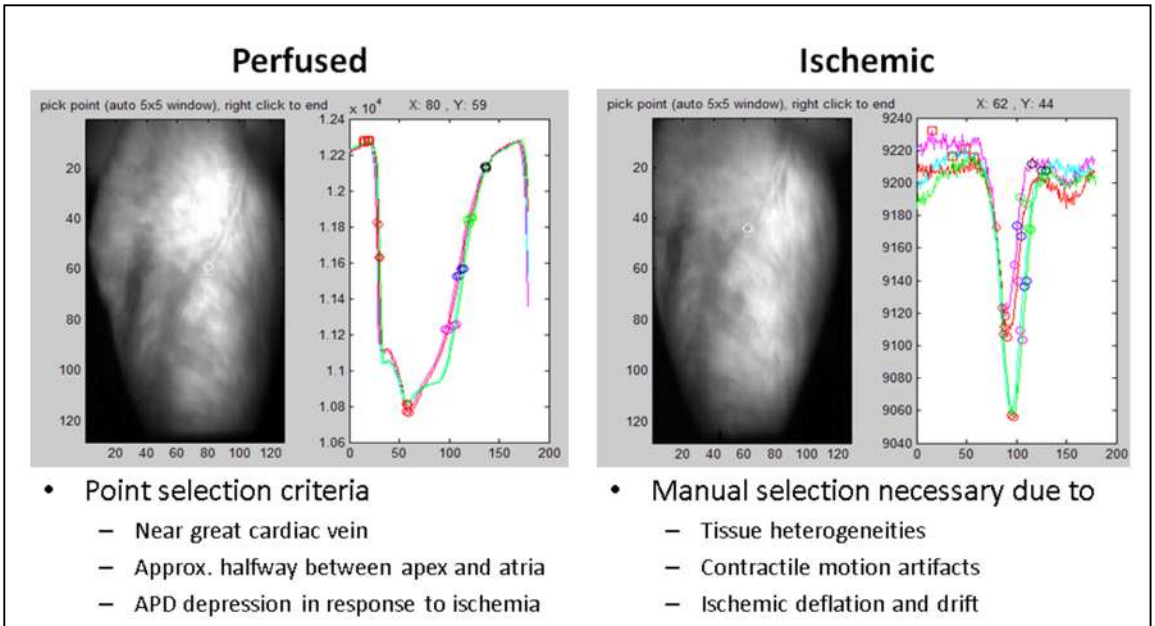

Figure 2-12. Identical points on the surface during perfusion and ischemia. During ischemia, the intraventricular pressure drops and the heart becomes smaller, necessitating manual datapoint selection to sample the same area of the heart.

finds a pixel in this region with minimal motion, which manifests as a lack of steady baseline, spikes or peaks in the action potential plateau or multiple identified “action potentials” in a single pacing interval (Figure 2-12).

Isoprostane and Isofuran Quantification

Frozen hearts were sectioned for isoprostane and isofuran analysis by first discarding approximately 2 g of tissue from the apex. This was done to remove any tissues that may have been damaged or suffered ischemia from the apical suture. A section of the left ventricular wall measuring approximately 0.5 cm by

0.5 cm was then removed and sent to Dr. Jackson Roberts's lab for isoprostane and isofuran analysis.

To test for isoprostanes and isofurans, the frozen sections were first added to a Folch solution (2:1 chloroform:methanol) containing 5 mg/100 ml butylated hydroxytoluene (BHT) at 20 ml/g of tissue in a conical tube and placed on ice. Tissues were then homogenized and the tubes sealed in nitrogen and allowed to sit at room temperature for 1 hour with occasional vortexing. A 0.9% NaCl solution was then added at 4 ml/1 g tissue and vortexed for 1 minute. The tubes were then centrifuged at 2000 rpm for 5 minutes to produce two layers. The upper aqueous layer was discarded and the organic layer transferred to a fresh tube. The organic liquids were dried under N_2 at 37°C

Depending on the amount of lipid present, 0.5-2 ml MeOH containing 5 mg/100 ml and an equal volume of 15% KOH was added. Samples were vortexed and, after the sides of the tube were scraped to suspend any adhered material, let sit at 37°C for 30 minutes. The pH was brought to ~7.0 with 1N HCl and then diluted to 10-40 ml with deionized water. Dilutions were made such that the volume of resuspension MeOH was less than or equal to 5% of the total volume. 1 ng of deuterated (d4) F2-isoprostane internal standard was added to ~1 ml deionized water, vortexed and transferred to each sample tube and mixed well by gently inverting the tubes. Samples were brought to ~pH3 with 1 N HCl and placed on ice for the free F2-Isoprostane assay.

A C18 Sep-Pak was attached to a 12cc syringe and pre-conditioned with 5 ml MeOH and 7 ml pH 3 deionized water. Samples were then slowly pushed

through the Sep-Pak at ~1-2 ml/min. Samples were then washed by running 10 ml of pH 3 water and then 10 ml of heptane through the Sep-Pak. Samples were eluted from the Sep-Pak with 10 ml of 1:1 ethyl acetate:heptane into 20 ml scintillation vials. A small scoop of sodium sulfate was used to remove any remaining water.

A new silica Sep-Pak was then pre-rinsed with 5 ml ethyl acetate and placed on the syringe. The sample from the scintillation vial was then slowly run through the Sep-Pak, being careful not to transfer any sodium sulfate, and washed with 5 ml ethyl acetate. Samples were eluted from the silica Sep-Pak with 5 ml 1:1 ethyl acetate:methanol into a 5 ml reactivial and dried under N_2 at 37°C.

Samples were esterified by adding 40 µl 10% pentafluorobenzyl bromide (PFBB) solution in acetonitrile (ACN) and 20 µl 10% diisopropylethylamine (DIPE) in ACN, vortexing and incubating at 37°C for 20 minutes. Samples were then dried under N_2 and reconstituted in 50 µl 3:2 methanol:chloroform.

The samples were purified using thin-layer chromatography (TLC) as 50 µl of sample were spotted on a TLC plate and allowed to separate in a solvent system consisting of 93% chloroform and 7% ethanol. The PGF2a TLC standard was measured and the area containing the desired bands was scraped onto a piece of creased weighing paper and poured into a microcentifuge tube. 1ml of 85% ethyl acetate 15% ethanol was added and vortexed to resuspend the solids.

Purified samples were then centrifuged for 2 minutes at 14,000 rpm and the ethyl acetate/ethanol was transferred into another centrifuge tube to remove

any silica solids and dried under N_2 at 37°C. 20ul BSTFA and 8 ul of dry (CaH_2 added) dimethylformamide (DMF) was then added to silate the samples for gas chromatography. Samples were again dried under N_2 and reconstituted in 10-20 ul dry (CaH2 added) undecane the day of GC/MS analysis.

For the GC/MS separation a 15 meter DB 1701 GC column was used at an inlet temperature of 2600 and helium carrier gas at a flow rate of 2 ml/minute. For each sample injected, the GC oven was programmed to run from 1900 to 3000 at 200/minute for 9 minutes. Samples were analyzed by selected ion

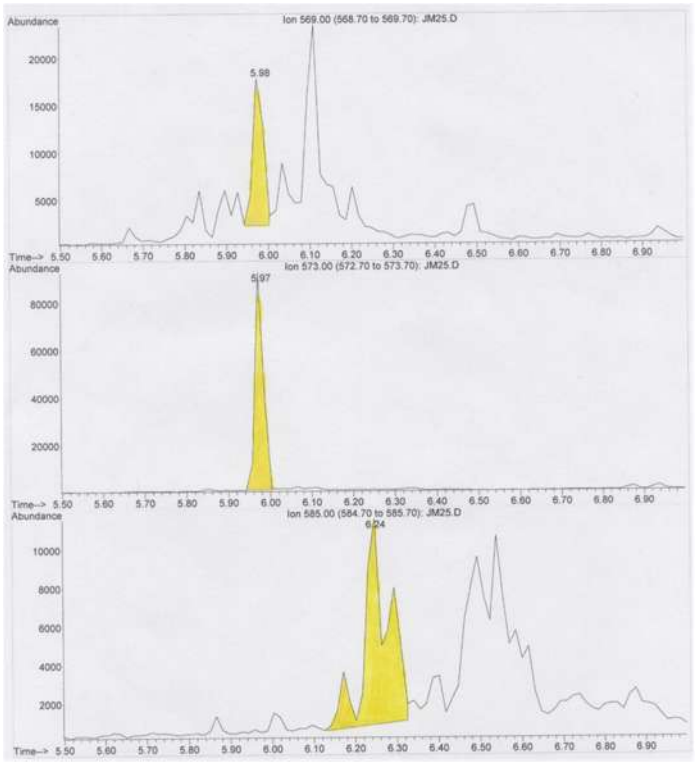

Figure 2-13. Isoprostane quantification. Ions monitored were m/z 569 for F2-Isoprostanes, m/z 585 for Isofurans, and m/z 573 for the internal standard d4 15-F2t-Isoprostane. Yellow areas indicate the area of the peak used to quantify isoprostane content of the samples.

monitoring GC/NICI/MS. Ions monitored were m/z 569 for F2-Isoprostanes, m/z 585 for Isofurans, and m/z 573 for the internal standard d4 15-F2t-Isoprostane (Figure 2-13).

Statistical Analysis

The statistical methods were previously published[65] and summarized here.

Action potential duration was modeled as follows: $APD(t) = k_0 + k_1[x_0(t) - x_1(t)] - k_2 t^2$, where k_0 is the baseline APD, and $x_0(t)$ and $x_1(t)$ are solutions to a pair of piecewise linear differential equations taking the form $x_j' = -l_j x_j$ during anoxia, and $x_j' = m_j(1 - x_j)$ otherwise, for $j = 1,2$ and $x_0(0) = x_1(0) = 1$. Thus the effect of anoxia on APD was modeled as an exponential decay, followed by exponential recovery upon reoxygenation. Whereas x_2' enters the anoxia state immediately, x_1' remains in the baseline state for a period of time determined by an offset parameter. This offsetting captures the transient elongation of APD just after the start of anoxia. The last term, $k_2 t^2$, models the secular trend (decay) in APD over the entire experiment. Nonlinear mixed effects regression[66] was used to account for the variability among hearts (random effects), and to quantify the effects of amino acid supplementation (fixed effects) on each of the model parameters and the resulting APD in response to anoxia challenges. The mixed-effects method is similar to a “two-stage approach”, in which the statistical model is fitted separately for each heart (stage 1), and the resulting model fits or their summaries are compared across treatment groups (stage 2). While simple, this approach fails to “propagate” statistical uncertainty

to the second stage, and cannot be used when only partial data are available for some hearts. The mixed-effects method combines the steps of the two-stage approach for a parsimonious solution. The differences in the average APD between groups over the course of the experiment were summarized using 95% confidence intervals (confidence band). Intervals that exclude the appropriate null value (zero) were considered statistically significant.

CHAPTER III

CARDIAC ANOXIA AND AMINO ACIDS

Published in Physiological Reports[67]

Physiol Rep. 2015 Sep; 3(9): e12535.

Introduction

Cardiac hypoxia/anoxia occurs during heart failure, carbon monoxide poisoning, drowning and other events where oxygen supply is interrupted without blockage of coronary arteries. While cardiac hypoxia/anoxia may not be as common or clinically applicable as cardiac ischemia, it allows dissection, and study of the physiological effects particularly related to oxygen deprivation without the sequelae associated with complete ischemia. During hypoxia/anoxia the heart receives adequate substrate throughput, and the blockage of oxidative phosphorylation can be isolated from the effects of waste accumulation or substrate depletion, as occur with no-flow ischemia.

Glucose, fatty acids, and other substrates require oxygen for full energy yield and produce significant levels of acidic by-products [68]. Amino acids are of particular interest due to their potential for nonoxidative metabolism and their low contribution to cellular acidification. In addition to their role as protein precursors, amino acids are essential components in many aspects of physiology and can serve as metabolic substrates [69]. We hypothesized that supplementation with

glutamate and glutamine maintains electrical properties of the heart during anoxia and improves electrical stability in the recovery period.

Glutamine and glutamate were chosen because glutamate can be easily transaminated to α-ketoglutarate and metabolized via the TCA cycle.[70] It is also a one-step transamidation reaction to turn glutamine into glutamate, making the two amino acids highly interconvertible in the cell.[71] Once the amino acids enter the TCA cycle as α-ketoglutarate, they can be converted to succinate, yielding one molecule each of GTP and NADH.[30] This process does not require any oxygen and does not contribute to cellular acidification. This anaplerotic reaction also serves to maintain the levels of TCA cycle intermediates so that the metabolic machinery is primed to resume normal function once oxygen returns.

To determine the effects of amino acid supplementation on the heart, we monitored the action potential duration (APD) of the heart in response to cardiac anoxia. APD is defined as the amount of time that the cell membranes remain above a given threshold, thereby enabling various ion channels to open or close to allow for the contraction of the muscle fibers. This particular parameter was chosen due to its importance as the linkage between cardiac metabolism and electrical function. Strictly metabolic readouts like ATP/ADP or $NADH/NAD^+$ ratios may not directly correlate with cardiac output, and a functional readout like ejection fraction is an aggregate readout of various metabolic and environmental inputs. Using APD as a readout, we are monitoring first-order effects of the metabolic state without any intermediate reactions to complicate the signal. In an isolated paced heart we remove many of the biochemical and neural signals that

control cardiac function and define the metabolic components being supplied to the heart, thus minimizing the number of variables that can affect APD.

In this study we subjected the hearts to repeated episodes of anoxia to elicit adaptive metabolic responses to the stressor. Six minutes of anoxia were found to result in a small but significant decrease in APD without inducing fibrillation or a loss of pacing. While glutamine and glutamate have been shown to improve outcomes when given to perioperative heart surgery patients[39, 41] it is possible that prophylactic doses of glutamine may reduce the damage from transient anoxia or ischemia with few apparent side effects in populations at risk for cardiovascular events.

Preliminary Data

Initial experiments focused on identifying optimal experimental parameters for anoxia and recovery periods. Initial experiments used four, six, eight and ten minute anoxic challenges followed by 30 minute recovery periods. Our criteria for optimal anoxia duration were:

1) APD depression during anoxia.

2) Moderate APD depression during recovery.

3) Equilibration at a steady APD during recovery.

4) Survival of the heart for the entirety of the experiment.

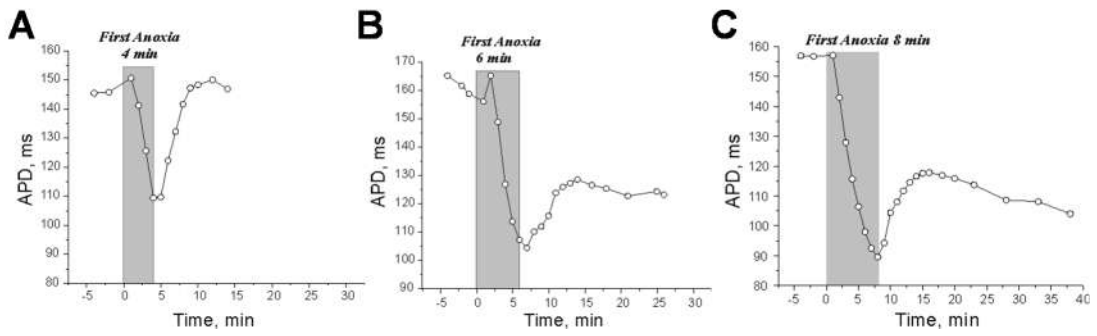

Figure 3-1. Preliminary studies of various durations of anoxia challenge. A. Four-minute anoxia. B. Six-minute anoxia. C. Eight-minute anoxia. Increasing the duration of anoxia markedly lowers APD in the recovery period, and anoxia lasting eight minutes or longer leads to an irreversible progressive decline in APD.

Four minutes of anoxia was found to result in minor APD depression during anoxia with a rapid return to baseline APD (Figure 3-1). There did not appear to be a significant difference between the baseline and recovery periods. Eight minutes of anoxia resulted in severe APD depression during anoxia and recovery, frequently with arrhythmia and occasionally with cardiac death. This effect was even more severe after ten minutes of anoxia and every challenge resulted in arrhythmia and irreversible APD decline followed by cardiac death.

We found that a six minute anoxia challenge resulted in significant APD depression during anoxia and a moderate decrease in APD during the recovery period. The APD decrease after six minutes of anoxia was found to be maintained for long periods after the challenge and the APD neither increased to pre-anoxia levels nor decreased beyond the post-anoxia steady state (Figure 3-2). These preliminary studies also showed that the hearts had no additional

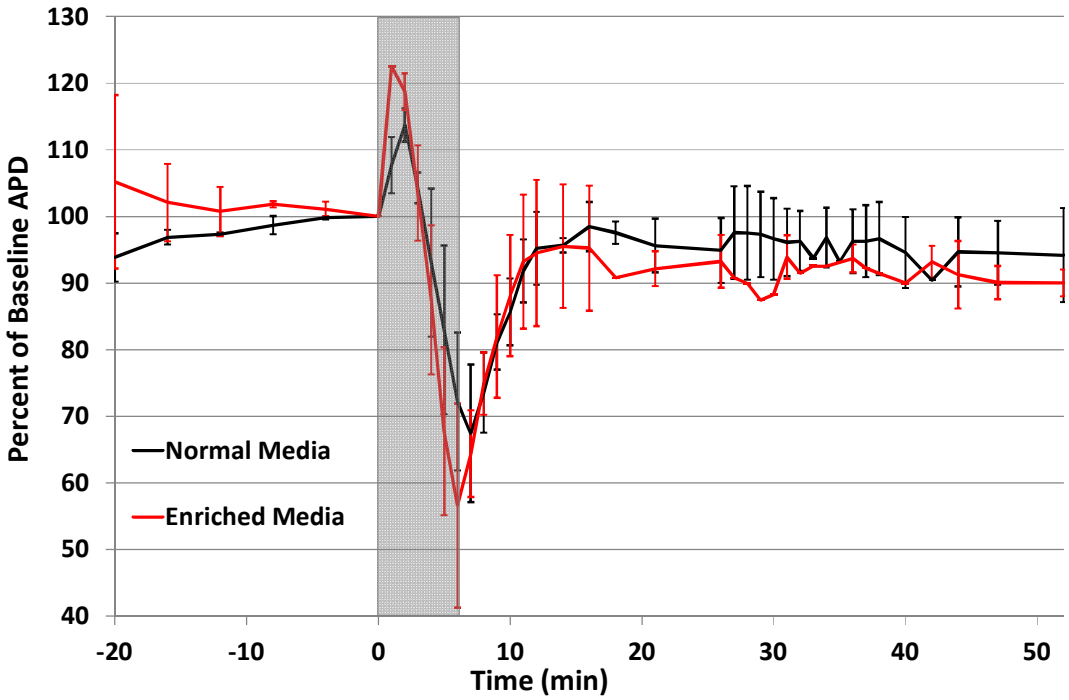

Figure 3-2. APD after a single anoxia. A total of 4 hearts (2 normal, 2 enriched) were exposed to a single six-minute episode of anoxia. To roughly account for baseline variation among hearts we normalized the hearts to a percent of the APD at time 0. A single anoxia has a minimal effect on APD and there does not appear to be a significant difference between the experimental groups.

changes in APD after 20 minutes of recovery, so this was chosen as an adequate time to allow the hearts to re-equilibrate after each anoxic episode.

There has been a great deal of attention paid to the phenomena of ischemic preconditioning wherein a heart exposed to a short episode of ischemia will suffer much less damage when exposed to subsequent, longer ischemias. There has not, to our knowledge, been a similar study of *anoxic* preconditioning so we decided to investigate this phenomena ourselves. Indeed, we found that

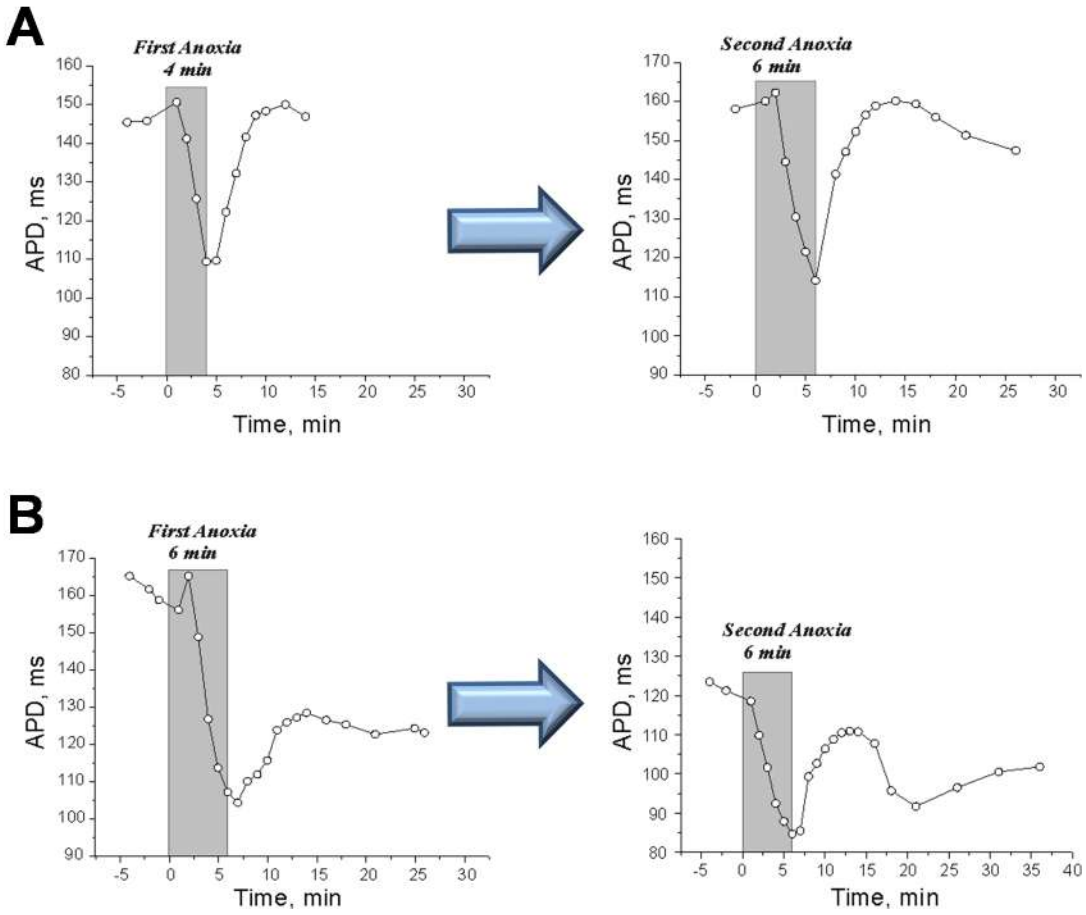

Figure 3-3. Initial anoxia challenges decrease the effects of subsequent challenges. A. An initial four-minute challenge results in no significant APD depression. A subsequent six-minute challenge results in only minor APD decrease. B. An initial six-minute challenge results in significant APD decline, while the next challenge results in a much smaller APD decrease, though this could be due to the lower APD at the beginning of the second challenge.

anoxia challenges given in series were found to elicit smaller effects from subsequent bouts of anoxia (Figure 3-3). An initial challenge of four minutes results in only minor APD decreases when followed by a six minute challenge. An initial challenge of six minutes results in significant APD decreases but the subsequent six minute challenge results in a much smaller APD decrease.

Using the sequential anoxia challenge described above, we exposed amino acid enriched hearts to an initial challenge of four minutes and a subsequent challenge of eight minutes which had previously been shown to be highly damaging to the hearts with profound effects on APD. The amino acid concentrations (2500 μM gln, 150 μM glu) were significantly higher than normal plasma levels but not beyond what could be induced by IV supplementation or

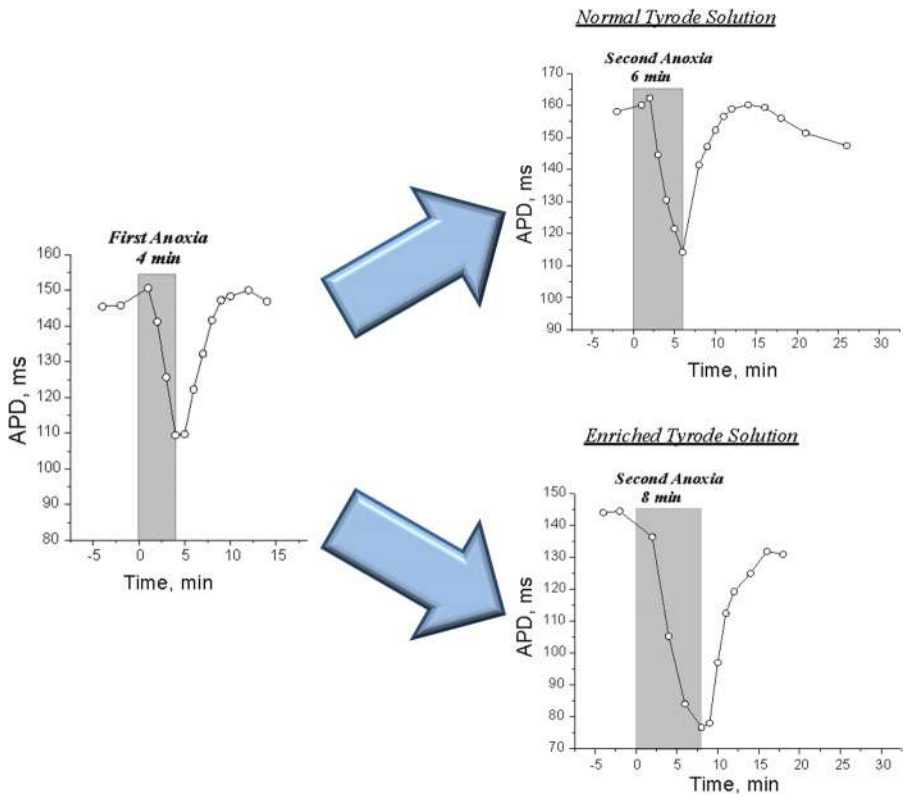

Figure 3-4. Hearts perfused with enriched media tolerate longer periods of anoxia. Hearts perfused with normal (top right) or enriched (bottom right) media were exposed to a four-minute anoxia challenge (left, representative image for both conditions) and then a subsequent challenge. The hearts perfused with enriched media showed approximately equal APD recovery to the control group, even though the enriched hearts endured two more minutes of anoxia.

even by consumption of oral amino acid supplements. [72-74] We saw that the enriched hearts suffered only moderate APD depression and had no arrhythmias even at the end of the eight minute anoxia (Figure 3-4). This was highly encouraging and we decided to test this phenomenon as a full scale experiment.

Results

In one set of experiments the heart was initially perfused with regular Tyrode's solution for 20 minutes, and then the perfusion system was switched to supply the heart with enriched Tyrode's solution for the next 20 minutes. The addition of

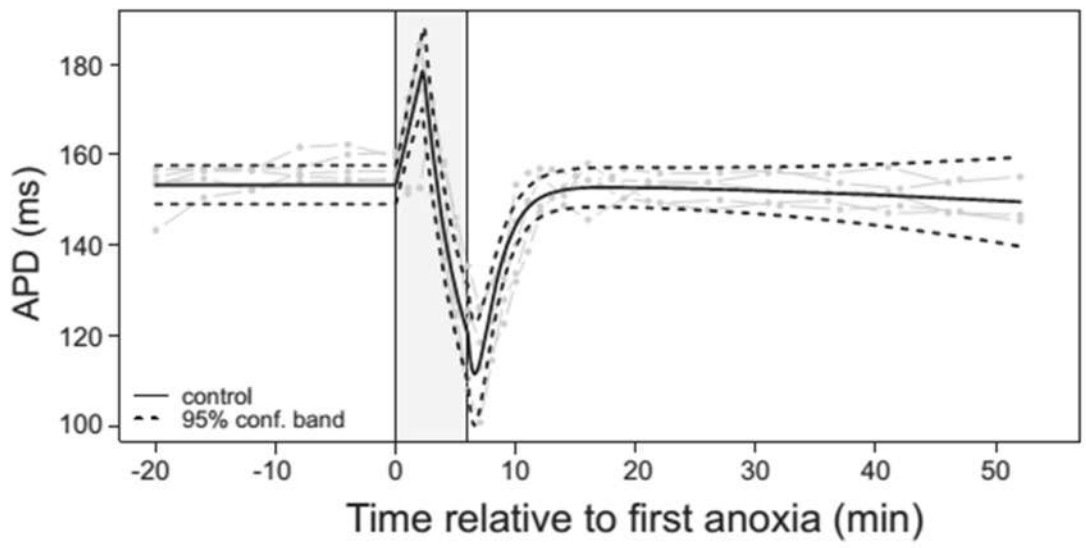

Figure 3-5. APD stability during a long recovery phase after single anoxia. For each experimental replicate (N = 6), the APD time series is illustrated in light gray. For the purpose of graphical presentation, each original time series was adjusted to the overall pre-anoxia mean. The solid black line represents mean APD from the fitted model. The dotted black lines define a pointwise 95% confidence band. The vertical gray bar delineates the six-minute anoxia challenge.

amino acids insignificantly increased APD from 150.5 ms (95% CI: [148.5 ms, 152.4 ms]) to 153 ms (95% CI: [149.9 ms, 156.1 ms]) (N = 24) (6 experiments, unpaired t-test). Another set of experiments (N = 5), wherein the hearts were exposed only to one anoxia, is presented in Figure 3-5. As the figure illustrates, mean APD recovers to 99% (152.7 ms, 95% CI: [148.3 ms, 157.0 ms]) of baseline APD within 10 minutes following cessation of anoxia; therefore, 20 minutes was chosen as a sufficient recovery interval between two sequential anoxias.

Figure 3-6 demonstrates the characteristic data of APD change in response to two successive anoxias. In this control experiment the heart was perfused with only glucose-containing media. Three phases can be readily distinguished in each set of anoxia. The first phase of abrupt APD increase starts immediately after onset of anoxia. This initial change in APD was more pronounced in the first insult of anoxia and was observed in 18 out of 21 conducted experiments. The first transient phase is followed by considerable APD decrease, which lasts until cessation of anoxia. This APD shortening was always greater during the second period of anoxia. The third phase of anoxia-induced change in APD takes place after recommencing the perfusion with oxygenated solution. The fast APD recovery phase continues for about 10 minutes. The insets in Figure 3-6 illustrate MAP traces recorded at different phases of APD change. The described APD dynamics were typical in both control and hearts perfused with enriched media.

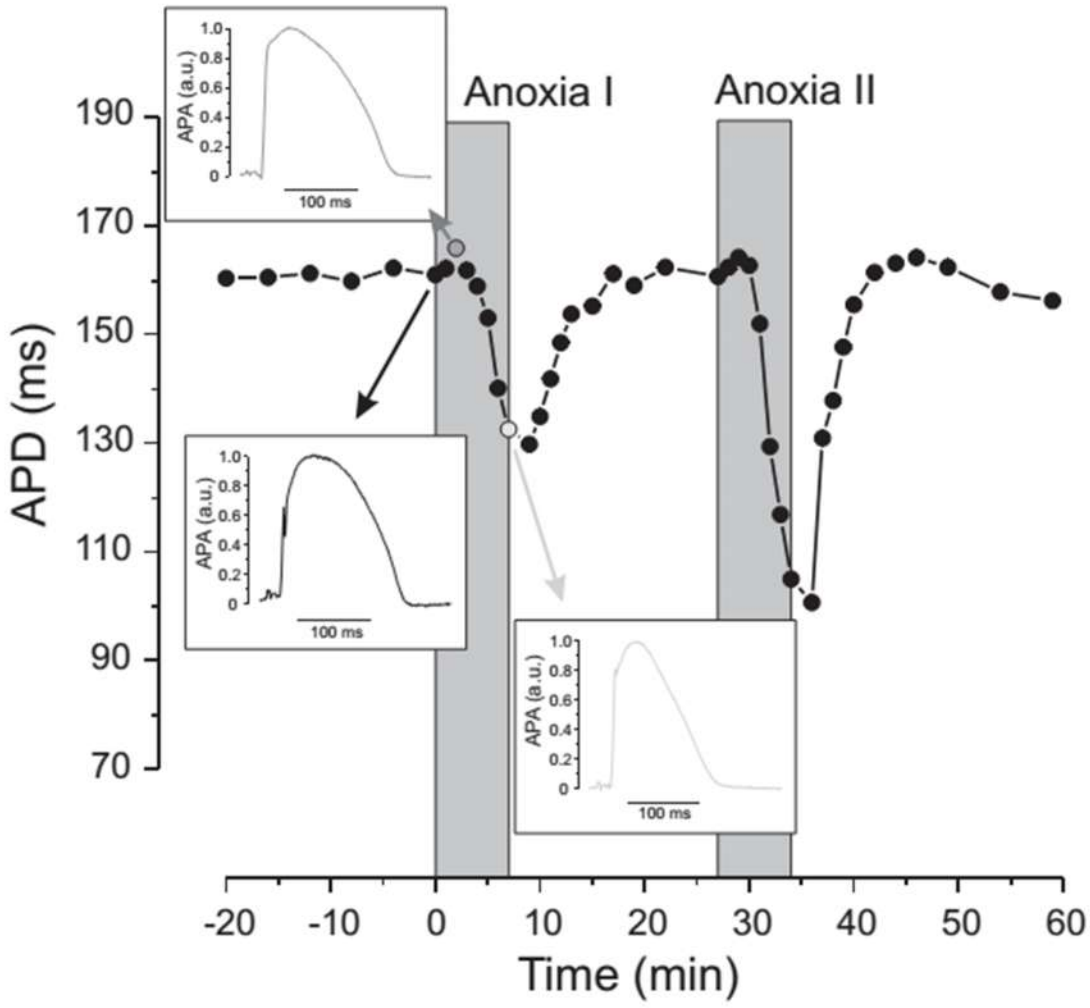

Figure 3-6. A typical double anoxia experiment. Two successive six-minute anoxic periods followed by 20 minutes of recovery. The insets demonstrate MAP recorded at different phases of anoxia-induced APD change.

Figure 3-7 represents the effect of glutamine/glutamate supplementation on mean APD dynamics in response to two insults of anoxia (N = 16). The upper panel in Figure 3-7 illustrates estimated mean APD curves from control (blue) and from experimental (orange) hearts with individual time series data superimposed in lighter color. The lower panel shows the estimated difference in

mean APD between control and enriched groups and the 95% confidence band. After onset of the first anoxia, the first phase of acute transient APD increase peaks at 2.27 min (95% CI: [2.01min, 2.54 min]) with amplitude of 13.7 ms (95% CI: [11.8 ms, 15.7 ms]) and 8.1 ms (95% CI: [9.4 ms, 10.7 ms]) above baseline

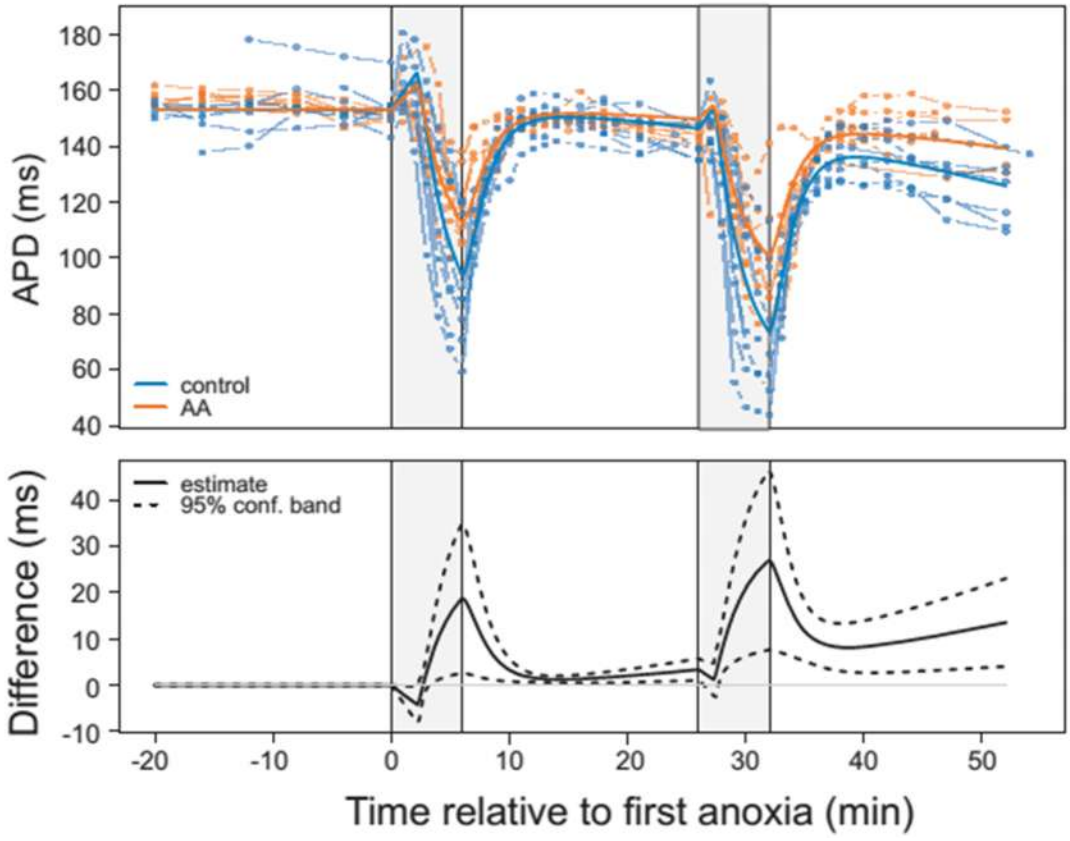

Figure 3-7. APD change in response to two sequential insults of anoxia. Vertical gray bars show the two periods of anoxia. Upper Panel: The solid blue and red colored lines depict mean APD for control (N = 8) and supplemented (N = 8) hearts, respectively. The dot-dash colored lines represent individual APD time series for each replicate. For the purpose of graphical presentation, each original time series was adjusted to the overall pre-anoxia mean. Lower Panel: Estimated difference in mean APD for enriched versus normally perfused hearts with pointwise 95% confidence band.

for control and supplemented media groups, respectively. The subsequent APD shortening is 39% (59.3 ms, 95% CI: [51.0 ms, 67.7 ms]) for control and 26% (40.5 ms, 95% CI: [32.4 ms, 48.6 ms]) for experimental groups. In the course of the second anoxia, the first phase transient APD elongation peaks at 1.3 minutes (95% CI: [1.0 min, 1.7 min]), which is about 0.9 minutes (95% CI: [0.5 min, 1.3 min]) faster than in the first anoxia. The magnitude (relative to mean APD just before the start of anoxia) is 5.1 ms (95% CI: [-0.4 ms, 10.8 ms]) and 7.4 ms (95% CI: [-2.0 ms, 16.7 ms]) for supplemented and normal hearts, respectively. The following APD shortening is 48% (73.7 ms, 95% CI:[59.0 ms, 88.4 ms]) in the hearts perfused with regular solution and 32.0% (100.8 ms, 95% CI:[86.2 ms, 115.2 ms]) in the hearts supplied with amino acids.

Thus the control group shows a significantly larger drop in APD than the supplemented group. The difference in dynamics of APD change in response to amino acid administration can be easily detected from the estimated difference in mean APD for enriched versus normally perfused hearts, as illustrated in the lower panel of Figure 3-7. It should be noted that anoxia induces gradual APD depression over the entire experiment. The rate of APD decay over the course of the experiments in the amino acid supplemented hearts (0.010 ms/s/s, 95% CI:[0.005, 0.015]) was less than in control (0.020 ms/s/s, 95% CI:[0.015, 0.025]). Notably, there was no evidence of significant decay in APD among hearts exposed to a single anoxia event (0.003 ms/s/s, 95% CI:[0.003, 0.009]). On average, the APDs for control hearts were 10.8% shorter (13.6 ms, 95% CI: [4.1

ms, 23.1 ms]) than hearts supplemented with glutamine and glutamate at the end of the experiment.

Discussion

Amino acids

This study investigated the effects of anoxia on cardiac action potential duration in the presence or absence of therapeutic doses of amino acids. According to the NIH, normal levels of glutamine and glutamate are approximately 390-650 μM and 18-98 μM for adults in the fasted state.[75] Hearts were perfused with glutamine (2500 μM) and glutamate (150 μM) at levels somewhat higher than those found in the body naturally. Glutamate was included in the media to reduce washout of the cellular stores, since ischemia and anoxia lead to ATP depletion and decreased function of the active transporters that maintain the high intracellular glutamate gradient.[76-78]

Glutamate is found at high tissue/plasma ratios in the heart and is associated with increased contractile strength, $NADH/NAD^+$ ratios and ATP levels when given to hearts before an anoxic event.[78] Glutamine supplementation has also been shown to improve contractile function and Ca^{2+} homeostasis during chemical hypoxia.[77, 79] Increased intracellular glutamate stores are correlated with improved metabolic recovery, increased cardiac output and elevated glutathione levels after an ischemic episode.[71-73] That said, glutamate is a potent neurotransmitter and elevated levels of circulating glutamate have been associated with neurological side effects.[72, 80]

Glutamine, on the other hand, has no known toxicity threshold and is normally the amino acid of highest concentration in circulation.[74] A single dose of oral or intravenous glutamine has been shown to improve tissue glutamate levels without the need for high levels of glutamate in the plasma.[81, 82] This is due to the presence of high-affinity transporters for glutamine in the heart, and a high level of glutaminase activity, allowing the heart to rapidly convert circulating glutamine into intracellular glutamate stores.[78] Improved cardiac performance has been found with circulating glutamine levels as low as 1.25 mM, a level easily achieved by an oral dose of glutamine.[72, 73] This has important clinical applications if it can be shown that glutamine improves disease outcomes, since there would be a wide therapeutic range and negligible risks associated with its use. The administration of these amino acids did not appear to alter the hearts normal APD since we did not observe any significant difference between control and supplemented hearts during the baseline period.

Anoxia

An interesting behavior occurs at the onset of anoxia: a rapid and significant increase in APD. This is of particular interest due to the greater energy demands associated with longer APD in the face of decreased metabolic capacity from the loss of oxidative phosphorylation. Such behavior was observed in 18 of 21 investigated hearts within 3 minutes of anoxia and was independent of amino acid supplementation. This phenomenon of initial prolongation of APD after metabolic inhibition has been described previously by Carmeliet and

Boulpaep in the frog heart[83] and later in sheep Purkinje fibers[84]. Isenberg *et al*.[85] suggested that initial prolongation of APD in guinea-pig ventricular myocytes results from block of the electrogenic Na pump due to ATP depletion. The biphasic response in rabbit and human cardiomyocytes to hypoxia and metabolic inhibition has been reported by Verkerk *et al*.[86] They detected this phenomenon in all subepicardial myocytes, but not in most subendocardial myocytes. They found that a decrease in I_{to}, which occurs prior to the opening of K_{ATP} channels, underlies the metabolic-induced initial increase in APD.

Reoxygenation of the heart results in a rapid increase in APD. In both groups there was a gradual decline after approximately 8 minutes of reoxygenation after both anoxic episodes. It was originally thought that the decline in APD seen after the second anoxia was simply a continuation of the APD decline caused by the first anoxia and that a single anoxia may result in a steady decline in APD regardless of subsequent anoxia. We showed that this was not the case by exposing hearts to a single anoxia and monitoring their behavior for the same length of time. These data showed that the challenged hearts reached a new, albeit lower, steady state 20 minutes post-anoxia and remained relatively constant for another 30 minutes. For this reason we chose to challenge the hearts multiple times to enhance the effects of the insult and to simulate a condition like CHF, where the anoxia may be transitory but repetitive in nature.

Repeating the anoxia also allowed us to explore the effects of cardiac preconditioning, a mechanism by which a challenged heart can adapt to the

insult and respond more effectively to subsequent insults. In our work the application of amino acids significantly decreased anoxia-induced APD shortening by 29.9% (18.9 ms, 95% CI:[2.6 ms, 35.1 ms]) in the first anoxia and by 36.6% (27.1 ms, 95% CI:[7.7ms, 46.6 ms]) in the second period of anoxia. In addition, the amino acids significantly reduced slow APD decay. Since our insults were only 20 minutes apart, the heart did not have adequate time to significantly change its transcription or translation profiles, so we were looking only at acute changes in substrate handling. Thus, the changes we saw are most likely due to metabolic effects of the intervention or responses from endogenous proteins. Due to the extremely high turnover in the ATP pool from oxidative phosphorylation, phosphocreatine cycling and glycolysis, we did not expect to see significant ATP/ADP differences between the conditions after the 20-minute recovery period.

While the outermost layer or two of cells may receive oxygen passively through contact with the air, this very low level of diffusion is not sufficient to supply the heart's high oxygen demands. Additionally, the MAP probe is in direct contact with the epicardium, but the signal it measures is derived from the surrounding tissues, possibly reaching as deep as the mid-myocardium. The presence of the electrode itself will block diffusion into the underlying tissue from the air. The integration of the MAP signal over a depth of underlying tissue further minimizes the impact of the few surface cells that receive diffused oxygen. Furthermore, we have extensive experience and there is also a large literature on the optical measurement of transmembrane potentials in the regionally or

globally ischemic heart. We have not seen nor have we found reports of any epicardial cardiomyocytes being able to sustain measureable electrical activity only through absorption of oxygen from the air.

Statistics

Our initial strategy was to use Student's t tests to assess the differences in average APD for control versus supplemented hearts following the second anoxic episode. However, this approach neglects the variability due to instrument calibration, and heart-specific variability in baseline APD. The differences observed did not achieve statistical significance using this technique, and subsequent numerical investigations revealed that this approach had very little statistical power.

The metabolic and electrophysiological response to ischemia can deviate depending on multiple factors, such as vasculature, hormonal status, heart rate and metabolic rate, concomitant diseases, gender and age [87-90]. The same factors could also underlie interspecies variability in the case of anoxia, and thereby complicate analysis of the response to anoxia, especially when anoxic stress is of short or moderate duration.

To account for the variability among hearts in the effects of anoxia on APD and to properly quantify statistical uncertainty in our work, we utilized nonlinear, mixed-effects regression[66] to develop a novel statistical method[91]. By fitting the entire time-course of APD measurements to a simple mechanistic model, and adjusting for heart-specific baseline variability, we demonstrated a clear and

statistically significant difference between the control and supplemented hearts (Figure 3-7). Table 3-1 compares the values from the fitted model compared with the raw APD measurements at each of the phase transitions. Related strategies are common in the analysis of pharmacokinetics and pharmacodynamics time series experiments.[92]

Table 3-1. Comparison of raw data and fitted model values. Values measured at the end of each experimental phase.

	Baseline	First Anoxia	First Recovery	Second Anoxia	Second Recovery
Minute	0	6	26	32	52
Data – Control	155.3	105.2	144.7	91.1	128.8
Data – Enriched	152.7	113.5	148.9	101.1	144.9
Model – Control	153.7 (148.6, 158.8)	113.7 (93.4, 138.0)	147.5 (140.4, 154.8)	93.0 (74.4, 118.3)	128.7 (112.7, 143.8)
Model – Enriched	153.7 (148.6, 158.8)	118.8 (99.5, 140.1)	151.3 (145.6, 157.1)	103.8 (84.8, 125.6)	144.0 (133.8, 153.4)

Finally, we relied heavily on 95% confidence intervals to summarize the differences between treatment groups. For example, the rate of APD decay in the normal media group was 3.2×10^{-6} ms/s/s faster, relative to the amino acid-supplemented media group. The 95% confidence interval for this quantity is $(2.8\times10^{-7}, 6.2\times10^{-6})$. Because this confidence interval does not include zero, there is statistically significant evidence that APD decays more slowly in hearts perfused with amino acid-supplemented media. This approach to statistical significance highlights the estimated magnitude and possible range (with 95% confidence) of differences between treatment groups. In particular, this supplants the more conventional, but less informative, hypothesis test and p-value summary.

Mechanisms

There are several mechanisms through which these amino acids could exert their effects.[1] Glutamine and glutamate are interconvertible via a transamidation reaction at the cell membrane and within the intracellular space.[71] Glutamate can then be transaminated and enter the TCA cycle as α-ketoglutarate.[70] The ability to produce ATP directly from glutamine and glutamate through substrate-level phosphorylation in the TCA cycle can provide a small amount of GTP without the need for oxygen (Figure 3-8).[30] This could be a crucial

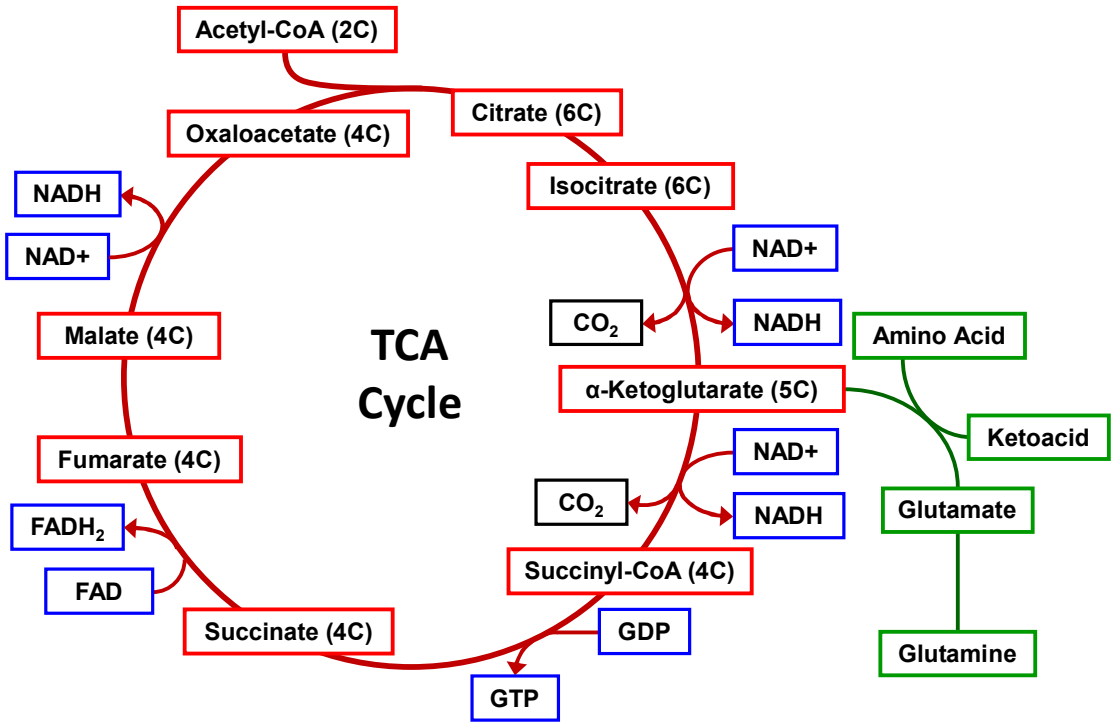

Figure 3-8. TCA Cycle GTP Production. GTP is directly created through substrate-level phosphorylation during the conversion of succinyl-CoA to succinate.

reaction that allows the heart to maintain a minimal level of pump and muscle function, giving the heart a slightly longer period of resistance to anoxia. When we began these experiments we found this theory quite compelling. However, only a very small amount of ATP can be produced through this mechanism since each molecule of glutamate or glutamine can produce only one GTP and one NADH molecule (which cannot be oxidized under anoxic conditions) in their conversion to succinate. In contrast, a single molecule of acetyl-CoA produces one GTP, 3 NADH and one $FADH_2$, which will yield approximately 10 ATP through oxidative phosphorylation. Also, the reducing environment of the ischemic heart inhibits these reactions, as does the accumulation of NADH. Since NADH requires oxygen for deprotonation, this can become a limiting reagent of the α-ketoglutarate to succinyl-CoA reaction before substrate-level phosphorylation can occur. We have shown that the control and supplemented hearts have no significant APD differences during the anoxic episodes and that the differences between the conditions emerge only after several minutes of reperfusion. This strongly suggests that the cardioprotective effects occur only after oxygen supply returns. Hence, we no longer believe that ATP production during anoxic challenge is the primary mechanism responsible for the cardioprotective effects of glutamine and glutamate.

Another possible method of glutamine-mediated metabolic support is anaplerosis, or replacement of depleted intermediates. As stated above, glutamine and glutamate readily enter the TCA cycle. This additional supply of TCA cycle intermediates could support the return of oxidative phosphorylation

during reperfusion by maintaining the levels of TCA cycle intermediates during ischemia and early reperfusion. Since ischemia normally results in losses of membrane integrity and ion compartmentalization, this reinforcement could be essential to return the heart to normal function. This mechanism is supported by the data in that the differences between the conditions emerge only during the late reoxygenation periods when oxidative phosphorylation should be recovered

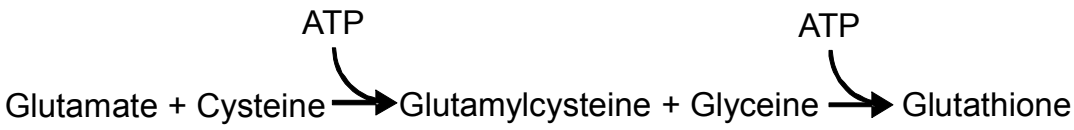

Figure 3-9. Mechanism of glutathione production from amino acid precursors.

and meeting the needs of the struggling heart.

A third explanation is that glutamate and, by extension, glutamine may reduce the effects of reactive oxygen damage through their conversion to the potent antioxidant, glutathione (Figure 3-9). Glutathione can be produced from amino acid precursors and is an effective antioxidant within the cell. It is possible that glutamine and glutamate contribute to cellular stores of glutathione, reducing the damage from reactive oxygen species (ROS). This is an ATP-dependent reaction that would necessarily take place before the onset of anoxia to effectively reduce ROS damage during anoxia. It also requires other amino acids to assemble the final glutathione molecule. For these reasons we do not believe

that this is the mechanism responsible for the APD enhancement we see in these experiments. That said, this pathway may play a role in long-term recovery from anoxic insults and may be another compensatory mechanism that would prepare the heart for subsequent anoxia.

CHAPTER IV

CARDIAC ISHEMIA AND AMINO ACIDS

Introduction

Cardiac ischemia is the leading cause of death and is responsible for the majority of hospital admissions in the United States.[93] These acute ischemic events are usually caused by asymptomatic atherosclerosis that reduces blood flow to the tissues and leaves the heart vulnerable to oxygen deprivation during exercise or elevated cardiac output. Due to the often subtle and transient nature of these episodes, cardiac ischemia is often undetected until it causes a fatal heart attack. In light of this, it is important to study cardiac ischemia as a "chronically acute" event in which the heart is repeatedly subjected to short, non-lethal ischemic episodes, much as it would happen *in vivo*.

The heart's ability to alter its metabolism and overall behavior to reduce the threat from ischemia means that its ischemic response will change over time, as will its post-ischemic recovery.[94, 95] Ischemic preconditioning is a well-known phenomenon in cardiology that is often overlooked in basic research settings of single-ischemia challenges.[30] We established in the previous chapter that the heart alters its electrophysiology in response to sequential anoxia challenges, and we now explore both the electrophysiology of ischemia and what happens to the heart over longer time scales. If the heart exhibits significant metabolic

changes after only two anoxic challenges over 52 minutes, then we expect to see even greater changes after three ischemic challenges over 90 minutes.

The principal reason for our use of ischemic challenge rather than more anoxic challenges is clinical relevance – far more patients suffer infarctions and atherosclerosis than drowning, carbon monoxide poisoning or pulmonary edema. A secondary consideration was that the original thesis proposal contained perfusate sampling techniques that were not possible during stopped-flow conditions and required constant flow. This necessitated anoxic challenges due to the ability to maintain perfusion. These methods were not used in our experiments, so there was no longer any concern about flow rates.

The importance of amino acids, however, remains highly relevant in the context of ischemia since the lack of oxygen still inhibits the normal functions of the heart.[28, 41] We continued to use the same media and the same amino acid levels as in the previous experiments to compare the responses in the anoxic and ischemic hearts. The glutamine and glutamate were expected to exert similar effects since the same pathways are expected to have similar dynamics in both conditions.

We expanded our action potential duration (APD) measurements from APD_{90} only to include dV/dt_{max}, APD_{50} and APD_{70} as well as APD_{90}. This allows us to more thoroughly explore the behavior of the heart and determine exactly how the heart's action potential (AP) is responding to the ischemia and the amino acids. Using these three additional parameters we are able to plot the shape of the AP to see how long the heart is maintaining calcium currents and other ion

channels. These parameters will help us link the metabolism and electrophysiology to calcium signaling and mechanical function. The AP shape will also help us determine the mechanism of amino acid-mediated cardioprotection.

To test the effect of amino acid anaplerosis of the TCA cycle, we introduced a new compound to our experiments: aminooxyacetate (AOA). This molecule is an amino acid transaminase inhibitor that has been shown to block the action of the glutamate transaminase that converts glutamate to α-ketoglutarate.[30] Since we proposed that this was the primary mechanism for the cardioprotective effects of these amino acids, this compound was expected to negate the APD increases in the supplemented group.

In the course of these experiments we found that the amino acid-enriched group did in fact have significantly higher APDs than the control group and that the AOA completely blocks this increase when given in conjunction with the amino acids. The effects are most prominent in the APD_{50} group, indicating that the amino acids exert significant effects on maintaining a longer, more normal AP than the control group. This has important implications in the clinical setting as it indicates that glutamine supplementation may significantly improve the most fundamental level of cardiac function: the action potential.

Results

A total of 31 hearts (8 AA-/AOA-, 8 AA+/AOA-, 8 AA-/AOA+, 7 AA+/AOA+) were perfused, paced and monitored over a period of 110 minutes (see Figure 2-5). This included 20 minutes to establish baseline APD and three 10-minute

episodes of ischemia with 20 minutes of recovery each. After the experiments the hearts were frozen at -80°C and later analyzed for isoprostanes, isofurans and tissue amino acid levels.

Action Potential Duration

APD was measured at three points along the AP curve: 50% of maximum AP amplitude (APD_{50}), 30% of maximum AP amplitude (APD_{70}) and 10% of maximum AP amplitude (APD_{90}). The data were used to construct a fitted model of APD behavior at each point over time with a 95% confidence interval (CI). The value and CI at the end of each stage of the experiment are shown in Table 4-1.

APD_{50}

AA-/AOA- hearts had a baseline APD_{50} of 96 ms (95% CI: [82 ms, 109 ms]) (Figure 4-1A). Each reperfusion period resulted in a small but significant increase in APD_{50} compared to baseline. The final APD_{50} was 113 ms (95% CI: [93 ms, 134 ms]).

AA+/AOA- hearts had a baseline APD_{50} of 119 ms (95% CI: [88 ms, 146 ms]) (Figure 4-1B). Each reperfusion period resulted in increasingly higher APD_{50} compared to baseline. The final APD_{50} was 164 ms (95% CI: [138 ms, 197 ms]).

AA-/AOA+ hearts had a baseline APD_{50} of 143 ms (95% CI: [112 ms, 173 ms]) (Figure 4-1C). The AA+/AOA+ group had a baseline APD_{50} of

Table 4-1. Mean values with 95% confidence intervals for model-fitted data. Each point is from the end of each period throughout the experiment.

APD_{50}		First		Second		Third	
	Baseline	Ischemia	Reperfusion	Ischemia	Reperfusion	Ischemia	Reperfusion
Minute	0	10	30	40	60	70	90
Control	95.89 (82.29 ms, 109.04 ms)	71.50 (36.51 ms, 101.02 ms)	97.85 (85.38 ms, 110.62 ms)	76.25 (42.26 ms, 105.82 ms)	103.76 (91.41 ms, 116.95 ms)	82.68 (51.82 ms, 110.85 ms)	113.61 (93.33 ms, 133.64 ms)
Enriched	118.73 (88.48 ms, 146.43 ms)	19.73 (-5.05 ms, 48.75 ms)	123.72 (96.00 ms, 148.68 ms)	29.60 (5.10 ms, 61.63 ms)	138.70 (116.28 ms, 160.16 ms)	44.31 (13.00 ms, 86.28 ms)	163.68 (137.67 ms, 196.87 ms)
AOA Control	142.97 (111.51 ms, 172.77 ms)	59.23 (33.36 ms, 84.21 ms)	142.56 (111.33 ms, 171.50 ms)	60.32 (35.69 ms, 85.33 ms)	141.33 (109.90 ms, 168.79 ms)	55.58 (30.43 ms, 80.79 ms)	139.30 (104.96 ms, 168.53 ms)
AOA Enriched	114.15 (87.09 ms, 139.26 ms)	75.50 (50.62 ms, 99.65 ms)	114.22 (88.28 ms, 137.97 ms)	77.32 (52.61 ms, 100.19 ms)	114.34 (89.31 ms, 137.71 ms)	76.09 (50.74 ms, 100.95 ms)	114.54 (85.87 ms, 145.88 ms)

APD_{70}		First		Second		Third	
	Baseline	Ischemia	Reperfusion	Ischemia	Reperfusion	Ischemia	Reperfusion
Minute	0	10	30	40	60	70	90
Control	114.98 (101.11 ms, 129.37 ms)	104.22 (66.27 ms, 138.77 ms)	118.68 (106.36 ms, 131.97 ms)	112.79 (76.53 ms, 146.59 ms)	129.81 (118.37 ms, 142.32 ms)	129.53 (95.62 ms, 160.55 ms)	148.36 (126.88 ms, 167.68 ms)
Enriched	136.22 (103.36 ms, 167.64 ms)	-24.28 (-53.30 ms, 6.92 ms)	141.12 (111.12 ms, 168.98 ms)	-11.10 (-40.49 ms, 21.57 ms)	155.83 (131.92 ms, 177.38 ms)	18.71 (-15.17 ms, 63.85 ms)	180.34 (151.44 ms, 216.94 ms)
AOA Control	161.48 (138.67 ms, 185.15 ms)	0.77 (-27.23 ms, 30.19 ms)	160.53 (138.87 ms, 183.02 ms)	4.17 (-21.48 ms, 32.92 ms)	157.67 (136.86 ms, 178.11 ms)	12.47 (-11.85 ms, 41.83 ms)	152.90 (126.41 ms, 176.46 ms)
AOA Enriched	139.55 (111.27 ms, 167.17 ms)	63.91 (33.21 ms, 92.70 ms)	138.81 (112.63 ms, 164.20 ms)	65.90 (36.17 ms, 92.48 ms)	136.53 (113.15 ms, 159.25 ms)	70.68 (42.47 ms, 98.20 ms)	132.72 (104.02 ms, 164.93 ms)

APD_{90}		First		Second		Third	
	Baseline	Ischemia	Reperfusion	Ischemia	Reperfusion	Ischemia	Reperfusion
Minute	0	10	30	40	60	70	90
Control	143.19 (130.71 ms, 157.82 ms)	167.62 (122.45 ms, 208.79 ms)	146.72 (135.52 ms, 160.47 ms)	176.20 (131.19 ms, 217.38 ms)	157.33 (143.68 ms, 171.12 ms)	191.46 (149.12 ms, 231.85 ms)	175.02 (146.44 ms, 197.20 ms)
Enriched	171.97 (145.77 ms, 195.54 ms)	61.70 (18.90 ms, 95.43 ms)	177.59 (154.02 ms, 198.83 ms)	78.51 (38.06 ms, 112.29 ms)	194.48 (174.11 ms, 215.80 ms)	114.12 (68.30 ms, 156.97 ms)	222.65 (188.48 ms, 263.15 ms)
AOA Control	189.89 (166.26 ms, 215.44 ms)	77.29 (36.80 ms, 114.10 ms)	190.30 (167.65 ms, 214.72 ms)	85.44 (47.30 ms, 120.00 ms)	191.56 (169.37 ms, 214.89 ms)	101.85 (64.12 ms, 136.74 ms)	193.65 (163.25 ms, 223.03 ms)
AOA Enriched	167.98 (143.02 ms, 192.79 ms)	163.90 (126.96 ms, 200.49 ms)	170.00 (146.64 ms, 192.19 ms)	170.95 (134.46 ms, 206.02 ms)	176.07 (152.64 ms, 199.03 ms)	183.38 (144.82 ms, 221.48 ms)	186.18 (139.92 ms, 222.96 ms)

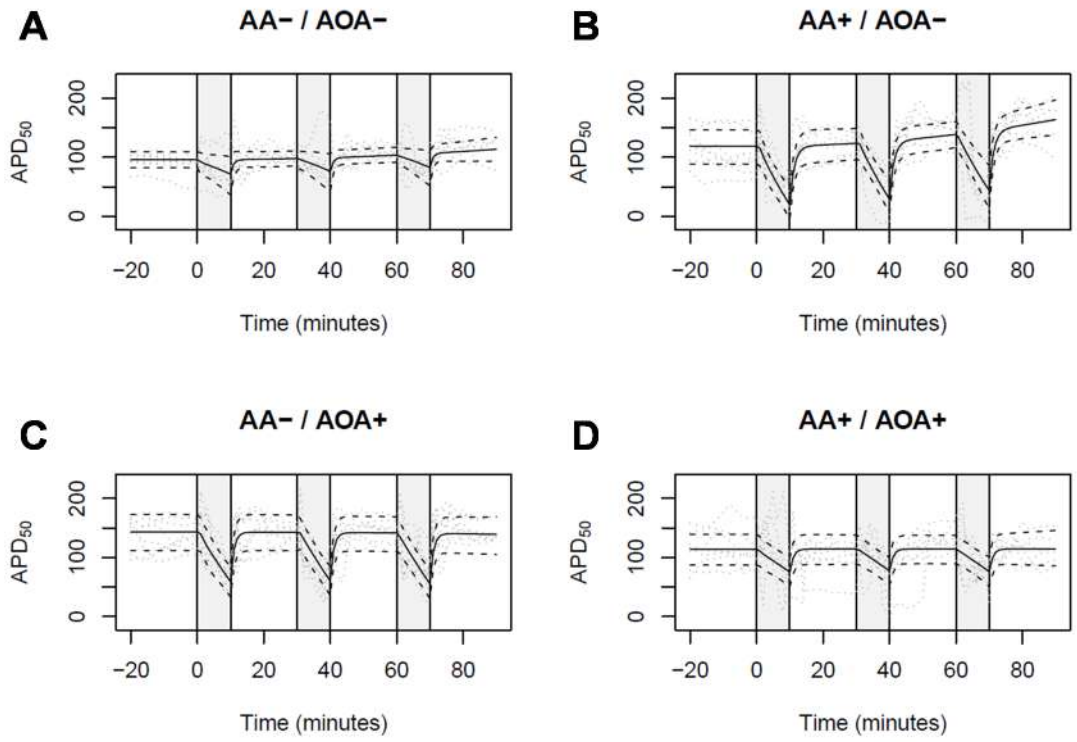

Figure 4-1. Model-fitted mean for APD_{50} (in ms) for each experimental condition. Gray bars show ischemic periods, the mean is shown in solid black, 95% CI is shown in dashed black, and raw data are shown in dashed gray lines. Of the four conditions, only the AA+/AOA- group exhibits a significantly longer APD compared to baseline measurements at the end of the experiment.

114 ms (95% CI: [87 ms, 139 ms]) (Figure 4-1D). Neither of these groups showed a significant change in APD_{50} at the end of the experiment.

APD_{70}

AA-/AOA- hearts had a baseline APD_{70} of 115 ms (95% CI: [101 ms, 129 ms]) (Figure 4-2A). Each reperfusion period resulted in a small but significant increase in APD_{70} compared to baseline. The final APD_{70} was 148 ms (95% CI: [127 ms, 168 ms]).

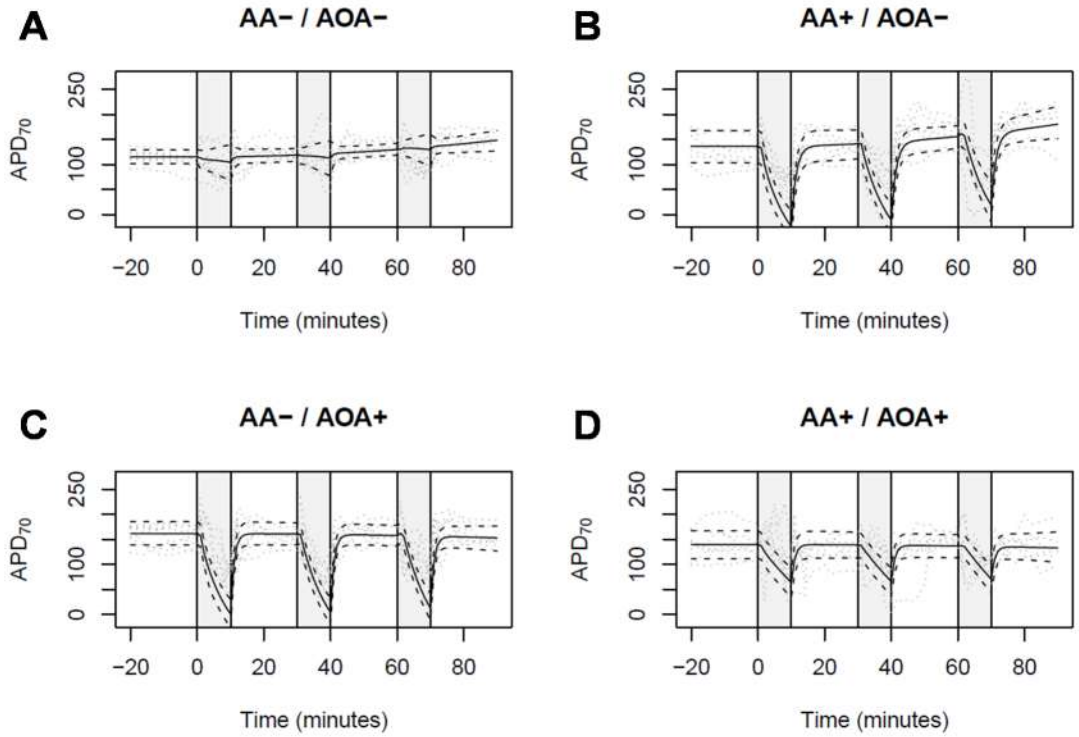

Figure 4-2. Model-fitted mean for APD_{70} (in ms) for each experimental condition. Gray bars show ischemic periods. Model-fitted mean is shown in solid black, 95% CI in dashed black, and raw data in dashed gray lines. The control group (AA-, AOA-) also exhibits slightly elevated APD at the end of the experiment, but not as high as the supplemented (AA+/AOA-) group.

AA+/AOA- hearts had a baseline APD_{70} of 136 ms (95% CI: [103 ms, 168 ms]) (Figure 4-2B). Each reperfusion period resulted in increasingly higher APD_{70} compared to baseline. The final APD_{70} was 180 ms (95% CI: [151 ms, 217 ms]).

AA-/AOA+ hearts had a baseline APD_{70} of 161 ms (95% CI: [139 ms, 185 ms]) (Figure 4-2C). The AA+/AOA+ group had a baseline APD_{70} of 140 ms (95% CI: [111 ms, 167 ms]) (Figure 4-2D). Neither of these groups showed a significant change in APD_{70} at the end of the experiment.

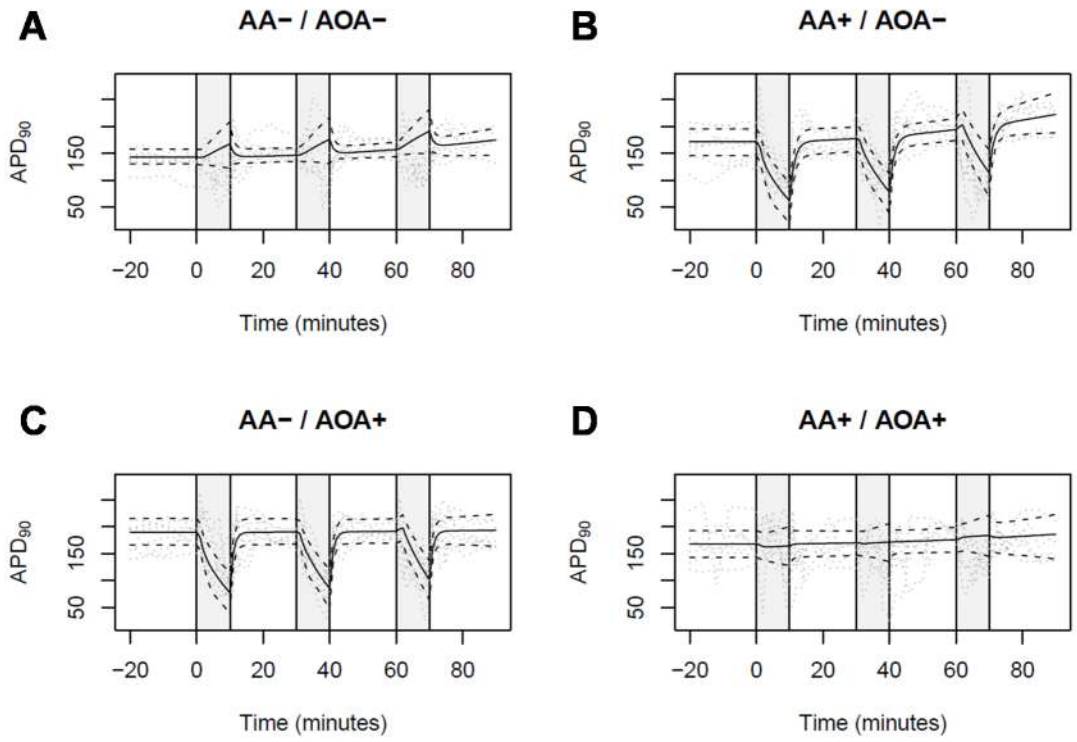

Figure 4-3. Model-fitted mean for APD_{90} (in ms) for each experimental condition. Gray bars show ischemic periods. Model-fitted mean is shown in solid black, 95% CI in dashed black, and raw data in dashed gray lines. APD_{90} results demonstrate a significant shortcoming as a measurement point, as the weak AP during ischemia can exhibit a long APD due to the sharp shape of the restitution curve and slow recovery to resting membrane potential. During the recovery periods, however, the AP shape recovers and shows that the AA+/AOA- group significantly increases APD over the course of the experiment.

APD_{90}

AA-/AOA- hearts had a baseline APD_{90} of 143 ms (95% CI: [131 ms, 158 ms]) (Figure 4-3A). Each reperfusion period resulted in a small but significant increase in APD_{90} compared to baseline. The final APD_{90} was 175 ms (95% CI: [146 ms, 197 ms]).

AA+/AOA- hearts had a baseline APD_{90} of 172 ms (95% CI: [146 ms, 196 ms]) (Figure 4-3B). Each reperfusion period resulted in increasingly higher APD_{90} compared to baseline. The final APD_{90} was 223 ms (95% CI: [188 ms, 263 ms]).

AA-/AOA+ hearts had a baseline APD_{90} of 190 ms (95% CI: [166 ms, 215 ms]) (Figure 4-3C). The AA+/AOA+ group had a baseline APD_{90} of 168 ms (95% CI: [143 ms, 193 ms]) (Figure 4-3D). Neither of these groups showed a significant change in APD_{90} at the end of the experiment.

APD Differences

We determined the difference between conditions by finding the difference between the fitted models and calculating a 95% CI for each comparison. The conditions were considered significant if the CI did not include zero. The difference between each condition at each stage of the experiment is shown in Table 4-2.

AA-/AOA- vs. AA+/AOA-

AA+/AOA- and AA-/AOA- hearts showed no significant difference in APD during the baseline period or first reperfusion. Over the course of the second reperfusion the AA+/AOA- hearts began to show significantly higher APD_{50} and APD_{90} than the AA-/AOA- hearts. By the end of the third reperfusion the AA+/AOA- hearts had significantly higher APD_{50}, APD_{70} and APD_{90} than AA-/AOA- (Figure 4-4).

Table 4-2. Differences between model-fitted groups. Bolded values indicate points where there was a significant difference between conditions.

APD_{50}		First		Second		Third	
	Baseline	Ischemia	Reperfusion	Ischemia	Reperfusion	Ischemia	Reperfusion
	0	10	30	40	60	70	90
Enriched - AOA Enriched	4.58 (-33.94, 42.70)	**-55.76 (-86.99, -19.36)**	9.50 (-26.28, 45.07)	**-47.72 (-79.17, -8.33)**	24.36 (-7.56, 56.80)	-31.78 (-70.69, 15.70)	**49.14 (8.94, 91.66)**
Enriched - Control	22.84 (-9.72, 53.69)	**-51.77 (-90.75, -4.87)**	25.86 (-4.19, 54.05)	-46.65 (-87.10, 2.49)	**34.94 (8.75, 59.78)**	-38.37 (-83.51, 16.82)	**50.07 (16.92, 87.96)**
Control - AOA Control	**-47.08 (-78.77, -13.96)**	12.28 (-32.91, 50.91)	**-44.70 (-75.48, -11.88)**	15.93 (-28.62, 54.15)	**-37.57 (-67.72, -3.66)**	27.11 (-15.40, 66.02)	-25.70 (-62.14, 14.99)
AOA Enriched - AOA Control	-28.82 (-68.05, 10.23)	16.27 (-17.07, 49.17)	-28.34 (-65.92, 9.95)	16.99 (-15.33, 48.90)	-26.99 (-63.42, 11.95)	20.52 (-12.63, 52.94)	-24.76 (-66.03, 19.55)

APD_{70}		First		Second		Third	
	Baseline	Ischemia	Reperfusion	Ischemia	Reperfusion	Ischemia	Reperfusion
	0	10	30	40	60	70	90
Enriched - AOA Enriched	-3.34 (-45.69, 37.96)	**-88.19 (-125.23, -45.18)**	2.30 (-36.07, 39.95)	**-77.01 (-113.08, -34.76)**	19.30 (-12.67, 50.88)	**-51.97 (-92.71, -2.13)**	**47.63 (5.47, 94.07)**
Enriched - Control	21.24 (-14.81, 55.50)	**-128.50 (-173.88, -77.73)**	22.43 (-10.07, 53.15)	**-123.90 (-170.18, -72.44)**	26.01 (-1.58, 51.05)	**-110.82 (-159.76, -50.97)**	31.98 (-2.44, 72.62)
Control - AOA Control	**-46.51 (-74.45, -19.97)**	**103.46 (54.67, 147.27)**	**-41.84 (-67.70, -16.97)**	**108.63 (60.78, 151.00)**	**-27.86 (-51.66, -3.57)**	**117.06 (70.46, 157.16)**	-4.54 (-36.26, 29.05)
AOA Enriched - AOA Control	-21.93 (-58.03, 12.32)	**63.15 (20.37, 101.94)**	-21.71 (-55.24, 10.42)	**61.73 (22.01, 96.56)**	-21.14 (-51.31, 8.44)	**58.21 (19.61, 92.37)**	-20.18 (-57.66, 20.98)

APD_{90}		First		Second		Third	
	Baseline	Ischemia	Reperfusion	Ischemia	Reperfusion	Ischemia	Reperfusion
	0	10	30	40	60	70	90
Enriched - AOA Enriched	3.98 (-31.59, 38.87)	**-102.20 (-148.08, -53.81)**	7.59 (-24.74, 39.41)	**-92.44 (-136.72, -44.05)**	18.42 (-12.28, 50.78)	**-69.26 (-120.44, -14.11)**	36.47 (-14.16, 96.02)
Enriched - Control	28.77 (-1.38, 55.88)	**-105.92 (-157.73, -50.72)**	**30.87 (3.09, 55.20)**	**-97.69 (-148.68, -41.71)**	**37.15 (11.86, 62.60)**	**-77.35 (-131.56, -18.17)**	**47.63 (8.17, 95.50)**
Control - AOA Control	**-46.69 (-75.44, -18.51)**	**90.33 (33.95, 142.12)**	**-43.58 (-70.81, -16.78)**	**90.76 (35.76, 140.88)**	**-34.22 (-61.29, -8.02)**	**89.62 (37.59, 137.60)**	-18.64 (-58.44, 18.65)
AOA Enriched - AOA Control	-21.91 (-57.24, 12.43)	**86.61 (35.11, 133.05)**	-20.30 (-53.55, 11.54)	**85.51 (36.72, 128.78)**	-15.49 (-47.74, 17.66)	**81.53 (34.12, 126.78)**	-7.48 (-59.86, 42.49)

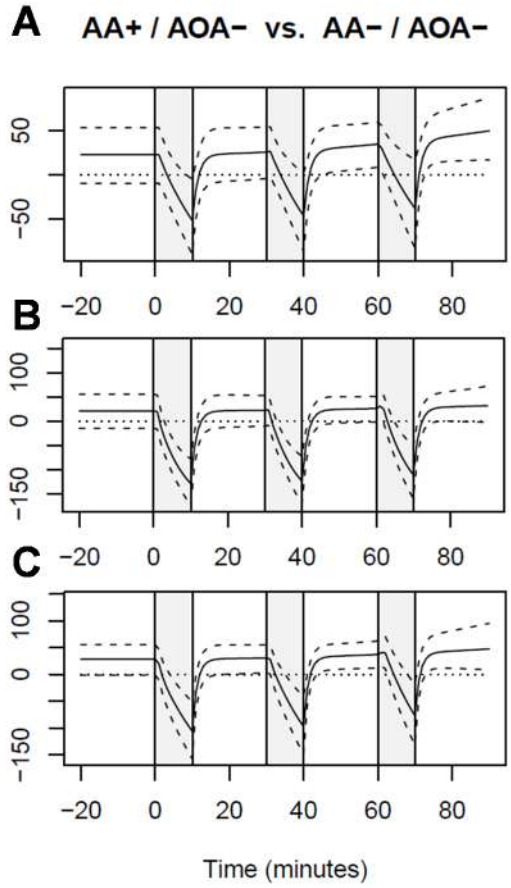

Figure 4-4. Difference between AA-/AOA- and AA+/AOA- hearts. A) APD_{50}, B) APD_{70}, C) APD_{90}. Amino acid supplementation significantly increases APD compared to controls after ischemic challenge.

AA+/AOA- vs. AA+/AOA+

AA+/AOA- and AA+/AOA+ hearts showed virtually no difference in APD during the baseline period. There were no significant differences in APD throughout the first and second reperfusion periods, but by the end of the third reperfusion the AA+/AOA- hearts had significantly higher APD_{50}, while APD_{70} and APD_{90} were not significantly higher compared to the AA+/AOA+ hearts (Figure 4-5).

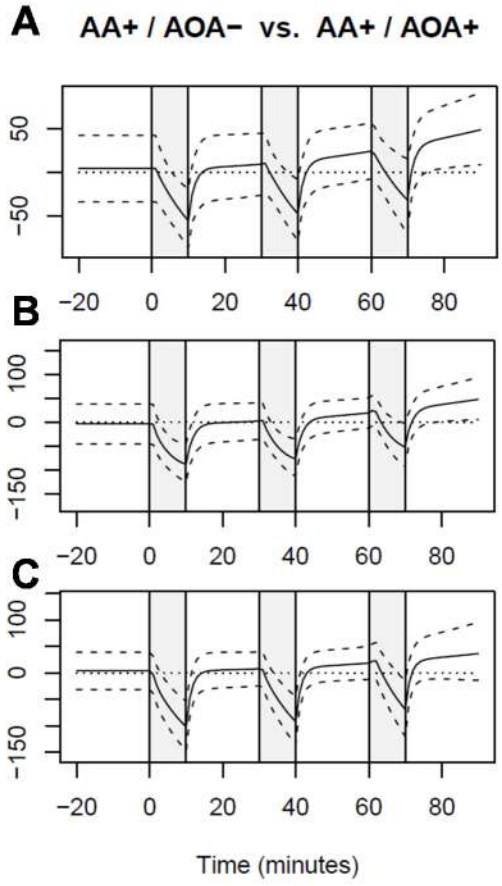

Figure 4-5. Difference between AA+/AOA- and AA+/AOA+ hearts. A) APD_{50}, B) APD_{70}, C) APD_{90}. Addition of the transaminase inhibitor AOA inhibits the effects of AA supplementation, as the AA+/AOA- group has significantly longer APD than the AA+/AOA+ group.

AA-/AOA- vs. AA-/AOA+

The AA-/AOA+ group had a significantly higher baseline APD than the AA-/AOA- group. This difference diminished over the course of the experiment, as the control group's APD increased in response to the ischemia and reperfusion

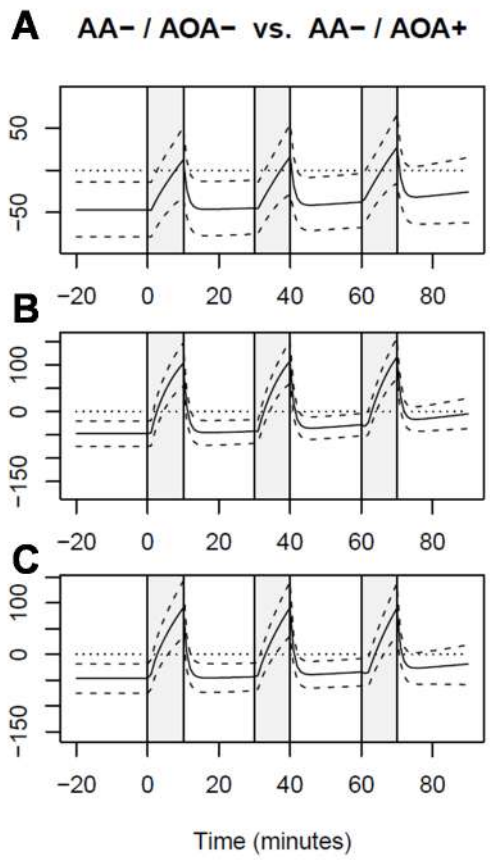

Figure 4-6. Difference between AA-/AOA- and AA-/AOA+. A) APD_{50}, B) APD_{70}, C) APD_{90}. Addition of AOA decreases AP in the normal heart, but by the end of the experiment there is no significant difference between AOA+ and AOA- hearts.

while the AA-/AOA+ did not. By the end of the experiment there was no significant difference between the two conditions at APD_{50}, APD_{70} or APD_{90} (Figure 4-6).

AA-/AOA+ vs. AA+/AOA-

There was no significant difference between the AA-/AOA+ and AA+/AOA+ groups at any time for APD_{50}, APD_{70} or APD_{90} (Figure 4-7).

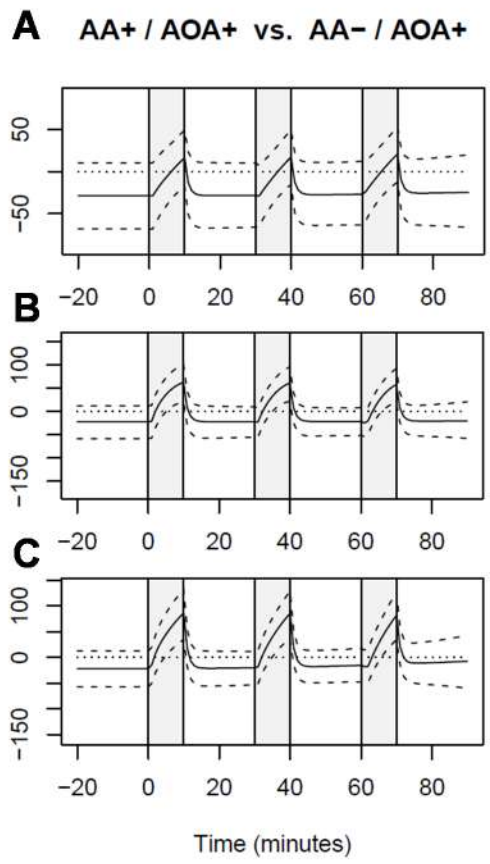

Figure 4-7. Difference between AA-/AOA+ and AA+/AOA+ hearts. A) APD_{50}, B) APD_{70}, C) APD_{90}. AOA negates the effects of amino acid supplementation as the AA+/AOA+ and AA-/AOA+ groups show no significant differences throughout the recovery periods.

Action Potential Slope

Action potential duration was measured at three points along the action potential curve: APD_{50}, APD_{70} and APD_{90}. These points measured jointly illustrate the shape of the action potential and can discriminate between strong and weak action potentials more accurately than a single point measurement (Figure 4-8). In this figure, a strong AP is shown in red with the characteristic "plateau and shoulder" followed by a rapid return to baseline. A weak AP, on the

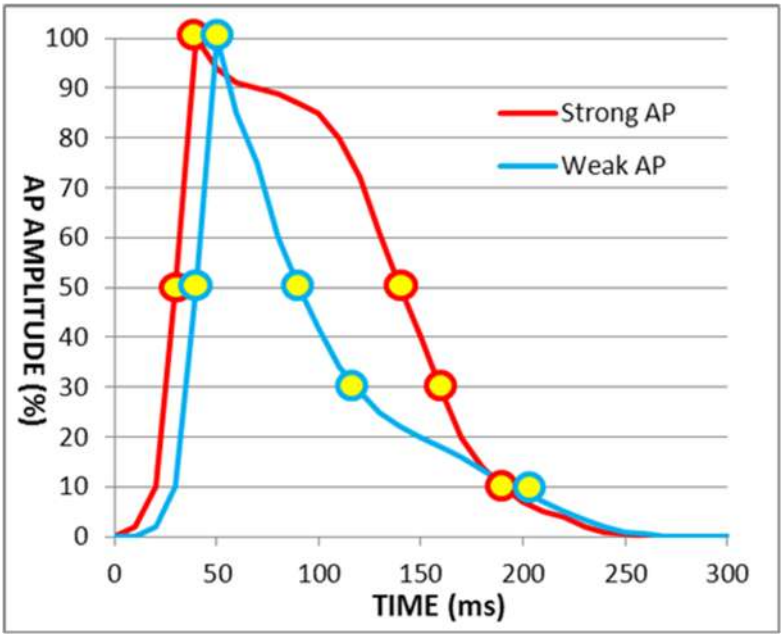

Figure 4-8. Comparison of strong and weak action potentials. Strong action potentials are characterized by a sustained membrane potential "plateau" around 90% of the maximum action potential, followed by a rapid repolarization. Weak action potentials exhibit little to no plateau and a repolarization that is initially rapid, but then slower as it nears the resting membrane potential.

other hand, will have little or no plateau and may have a fast or slow return to baseline. If a weak AP has a slow return to baseline, then a single APD_{90} measurement may not be able to distinguish between a strong or weak AP. However, if multiple points are measured on the curve then it becomes much easier to distinguish strong and weak APs.

We plotted the AP repolarization slope at the end of each recovery by applying a linear best fit through APD_{50}, APD_{70} and APD_{90} (Figure 4-9). A higher slope equates to faster membrane repolarization through robust ion transporter function, indicating healthy cellular function. The slopes for all groups experience

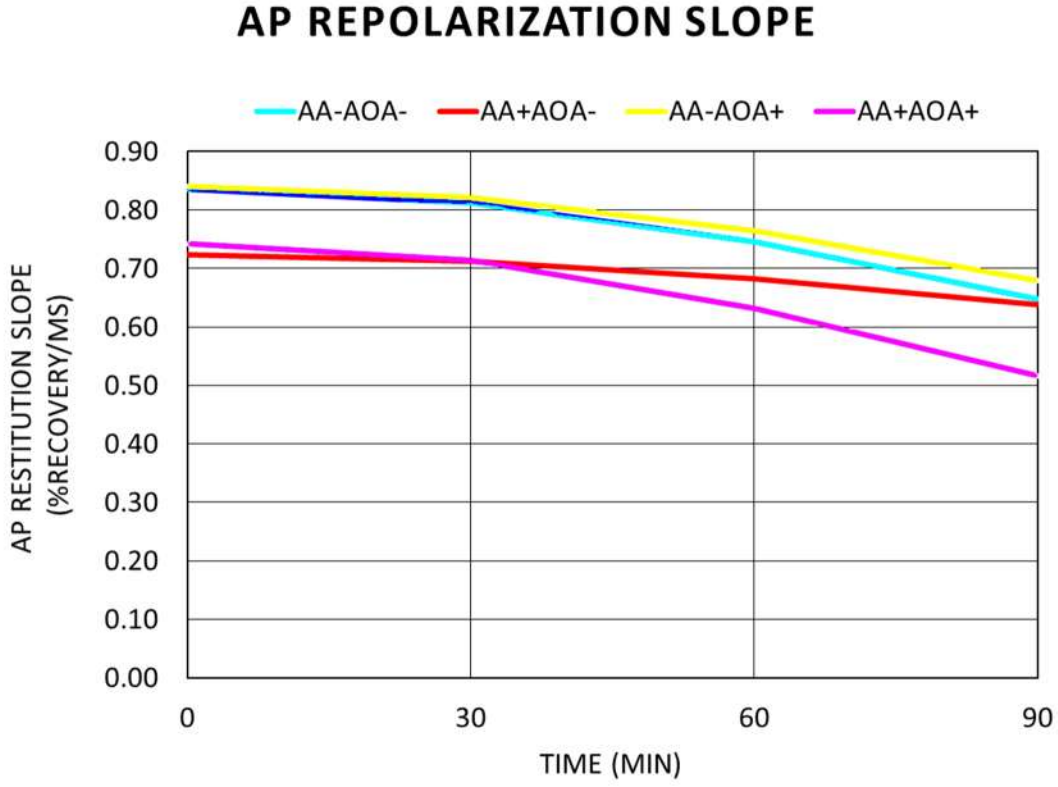

Figure 4-9. Slopes of the AP repolarization at the end of each recovery period. Over the course of the experiment there is a gradual decrease in the rate of repolarization for all hearts, but the AA+/AOA- group has a slower rate of repolarization decay than the other groups. Repolarization slope was defined as the slope of the linear regression through the APD_{50}, APD_{70} and APD_{90} for each condition.

recovery decay over the course of the experiments but the enriched (AA+/AOA-) group appears to show less recovery decay than the other groups.

By normalizing the data to highlight the change in AP slope over the course of the experiment we could more easily visualize the trends in AP slope at the end of each reperfusion stage (Figure 4-10). There is a steady trend in all of the data toward a less negative slope, but the enriched group shows markedly

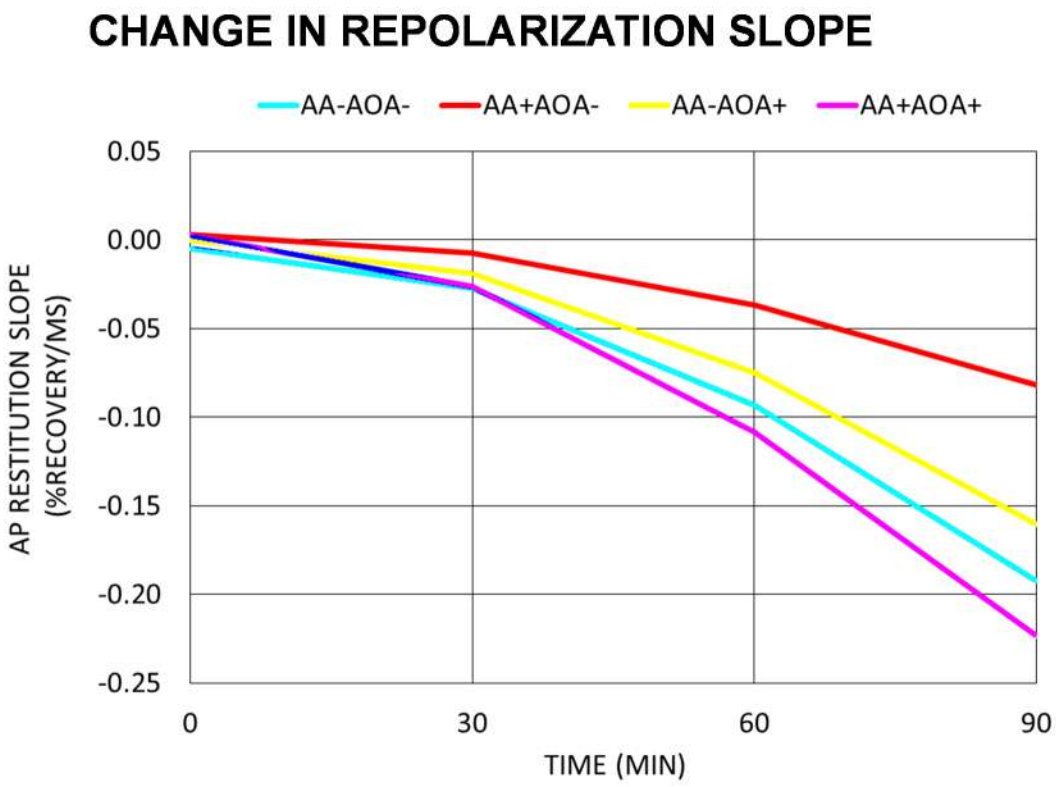

Figure 4-10. Baseline-adjusted AP repolarization slopes at the end of each recovery period. Repolarization slopes were recalculated by finding the change in the repolarization rate from the baseline period. Using this analysis, we found that the amino acid enriched group (AA+/AOA-) decayed 50% slower than the next closest group (AA-/AOA+) (.08 vs. .16 % recovery/ms).

less decay than the other groups (.08 vs .16 % recovery/ms). The significance of these values has not yet been evaluated.

Isoprostanes and Isofurans

Frozen samples of the ventricular wall were sent to Jackson Roberts's lab in two batches. The initial results indicated that the amino acid-enriched group

may have lower isoprostane and isofuran levels than the other groups, but the results were not significant (p=.09) (Figure 4-11).

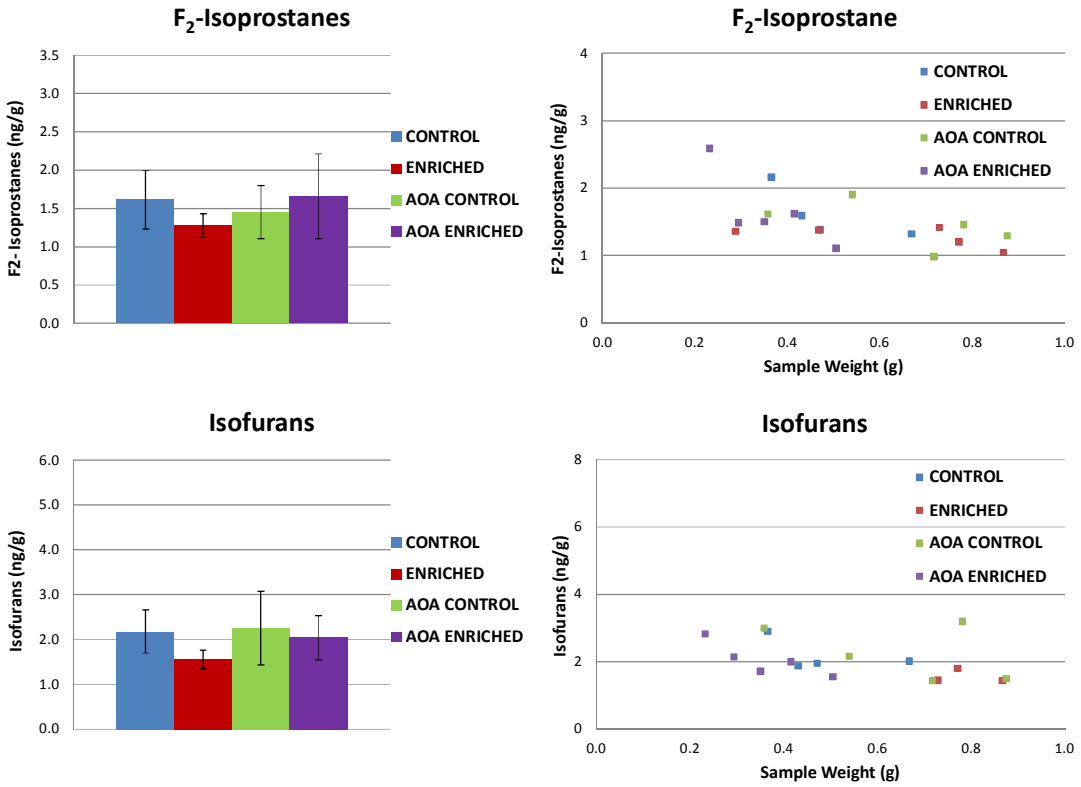

Figure 4-11. Initial results from the isoprostane analysis. This initial group of samples was small but exhibited tantalizing suggestions of cohort groupings in both isoprostane and isofuran analyses.

To increase the power of the study we analyzed additional hearts. Unfortunately, these were slightly smaller tissue samples and, according to the Roberts lab, smaller samples will have higher levels of auto-oxidation during the preparation, resulting in higher levels of isoprostanes and isofurans. We discovered this phenomenon once we plotted the sample mass in relation to the

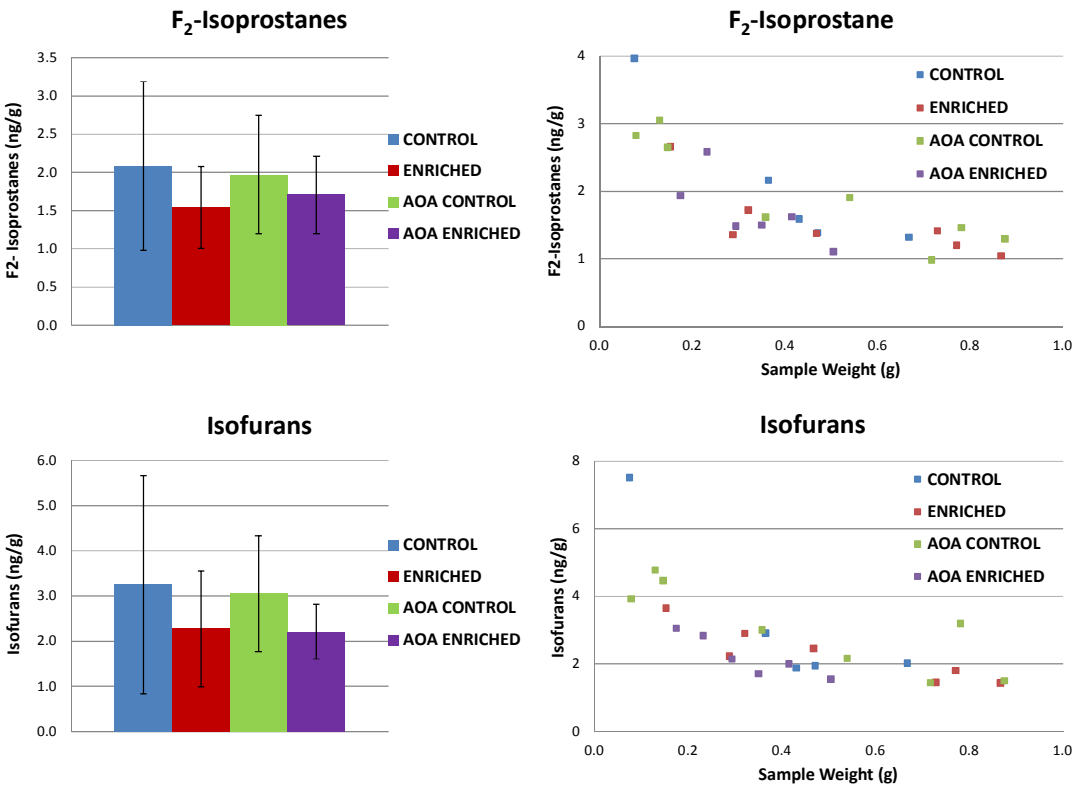

Figure 4-12. Complete isoprostane dataset. Enlarging the number of samples in the analysis eliminated any suggestion of experimental differences, revealing instead a relationship between the sample mass and the isoprostane and isofuran content. It is unclear how these are related, but the final result showed no significant difference between any of the experimental groups.

isoprostane levels (Figure 4-12). The smaller samples have significantly higher isoprostane and isofuran levels regardless of the experimental conditions. This introduced huge variability into the dataset and we could therefore draw no conclusions due to the large uncertainties in the results.

Discussion

Overall the data support the hypothesis that glutamine and glutamate supplementation increases APD, especially APD_{50}, and that this effect is mediated at least partially through the transamination of the amino acids. Based on the model-fitted data, APD_{50} increased by 38% in the AA+/AOA- compared to 18% in the AA-/AOA- and less than 1% in both the AA-/AOA+ and AA+/AOA+ groups over the course of the experiment. APD_{70} showed a less significant increase of 33% in the AA+/AOA- group, 28% increase in the AA-/AOA- and 5% decreases in the AA-/AOA+ and AA+/AOA+ groups. APD_{90} also showed a significant increase of 29% in the AA+/AOA- group compared to the 22% increase in the AA-/AOA- group, 10% increase in the AA+/AOA+ group and 2% increase in the AA-/AOA+ and group.

In the context of APD it is important to note that the shape of the AP is equally significant as (if not more significant than) a single duration measurement. For this reason it is of special note that the AA+/AOA- group appears to have a steeper AP return stroke than the other groups (though additional statistics will be required to verify this). This is a highly encouraging finding when coupled with the longer APD of the AA+/AOA- group as it indicates that the plateau and shoulder phase of the AP are longer in this group and that the cardiomyocytes are repolarizing more quickly. Since the plateau of the AP is associated with calcium signaling we can reasonably expect the enriched group to have greater contractile function than the other groups.

Since the AOA treatment results in a significant increase in baseline APD compared to the AA-/AOA- group, there is apparently an amino acid-independent effect of this treatment. This is likely due to inhibition of the malate-aspartate transaminase, though how this would lead to increased baseline APD is unclear. Further studies will be necessary to elucidate this link.

Based on this study alone we can reasonably conclude that glutamine and glutamate supplementation may significantly improve the electrical function of the heart in the context of acute and “chronically acute” myocardial ischemia and that further studies are warranted. It may be that prophylactic doses of amino acids will become *de rigueur* for those at risk of an ischemic event along with current low-dose aspirin regimens.

CHAPTER V

SUMMARY AND FUTURE DIRECTIONS

Summary

In this work we investigated, for the first time to our knowledge, the effect of amino acid administration on the electrical properties of the heart during sequential transitional periods of anoxic and ischemic challenge. Because of the variability among hearts in baseline APD, and in their response to anoxic events, conventional statistical analysis (e.g., using a series of two-sample t-tests) was not appropriate. We accounted for this variability by fitting a simple mechanistic model using nonlinear mixed-effects regression.[91] Thus we could clearly distinguish the effect of amino acid supplementation on mean APD dynamics in response to these challenges. Our findings provide valuable insights into the interplay of metabolism and electrophysiology by showing that mitigation of energy deficits has immediate effects on electrical function, which may improve survival rates during anoxic or ischemic events. These results are significant and conserved across both anoxia and ischemia, indicating that this is a reliable and effective intervention for extending APD and possibly improving cardiac function.

The results indicate that a significant portion of the cardioprotective effect is exerted through the transamination of glutamate and glutamine into α-ketoglutarate since blockage of transamination blocked the effect of amino acid supplementation. This is not to say that glutathione production is not also a factor

in the cardioprotective effect. The reduction in ROS may be significant for long-term recovery and ischemic pre-conditioning, but this did not have a significant effect over the course of our experiments.Our model system was the Langendorff perfused heart system, which is a valuable experimental approach that allows a vast amount of flexibility in measurements and interventions but with one significant difference from an *in vivo* heart: it is not a “working heart”. A working heart model has either an intraventricular balloon or an aortic hydrodynamic load that provides resistance to the contraction of the ventricle to more accurately model the behavior of the intact organ.[96, 97] The increased workload on the heart would increase the energetic demands of the heart and also allow measurement of cardiac mechanical function in addition to action potentials. We did perform a few early experiments with the contraction blocker blebbistatin but this complete elimination of contractile work made the hearts extremely resistant to ischemic and hypoxic APD shortening. These results indicate that the ATP consumption through mechanical function is a significant portion of the total metabolic load of the heart which is suported by the literature.[98] However, we felt that the increased complexity of the system would not be justified for a minimal increase in clinical significance of what we viewed as a pilot study. This may be a valuable component to add in the future to investigate the increase in energy demand and degree of challenge from an ischemic episode.

We are eager to see these studies extended to the clinical setting as the intervention they indicate has immediate applicability and is an immediate necessity. With heart disease and other metabolic disorders on the rise, we can

ill afford to neglect treatments that could reduce medical costs and patient suffering.

Future Directions

Although these studies have revealed many heretofore unknown behaviors, they have also suggested additional lines of questioning. We have established the significance of metabolism in the development of APD and the effect of amino acid supplementation, but it is apparent that we need to quantify the TCA cycle intermediates. This will conclusively establish the degree to which amino acids affect the TCA cycle and the energetic state of the cells.

It is not entirely clear how AOA interacts with the cell as a whole, since we found a significant increase in baseline APD in AA-/AOA+ hearts compared to AA-/AOA-. Further replicates may reveal that our sample size was not large enough or that the AOA does in fact have some heretofore unknown effect on the AP.

These experiments also revealed an interesting feature in the shape of the AP itself. The initial ischemic and anoxic responses both produced a significant transient increase in APD of approximately 10-20 ms that lasted for one to two minutes. This was followed by a larger APD reduction of up to 50 ms that lasted for the remainder of the ischemic or anoxic episode. These initial increases occured rapidly in the first challenge, and slightly slower and with a shorter duration and amplitude in subsequent challenges. It is as yet unknown what

gives rise to this feature but this may be a response to a novel insult that is reduced or mitigated after the first exposure.

We must also begin using our dual-camera imaging system to measure other important intermediates, especially calcium and NADH. These investigations were not included in these studies due to the additional instrumentation and, in the case of calcium imaging, additional dyes. Now that the experimental protocol is fully developed and the other detection methods are fully operational, it is appropriate to consider these imaging modalities. They will allow us to quantify the specific energetic and contractile intermediates responsible for the action potential with negligible difficulty.

There were apparent differences in APD during the anoxic and ischemic periods but the high variability in the data requires additional analysis and experimentation to determine the significance in these differences. The recovery periods exhibited clear and significant differences in the amino-acid-enriched groups in the absence of AOA. We hypothesize that the maintenance of the metabolic machinery via anaplerosis was responsible for the rapid recovery of these groups and the sustained improvements over subsequent challenges.

To identify the contributions of the TCA cycle products, we could expose the heart to ischemia and hypoxia in the presence of the electron transport inhibitors listed in Table 5-1. These interventions would fully test the aerobic respiratory pathway to determine at what step of the TCA cycle, shown in Fig.1-2, the amino acids exert their effects. Both glutamine and glutamate enter the TCA cycle as α-ketoglutarate. From this point they continue through the cycle to produce NADH, GTP and $FADH_2$. These high-energy metabolites are then used to power proton pumps in the inner mitochondrial membrane through a series of enzymes that gradually release the energy stored in the NADH and $FADH_2$. By selectively inhibiting the activity of these intermediate electron transport complexes, we can determine which high-energy metabolites are most essential for the cardioprotective effects of these amino acids.

Table 5-1. List of electron transport inhibitors and their mechanisms of action.

Chemical Agonist	**Mode of Action**	**Result**	**Expected Degree of Survival**
Rotenone	Blocks complex I	NADH Blocked	**High** – $FADH_2$ oxidation still produces significant levels of ATP
Antimycin	Blocks complex III	NADH/$FADH_2$ Blocked Early	**Low** – Early transport blockage, minimal ATP produced
Carbon monoxide	Blocks complex IV	NADH/$FADH_2$ Blocked Late	**Moderate –** Late transport blockage, significant ATP produced
Anoxia	Blocks complex IV	NADH/$FADH_2$ Blocked Late	**Moderate** – Late transport blockage, significant ATP produced
Oligomycin	Blocks the ATP synthase proton channel	No Blockage, but no ATP produced	**Very Low** – Free radical production, but no ATP produced

Rotenone specifically inhibits complex I of the ETC, the complex responsible for removing the electrons from NADH (Fig. 5-1). It does not, however, affect the oxidation of $FADH_2$ as this enters the cycle in complex III via complex II, which converts succinyl-CoA to fumarate to produce the $FADH_2$. We would predict that rotenone would increase the uptake of glutamate and glutamine, as they will still be able to provide electron donors through this mechanism, thereby maintaining the proton gradient and ATP production. It may also lead to release of aspartate and asparagine through cataplerosis, as they

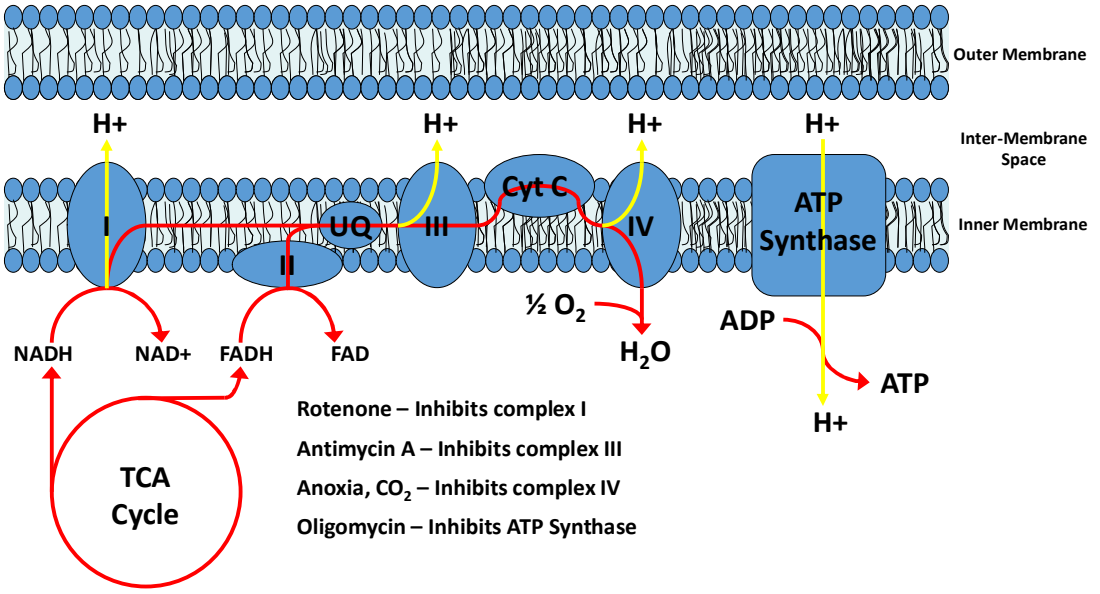

Figure 5-1. Electron transport chain (ETC) and oxidative phosphorylation. NADH and $FADH_2$ are produced through metabolism of TCA cycle intermediates. They are oxidized by complexes I and II, respectively, to generate the proton gradient across the inner mitochondrial membrane. The elevated proton concentration in the inter-membrane space is then coupled to ATP generation by ATP synthase. The final electron acceptor in the electron transport chain is oxygen. A lack of oxygen or inhibition of any of the ETC complexes will result in a reduction or abolishment of oxidative phosphorylation.

are possible products of an abundance of oxaloacetate. Since rotenone does not completely block electron transport, we would expect this to have only minor effects on APD since oxidative phosphorylation could still occur.

Blockage of complex III will likely be much more damaging than complex I blockage, since this stops both NADH and $FADH_2$ oxidation. Even complex IV inhibition still allows partial energy capture through the early steps of electron transport, and partial maintenance of proton flux. All of these inhibitors will likely dramatically reduce glutamine and glutamate uptake, as well as alanine release and cell survival. APD depression and arrhythmias would be expected to occur in most cases.

We would predict oligomycin to be the most damaging of the ETC inhibitors, as it blocks the activity of the ATPase responsible for harnessing the energy of the proton gradient. Its inhibition would allow the cell to burn metabolites and produce acidic by-products, and yet produce no energy. This intervention is expected to have a very low survival and very little metabolic activity after even short exposures.

To determine the effect of glutathione production on amino-acid-induced cardioprotection we could use buthionine sulfoximine (BSO) to selectively inhibit gamma-glutamylcysteine synthetase, an essential enzyme for the synthesis of glutathione. Blockage of this enzyme would eliminate this pathway as a possible mechanism for cardioprotection in the heart.

The glutamine used in these studies is the same L-glutamine found in high levels in many Asian diets. It may be that people with higher dietary glutamine

intake have higher levels of plasma glutamine, but we have not investigated this. According to our findings, if there are higher levels of glutamine in the blood there may be an increase in hypoxia resistance. This might make an interesting case study: dietary glutamine intake and anoxia tolerances of indigenous Everest sherpas vs. Western climbers. However, this type of study is obviously beyond the purview of our lab.

We would also need to include a down-stream analysis of cardiac effluent and post-ischemic tissues to determine the metabolic flux of the heart. By using an approach like UPLC-IM-MS we could very accurately measure the molecular composition of the proteome and metabotolome and clearly identify the pathways through which these amino acids exert their effects. Coupling this with microdialysis techniques we could also measure the uptake and release of key molecules within the interstitium of the myocardium over the course of the experiment. This approach would allow us to measure metabolites immediately around the cells before these metabolites enter the circulatory system, thereby eliminating the problems of time delay and dilution inherent in the sampling of whole heart effluent, as the metabolites do not travel through the blood vessels or across the endothelium before being detected.

It would also be valuable to quantify the activity of hypoxia-inducible factor (HIF) in ischemic and anoxic hearts. HIF is a heterodimeric protein with a constitutively-expressed β-subunit and an α-subunit that is readily ubiquitinated and degraded by prolyl hydroxylases in the presence of oxygen and α-ketoglutarate.[99-101] In the absence of oxygen, the dimers bind and activate a

significant portion of the transcriptome associated with angiogenesis, anti-oxidant production, enhanced glycolysis and reduced inflammation. While this pathway is not likely to significantly alter the outcomes of acute ischemic and anoxic challenges over the course of our experiments, it will likely have a major impact on longer term processes that would be involved in ischemic pre-conditioning in clinical settings. Hence affinity assays or targeted mass spectrometry might detect a transient increase in HIF-1α following each of the ischemic/anoxic challenges, and analysis of the transcriptome might reveal changes in gene transcription associated with modulation of HIF by hypoxia.[99, 100]

The over-arching goal of our research has been to unite the disparate fields of electrophysiology and cardiac metabolism. Existing models of cardiac electrophysiology have focused exclusively on ion flux, channels, and potentials and as a result there is very little metabolic regulation within the models.[102-107] More recent advances in the models have used TCA cycle “energy output” as a metabolic input,[108, 109] but this neglects the rich metabolic network responsible for the various forms of energy sources including NADH, $FADH_2$, ATP, creatine phosphate and even energy stores like glucose and fatty acids. Given the complex signaling and metabolic networks that regulate the heart, it would be ideal were the models to have metabolic demand, e.g., exercise, and nutrients as the inputs to the model, such that one could observe how changes in either demand or nutrients affected cardiac metabolism and electrophysiology. By coupling electrophysiological outputs like APD and AP propagation to metabolic perturbations we hope to better bridge this gap and encourage more discussions

between these “disparate” fields. Metabolic flux analysis or other approaches would allow the cardiac modeling community to begin incorporating these metabolites and processes using real data with measurable changes over time, especially if this analysis included simultaneous measurements of the electrical function of the heart. To our knowledge, experiments such as those described in this dissertation have not been carried out before and we hope that our pilot studies mark the start of a larger trend toward integration of the separate fields of cardiac physiology. These steps will, in the future, contribute to the eventual integration of all organ systems and models into all-encompassing whole organism predictive models capable of predicting disease outcomes and treatments *in silico*.

Future experiments will clearly be needed to more fully explore the exact mechanism of cardioprotection exerted by these amino acids and their effect on electrophysiology and clinical outcomes. Should these amino acids prove beneficial, we could foresee a time when at-risk patients would be prescribed glutamine supplements just like the aspirin regimens we see today. Due to the low risk and the low cost of the amino acids themselves, this could have a significant impact on morbidity and mortality with very little increase in medical costs.

Biometrics 69, 741–747
September 2013

DOI: 10.1111/biom.12066

Mechanistic Analysis of Challenge–Response Experiments

M. S. Shotwell,* K. J. Drake, V. Y. Sidorov, J. P. Wikswo

Vanderbilt University, Nashville, Tennessee 37232, U.S.A.
**email:* matt.shotwell@vanderbilt.edu

SUMMARY. We present an application of mechanistic modeling and nonlinear longitudinal regression in the context of biomedical response-to-challenge experiments, a field where these methods are underutilized. In this type of experiment, a system is studied by imposing an experimental challenge, and then observing its response. The combination of mechanistic modeling and nonlinear longitudinal regression has brought new insight, and revealed an unexpected opportunity for optimal design. Specifically, the mechanistic aspect of our approach enables the optimal design of experimental challenge characteristics (e.g., intensity, duration). This article lays some groundwork for this approach. We consider a series of experiments wherein an isolated rabbit heart is challenged with intermittent anoxia. The heart responds to the challenge onset, and recovers when the challenge ends. The mean response is modeled by a system of differential equations that describe a candidate mechanism for cardiac response to anoxia challenge. The cardiac system behaves more variably when challenged than when at rest. Hence, observations arising from this experiment exhibit complex heteroscedasticity and sharp changes in central tendency. We present evidence that an asymptotic statistical inference strategy may fail to adequately account for statistical uncertainty. Two alternative methods are critiqued qualitatively (i.e., for utility in the current context), and quantitatively using an innovative Monte-Carlo method. We conclude with a discussion of the exciting opportunities in optimal design of response-to-challenge experiments.

Key words: Bootstrap; Differential equation; Longitudinal data; Mechanistic model; Optimal experimental design.

1. Introduction

Observing the time series of response to designed physiological challenges is a powerful tool for biomedical research and diagnostics. The cardiac stress test is a well-known example. There is an emerging effort to utilize this methodology in studies of isolated tissues, and even single cells (Wikswo, Lin, and Abbas, 1995; Wikswo et al., 2006; Faley et al., 2008; Eklund et al., 2009; Enders et al., 2010; Snider et al., 2010; LeDuc, Messner, and Wikswo, 2011). This *response-to-challenge* methodology is part of a system-level approach (opposite a reductionist approach), and has become more prominent in the study of complex metabolic, signaling, and gene regulatory pathways (Garcia et al., 2011). Mechanistic mathematical models (e.g., systems of differential equations) are often used to characterize the mechanisms that underlie a biological system. The system is studied by making empirical observations on some of its parts, and then drawing inferences about the unobserved parts. This type of modeling and inference is common in epidemiology and pharmacology, for example (see Edelstein-Keshet (2005) for a comprehensive introduction), but is largely neglected in other basic sciences.

While the experimental response-to-challenge methodology has advanced, tailored statistical methods have lagged. As a result, the statistical methods employed often make unrealistic assumptions, fail to account for complexities in the data, or fail to adequately characterize (or worse, misleadingly characterize) the evidence about important scientific questions. Indeed, May (2004) highlights the use of conventional statistical methods and assumptions in highly nonlinear dynamical processes as an *abuse of mathematics in biology*. The impetus for the current work was a concern that important biological insights might be missed at the time of statistical analysis; that without sufficient care, statistical analysis might hinder rather than promote scientific discovery.

The response-to-challenge approach was implemented to study the connection between cardiac electrophysiology and metabolism using a series of measurements on isolated rabbit hearts. The cardiac tissue was perfused with either normal media or amino acid enriched media. Cardiac action potential duration (APD) was measured in a time course of intermittent metabolic challenges. In this experiment, two intermittent challenges were imposed by withholding oxygen from perfusion media (anoxia), thereby simulating the effect of acute lung injury, pulmonary embolism, asphyxia, and other respiratory conditions. The primary biological endpoint of the experiment was to draw inferences about the cardioprotective effect of amino acid enrichment under intermittent anoxia challenges.

In separate experiments (data not shown), no cardioprotective effect was evident in the absence of anoxia challenge, or when only one anoxia challenge was applied. We hypothesized that repeated anoxia would further strain the cardiac tissue, and be more likely to reveal a cardioprotective effect for amino acid enrichment.

We employed a mechanistic differential equation model for the change in cardiac APD over time, accounting for initiation and termination of the metabolic challenge events, and to parameterize the effect of amino acid enrichment. This type of mechanistic model serves the immediate goal of drawing statistical inferences about the effect of amino acid enrichment,

but is also useful in making predictions about how cardiac tissue behaves under anoxic stress. In particular, we are interested in predicting the consequence of modifying the challenge characteristics (e.g., extending the duration of anoxia) on the mean APD response. This type of prediction is useful, for example, in the design of new response-to-challenge experiments.

Complex variability, including residual autocorrelation and heteroscedasticity, is a prominent feature of the cardiac APD data. As the evidence presented below suggests, the anoxia challenge affects both mean *and* variance of the response. Because of this complexity and the small-sample nature of these data, there was concern about the use of asymptotic results (under strong parametric assumptions) for statistical inference. Indeed, Sohn and Menke (2002) reported that inference based on asymptotic results had underestimated uncertainty in a related nonlinear regression application, and recommend a bootstrap alternative.

Three distinct estimation and inference strategies were evaluated in the current context: ordinary least squares (OLS) estimation with nonparametric bootstrap inference, maximum likelihood estimation (MLE) with nonparametric bootstrap inference, and MLE with asymptotic inference. The frequent coverage of pointwise (i.e., points in time) confidence bands, and the power associated with pointwise hypothesis tests were examined using a novel Monte-Carlo method. Surprisingly, coverage was similar for the bootstrap OLS and bootstrap MLE methods. The asymptotic MLE method had lesser coverage in general, and especially less for time points within the anoxia challenge periods.

Our objective in studying alternative estimation and inference strategies was to better inform our analysis of the cardiac APD data. We make no generalized claims about the relative merits of these methods. However, we anticipate that these findings will inform the analysis of future response-to-challenge experiments. In addition, we have not attempted to demonstrate the asymptotic validity of the bootstrap procedures considered herein. While others continue to establish the validity of various bootstrap estimators in nonlinear regression (Hu and Kalbfleisch, 2000; Gonçalves and White, 2004, 2005; Chatterjee and Bose, 2005), we show that a numerical strategy can be successful in evaluating a bootstrap procedure in a narrow context.

Design, implementation, and analysis of response-to-challenge experiments is a developing, multidisciplinary endeavor to study complex biology. This manuscript considers several key statistical issues that are likely to emerge in the analysis of data resulting from response-to-challenge experiments. We conclude with a discussion of the outstanding statistical problems, including the promising opportunities associated with optimal experimental design.

2. Experimental Data

The experiments we consider were conducted on 14 isolated live rabbit hearts. Seven hearts were perfused with normal media and seven with amino acid enriched media (i.e., with the amino acids glutamine and glutamate). The experiment was designed to assess the cardioprotective effect of amino acid enrichment under anoxic challenge. The durations of cardiac action potentials (APD) were observed at 1 or 2 minute intervals for up to 72 minutes. All hearts were observed at baseline for up to 20 minutes. In two subsequent time periods, hearts were challenged with anoxia by withholding oxygen from the perfusion media. The two challenges lasted for 6 minutes each, and were separated by 20 minutes of recovery. Hence, the time series is characterized by a sequence of five adjacent time periods: baseline, first anoxia, first recovery, second anoxia, and second recovery. Figure 1 illustrates the time course of raw APD measurements on each heart.

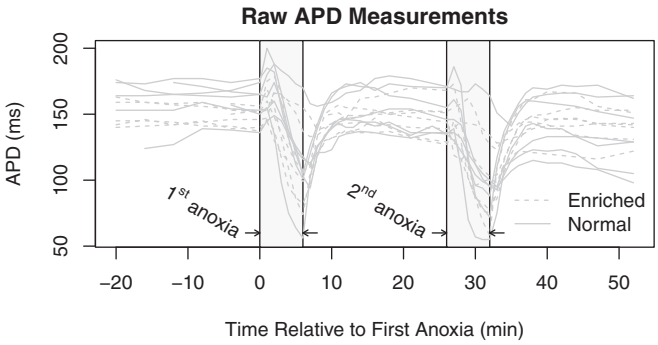

Figure 1. Raw action potential durations for 14 isolated rabbit hearts. Each heart was observed for up to 72 minutes. The vertical gray bars represent the periods of anoxia challenge.

3. Statistical Modeling Approach

We considered a nonlinear regression model of the form

$$y_{ijk} = \alpha_j + \eta(t_k, \theta_i) + \epsilon_{ijk} \tag{1}$$

where y_{ijk} is the measured APD on heart $j \in \{1, 2, \ldots, 14\}$ at time $t_k \in \{-20, -19, \ldots, 50\}$, under perfusion with media type $i \in \{E, N\}$. The intercept α_j represents the baseline APD for heart j. This varies among hearts due to innate differences and instrument recalibration. The function $\eta(t_k, \theta_i)$ gives the average change in APD from baseline until time t_k, given a fixed parameter θ_i. Finally, ϵ_{ijk} is a random error with mean zero. The intercepts were considered fixed rather than random to avoid the multiplicity of definitions for "residuals" in models that have random effects (Nobre and Singer, 2007), and more importantly, because the correlations among errors were modeled directly. The disadvantages of this approach are that (1) each α_j must be estimated and (2) no model is available for the purpose of simulating new α values. The former is not serious because there were many measurements on each heart. In the simulations described below, new α values were drawn from the empirical distribution defined by the estimated values $\{\hat{\alpha}_1, \hat{\alpha}_2, \ldots, \hat{\alpha}_{14}\}$.

Controlled anoxia challenges demonstrated a strong effect on cardiac APD. Within each anoxia period, the time course of APD was characterized by a small initial upswing, followed by a sharp decline. The recovery periods were characterized by a sharp initial upswing, followed by a period of stability. APD also exhibited a slow decay in time starting at the first exposure to anoxia and persisting throughout the experiment. This sharp, irregular response led us to develop

a piecewise differential equation model for the change in mean APD over time. We had briefly considered a restricted cubic splines (Harrell, 2006) model, but found that the cubic splines enforced a high degree of smoothness (Wegman and Wright, 1983) that failed to capture the sharp transitions between the baseline, anoxia, and recovery periods. More importantly, the splines model is not mechanistic, in the sense that predictions about APD under alternative experimental designs (i.e., different types of challenge) are not possible.

We rationalized that the heart would initially compensate for mildly anoxic conditions by contracting longer and with more force, resulting in lengthened cardiac action potentials. However, prolonged anoxia restricts oxidative metabolism and deprives cardiac tissue of the energy needed for contraction, resulting in shortened action potentials. On reintroduction of oxygenated media, oxidative metabolism is restored and APD quickly recovers to near pre-challenge levels. The heart is weakened as a result of anoxia, causing a slow decay in APD over time. We hypothesized that perfusion with amino acid enriched media would decelerate this anoxia-initiated decay in APD. These mechanisms were modeled using a system of piecewise ordinary differential equations that relate action potential duration (D), the proportion of oxygen available for oxidative metabolism (O), and a third proportion (E) that represents the unspecific cellular and metabolic resources that are necessary to sustain a cardiac action potential.

Using $X' = \frac{dX}{dt}$ to denote the derivative of X with respect to the time variable t, consider the following system of differential equations:

$$D' = \begin{cases} 0, & t \le t_{a_0}, \\ k_0(E' - O') - k_1 t, & t_{a_0} < t, \end{cases}$$

$$O' = \begin{cases} 0, & t \le t_{a_0}, \\ -l_0 O, & t_{a_0} < t \le t_{r_0}, \\ l_1(1 - O), & t_{r_0} < t \le t_{a_1}, \\ -l_0 O, & t_{a_1} < t \le t_{r_1}, \\ l_1(1 - O), & t_{r_1} < t, \end{cases} \tag{2}$$

$$E' = \begin{cases} 0, & t \le t_{a_0} + t_{\text{off}_0}, \\ -m_0 O, & t_{a_0} + t_{\text{off}_0} < t \le t_{r_0}, \\ m_1(1 - O), & t_{r_0} < t \le t_{a_1} + t_{\text{off}_1}, \\ -m_0 O, & t_{a_1} + t_{\text{off}_1} < t \le t_{r_1}, \\ m_1(1 - O), & t_{r_1} < t, \end{cases}$$

where t_{a_0} and t_{a_1} are the first and second anoxia start times, respectively, and t_{r_0} and t_{r_1} are the corresponding anoxia stop times. The expressions for O' and E' are each given in five pieces, corresponding to the five distinct experimental phases. Each anoxia is associated with an "offset;" the period of time between the start of anoxia, and the point where metabolic resources (i.e., the quantity modeled by E) begin to deplete. The lengths of the "offset" periods are denoted t_{off_0} and t_{off_1} for the transitions from baseline to the first anoxia, and from the first recovery to the second anoxia, respectively. The times t_{a_0}, t_{a_1}, t_{r_0}, and t_{r_1} are fixed aspects of the experimental design. The unknown times t_{off_0} and t_{off_1} are treated as model parameters.

The parameter k_1 represents the rate of slow decay in APD. All remaining parameters affect the behavior of APD in response to anoxia. The values of l_0 and m_0 represent the rates of oxygen and bioenergetic resource depletion during the anoxia periods, respectively, and l_1 and m_1 are the corresponding rates of replenishment during the recovery periods. All unknown model parameters were estimated simultaneously using one of the methods described below, under "Estimation and Inference Strategies."

While D measures APD in milliseconds, O and E are unitless proportions, where 1 represents full availability and 0 represents complete exhaustion. The initial (baseline) values for D, O, and E were fixed to 0, 1, and 1, respectively. This system of equations (3) yields analytical solutions for $D(t)$, $O(t)$, and $E(t)$ (see Web Appendix and Web Figure 4). For the analysis at hand, only the solution for $D(t)$ is used.

The solution for $D(t)$ given $\theta_i = \{k_0, k_{1i}, l_0, l_1, m_{0i}, m_{1i}, t_{\text{off}_0}, t_{\text{off}_1}\}$ is denoted $D_i(t_k)$, and substituted for $\eta(t_k, \theta_i)$ in Equation (1). Because the degree of anoxia was controlled, and since amino acid enrichment was thought to affect the metabolic process, only the parameters k_{1i}, m_{0i}, and m_{1i} were allowed to vary by perfusion media type (i.e., by index i). Hence, this mechanistic model permits comparisons of normal and amino acid enriched media treatments in terms of their effect on (1) the rates of depletion and replenishment of bioenergetic resources (m_{0i}, and m_{1i}) during and after an anoxic challenge, and (2) the severity of cardiac tissue weakening caused by the initial anoxic stress (k_{1i}).

4. Estimation and Inference Strategies

Accurate assessment of variability is important for inferential purposes, but also for our secondary objective: to predict the variability in cardiac responses to alternative experimental challenges (e.g., more frequent challenges, or for longer durations). The covariance structure in the cardiac APD data is complex. In order to characterize the variability in these data, three different methods for estimation and inference were considered.

In the following discussion, the terms "parametric" and "nonparametric" refer to the methods used to evaluate the sampling distribution of estimators. A method was considered parametric if the errors (i.e., ϵ_{ijk}, for all i, j, and k) were modeled as having arisen from a parametric probability distribution, *and* variability about sample estimators was evaluated under this assumption. Methods that fail to meet this criterion were considered nonparametric. The terms "parametric" and "nonparametric" are not used in regard to the mean model ($E[y_{ijk}] = \alpha_j + \eta(t_k, \theta_i)$), which is clearly parameterized.

The first method is nonparametric. The model parameters θ_i were estimated using the method of OLS. This method was selected initially to help characterize the structure of residual covariability in these data without specifying a parametric error distribution. The adjusted (BCa) percentile method (Efron, 1987; Davison and Hinkley, 1997) was used to construct 95% confidence intervals for each model parameter, and a pointwise 95% confidence band for the difference in mean APD ($D_{\text{E}}(t) - D_{\text{N}}(t)$) associated with amino acid enriched media versus normal media. A pointwise (versus simultaneous) confidence band was used in order to

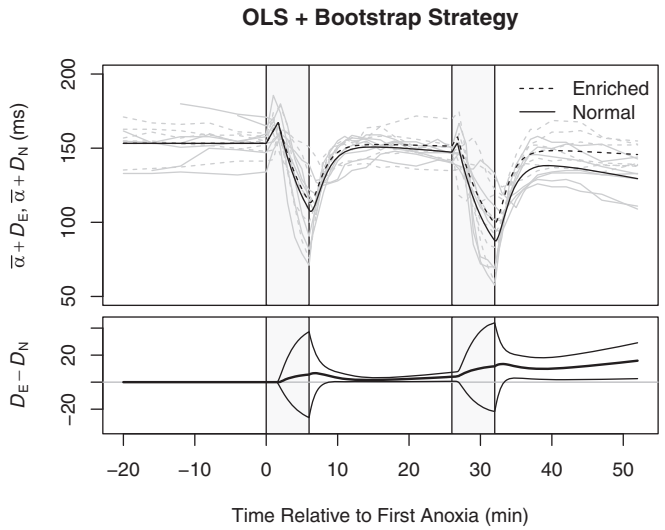

Figure 2. Ordinary least squares model fit. The top panel shows raw APD measurements (dotted lines) adjusted vertically by subtracting the corresponding $\hat{\alpha}_j - \bar{\alpha}$. Estimated mean APD curves (solid lines) are overlaid. The lower panel shows the estimated difference in mean APD for enriched versus normal media groups, with pointwise **bootstrap** 95% confidence band. In either panel, vertical gray bars delineate the periods of anoxia challenge.

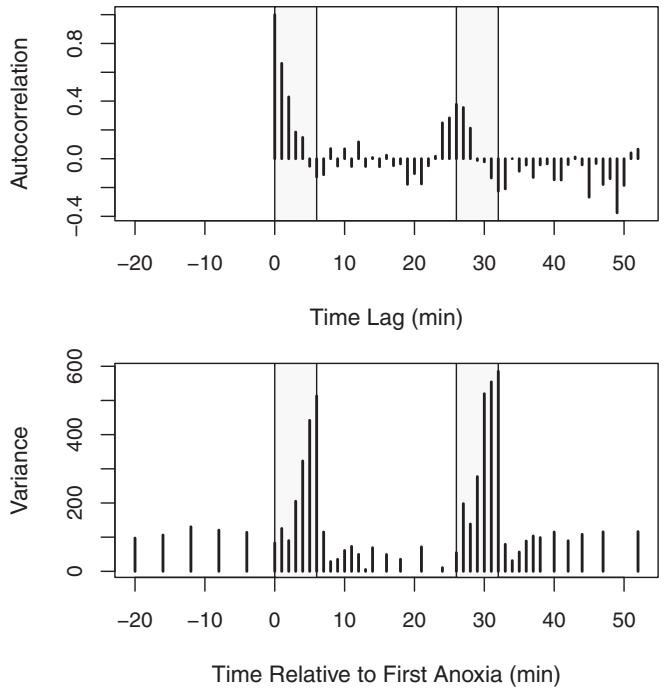

Figure 3. Residual analysis of the OLS model fit. Upper panel: estimated residual autocorrelation among time series measurements, in lags up to 52 minutes. Lower panel: estimated residual variance at each time where measurements were collected. The zero-lag time in the upper panel was aligned with time zero in the lower panel to illustrate the effect of repeat anoxia challenge on the estimated autocorrelation. However, note that autocorrelation estimates are increasingly uncertain for higher lag times. The autocorrelation for lags near 26 minutes are artifacts of the experimental design (i.e., repeat anoxia). No significant autocorrelation was observed among the MLE standardized residuals (see Web Figure 2).

assess the difference in mean APD at the final measurement (52 minutes). Hence, the reader should be cautioned against drawing simultaneous inferences about the difference in mean APD.

In order to preserve the complex covariance structure among resamples, the time series of measurements on individual hearts were considered clustered. Hence, whole clusters were resampled with replacement. This method corresponds to the *cluster bootstrap* of Field and Welsh (2007), a simplification of the *multi-stage bootstrap* for hierarchically structured data (Davison and Hinkley, 1997). Seven clusters were resampled from each of the normal and amino acid enriched media groups. Recently, Crainiceanu et al. (2012) advocate for an extension of this approach in a related application.

Ten thousand resamples were used for all bootstrap procedures. The bootstrap size was selected to ensure that the 2.5% and 97.5% bootstrap percentiles had coefficient of variation (CV) < 0.01 for each estimator. The method of Maritz and Jarrett (1978) and Efron (1979) was used to estimate the variance of bootstrap percentiles.

It is well known that the bootstrap distributions for certain types of estimators do not have the expected limiting behavior (e.g., see Example 2.15, Davison and Hinkley, 1997). We have not examined the asymptotic properties of the bootstrap methods used herein. However, empirical studies have shown the bootstrap to be reasonable for similar types of inferences (Hinkley and Schechtman, 1987; Duggins, 2010).

Figure 2 illustrates the OLS-fitted data, the estimated difference in mean APD, and the bootstrap-constructed 95% confidence band. Web Figure 5 illustrates the raw APD means plotted against OLS-fitted means, with good agreement. Web Table 1 gives estimates and 95% confidence intervals for each model parameter. In particular, the rate of slow APD decay (k_{1N} vs. k_{1E}) for the amino acid enriched media group was improved by $1.2\text{E}{-2}$ ms min^{-2} (95% CI: $2.6\text{E}{-3}$, $2.2\text{E}{-2}$), relative to the normal media group. The rates of depletion and replenishment of bioenergetic resources during anoxia and recovery periods (m_{0N}, m_{1N}, m_{0E}, m_{1E}) were not significantly different for the enriched versus normal media groups. However, bioenergetic resources began to deplete 55 seconds ($t_{\text{off}_0} - t_{\text{off}_1}$; 95% CI: 39, 72) earlier following the second onset of anoxia (t_{off_1}; 48 s, 95% CI: 31, 84) than at the first (t_{off_0}; 102 s, 95% CI: 90, 138). Although parameter estimates were slightly different under the two subsequent statistical strategies, the findings were qualitatively consistent.

Analysis of residuals from the OLS-fitted model revealed significant residual autocorrelation in APD measurements, and increasing residual variance within the anoxia challenge periods (heteroscedasticity). Figure 3 illustrates these findings.

The second estimation and inference strategy is fully parametric. Using the evidence illustrated by Figure 3, ϵ_{ijk} was modeled as having arisen from the normal distribution with

mean zero and covariance such that

$$\begin{aligned} \mathrm{var}(\epsilon_{ijk}) &= \begin{cases} \sigma^2, & \text{baseline, recovery,} \\ \sigma^2 e^{\psi(t_k - t_a)}, & \text{anoxia,} \end{cases} \\ \mathrm{cor}(\epsilon_{ijk}, \epsilon_{ijk'}) &= \rho^{|t_k - t_{k'}|}, \end{aligned} \tag{3}$$

where all other correlations are zero, and t_a is the time anoxia was initiated (i.e., $(t_k - t_a)$ measures the duration of anoxia). This *autoregressive* construction approximates the types of heteroscedasticity and autocorrelation observed in the cardiac APD data. Specifically, the variance in APD measurement is constant for baseline and recovery, but grows exponentially within the anoxia periods. Hence, this parameterizes the notion that perturbed biological systems behave more variably (or measured with less precision) than systems at rest.

Given this distributional information, a MLE was constructed for θ_i, σ^2, ψ, and ρ. Variability about the MLE was assessed using its asymptotic (i.e., normal) distribution, where the covariance was estimated by the inverse observed Fisher information, evaluated at the MLE. Monte-Carlo integration was used to construct a pointwise 95% confidence band for the difference in mean APD.

He and Severini (2010) demonstrated that the maximum likelihood estimator for parametric models with multiple unknown change-points is consistent, and has a multivariate normal limiting distribution with covariance matrix identical to the inverse Fisher information. Their result is valid under mild regularity conditions.

Web Figure 1 illustrates the MLE-fitted data, the estimated difference in mean APD, and the pointwise asymptotic 95% confidence band. Web Figure 2 shows the estimated autocorrelation and variance for the MLE standardized residuals. Because no significant autocorrelation was found among the standardized residuals, the parametric correlation structure given by expression (3) was considered sufficient. Web Table 1 gives estimates and 95% confidence intervals for each parameter in θ_i, σ^2, ψ, and ρ.

The third and final approach utilizes a likelihood-based estimator, but characterizes its variability nonparametrically: the MLE was used, but variability about the MLE was assessed using the nonparametric bootstrap, as before. The corresponding estimates and 95% confidence intervals are given in Web Table 1. Web Figure 3 illustrates the MLE-fitted data and estimated difference in mean APD as before, and the pointwise *bootstrap* 95% confidence band.

5. Simulation and Results

Because the processes that generate these experimental data are unknown, it is impossible to assess the utility of competing statistical methods under the "true" data-generating mechanism. However, if a *parametric* process is assumed (as is often done, for analytical and practical reasons), then our assessment may artificially favor a parametric strategy, and *vice versa* when empirical (nonparametric) or semiparametric processes are assumed. We refer to this as "simulation bias." Indeed, nonparametric methods are often less efficient than parametric methods when the underlying data arise from the corresponding parametric process (for a specific example, see Hollander and Wolfe, 1999, pp. 104–105).

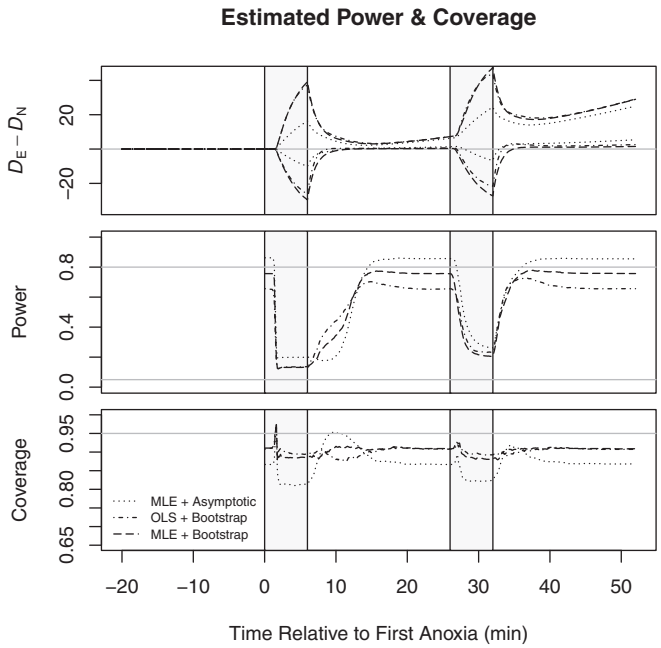

Figure 4. Estimated pointwise power and coverage for each of three strategies. The upper panel displays the pointwise 95% confidence bands for each method using the original cardiac APD data. The middle panel illustrates the estimated power associated with tests of the pointwise null hypothesis $H_0: D_E(t) - D_N(t) = 0$. The gray horizontal lines represent typical values of interest (i.e., 0.80 and 0.05). The lower panel shows the estimated coverage for pointwise 95% confidence bands. The gray horizontal line represents the nominal coverage (0.95).

To counter this potential bias, we constructed a data generating mechanism from an equal mixture (i.e., with mixing probability 0.5) of parametric and nonparametric processes. The former was taken as the MLE-fitted model in the section above. The nonparametric process was identical to the empirical distribution over clustered APD measurements, adjusted so that the mean APD at each time point matched that of the parametric process. Five hundred new data sets were simulated by this mechanism. The size of treatment groups, and frequency and spacing of measurements in time were simulated to match the original cardiac APD experiment.

For each of the estimation and inference alternatives described in the preceding section, the pointwise coverage and power associated with pointwise null hypotheses were evaluated. For each time point, the pointwise coverage was computed as the frequency of 95% confidence intervals that covered the "true," simulated difference in mean APD. The pointwise null hypothesis $H_0(t): D_E(t) - D_N(t) = 0$ was rejected when the corresponding 95% confidence interval failed to include zero. Note that this testing strategy does not ensure a fixed type I error rate. Statistical power was approximated by the rejection frequency in simulated experiments.

Figure 4 illustrates the pointwise coverage and power for 1500 simulated experiments. In particular, the asymptotic MLE method is anticonservative about the mean APD

estimate, especially within the anoxia periods. As a consequence, the coverage was lesser in these regions, and generally worse than that of the bootstrap methods. However, all methods exhibited less coverage than the nominal level.

Statistical power was generally greater for the asymptotic MLE method versus the bootstrap MLE method. In the most powerful regions (i.e., late in the recovery periods), the difference in estimated power was near 0.10.

Because the simulated difference in mean APD was nonzero at every time point beyond the baseline period, the pointwise type I error rate was not estimated. However, the simulated difference was *near* zero shortly after initiating the first anoxia challenge. Hence, the estimated power is a rough gauge of the type I error rate in this region. Figure 4 indicates that the approximate type I error rate for the asymptotic MLE method was near 0.20. Rates for the bootstrap methods were near 0.10.

It is of particular interest that the bootstrap OLS method did not have significantly better or worse estimated coverage than the bootstrap MLE method, even though the MLE explicitly accounts for the complex covariation observed in these data, and is asymptotically more efficient (i.e., under certain regularity conditions that were not verified in the present context; Casella and Berger, 2001, p. 472).

6. Discussion

There are significant costs and benefits associated with parametric methods that cannot be quantified in simple statistical measures (e.g., coverage and the rates of type I and II errors). For example, parametric error strategies often require greater human effort and other resources (e.g., model building, diagnostics, additional computer optimization, etc.). When the error structure has little inherent scientific value, the additional effort may not be worthwhile. Indeed, our analysis of the cardiac APD data revealed little benefit, in terms of coverage and power, associated with the bootstrap MLE versus bootstrap OLS methods.

In the current context, there is scientific value in characterizing the changes in variability of APD as a consequence of anoxia challenge. In particular, this is important in the design of future response-to-challenge experiments, where the number, duration, and spacing of challenges are design parameters.

To illustrate, consider a hypothetical experiment that aims to evaluate whether average APD continues to decline under anoxic conditions, or stabilizes at some time after the onset of anoxia. Let the design be identical to the cardiac APD experiment considered above, except that each anoxia challenge is prolonged by some amount t_{pro}. An alternative mechanistic model that accommodates the stabilization behavior is then proposed in order to evaluate the competing hypotheses. Both models may be fitted to preliminary data, and used to predict the behavior of APD under the hypothetical experiment.

The value of t_{pro} may then be selected to render the largest discrepancy in predictions between the two competing models (e.g., using the KL-optimality criterion of López-Fidalgo, Tomassi, and Trandafir (2007)). Because the variance in APD increases exponentially within the anoxia periods, a model and design criterion that account for this are necessary to fully evaluate the hypothetical experiment. In other words, prolonged anoxia is expected to result in continued APD decline, but the accompanying increase in variability may impose a constraint on the length of anoxia challenges. Indeed, sufficiently long exposure to anoxia results in fibrillation (and ultimately cardiac arrest), a physiological state where APD measurements are variable in the extreme.

Other types of hypotheses about the cardiac APD mechanism may benefit from the application of more conventional optimal design methods (i.e., those that aim to maximize a function of the Fisher information about one or more model parameters; see Fedorov (2010) for a recent review). The combination of mechanistic mean modeling and parametric error modeling makes this possible. Because the challenge characteristics are the crux of a response-to-challenge experiment, strategies for optimizing its design promise significant and powerful new insights in this field.

Supplementary Material

The Web Appendix, Figures, and Table referenced in Sections 3 and 4 are available with this paper at the Biometrics website on Wiley Online Library.

Acknowledgements

This work was supported in part by National Institutes of Health grant R01 HL58241-11, through the American Recovery and Reinvestment Act of 2009, U.S. Defense Threat Reduction Agency grant HDTRA-09-1-0013, and the Vanderbilt Institute for Integrative Biosystems Research and Education. We thank Allison Price for her editorial assistance, and two anonymous referees for their thoughtful comments.

References

Casella, G. and Berger, R. L. (2001). *Statistical Inference*, 2nd ed. Duxbury Press, Pacific Grove, CA, USA.

Chatterjee, S. and Bose, A. (2005). Generalized bootstrap for estimating equations. *The Annals of Statistics* **33**, 414–436.

Crainiceanu, C. M., Staicu, A.-M., Ray, S., and Punjabi, N. (2012). Bootstrap-based inference on the difference in the means of two correlated functional processes. *Statistics in Medicine* **31**, 3223–3240.

Davison, A. C. and Hinkley, D. V. (1997). *Bootstrap Methods and Their Applications*. Cambridge: Cambridge University Press. ISBN 0-521-57391-2.

Duggins, J. W. (2010). Parametric resampling methods for retrospective changepoint analysis. PhD thesis, Virginia Polytechnic Institute and State University.

Edelstein-Keshet, L. (2005). *Mathematical Models in Biology*. Society for Industrial and Applied Mathematics, Philadelphia, PA, USA.

Efron, B. (1979). Bootstrap methods: Another look at the jackknife. *Annals of Statistics* **7**, 1–26.

Efron, B. (1987). Better bootstrap confidence intervals. *Journal of the American Statistical Association* **82**, 171–185.

Eklund, S. E., Thompson, R. G., Snider, R. M., Carney, C. K., Wright, D. W., Wikswo, J. P., and Cliffel, D. E. (2009). Metabolic discrimination of select list agents by monitoring cellular responses in a multianalyte microphysiometer. *Sensors* **9**, 2117–2133.

Enders, J. R., Marasco, C. C., Kole, A., Nguyen, B., Sevugarajan, S., Seale, K. T., Wikswo, J. P., and McLean, J. A. (2010). Towards monitoring real-time cellular response using an integrated micro-fluidics matrix-assisted laser desorption ionisation/nanoelectrospray ionisation-ion mobility-mass spectrometry platform. *IET Systems Biology* **4**, 416–427.

Faley, S., Seale, K., Hughey, J., Schaffer, D. K., VanCompernolle, S., McKinney, B., Baudenbacher, F., Unutmaz, D., and Wikswo, J. P. (2008). Microfluidic platform for real-time signaling analysis of multiple single T cells in parallel. *Lab Chip* **8**, 1700–1712.

Fedorov, V. (2010). Optimal experimental design. *Wiley Interdisciplinary Reviews: Computational Statistics* **2**, 581–589.

Field, C. A. and Welsh, A. H. (2007). Bootstrapping clustered data. *Journal of the Royal Statistical Society; Series B* **69**, 369–390.

Garcia, J., Sims, K. J., Schwacke, J. H., and Del Poeta, M. (2011). Biochemical systems analysis of signaling pathways to understand fungal pathogenicity. *Methods in Molecular Biology* **734**, 173–200.

Gonçalves, S. and White, H. (2004). Maximum likelihood and the bootstrap for nonlinear dynamic models. *Journal of Econometrics* **119**, 199–219.

Gonçalves, S. and White, H. (2005). Bootstrap standard error estimates for linear regression. *Journal of the American Statistical Association* **100**, 970–979.

Harrell, Jr., F. E. (2006). *Regression Modeling Strategies*. Springer-Verlag, New York, Inc, New York, NY, USA.

He, H. and Severini, T. A. (2010). Asymptotic properties of maximum likelihood estimators in models with multiple change points. *Bernoulli* **16**, 759–779.

Hinkley, D. and Schechtman, E. (1987). Conditional bootstrap methods in the mean-shift model. *Biometrika* **74**, 85–93.

Hollander, M. and Wolfe, D. A. (1999). *Nonparametric Statistical Methods. Wiley Series in Probability and Statistics: Texts and References Section*. Wiley, New York, NY, USA.

Hu, F. and Kalbfleisch, J. D. (2000). The estimating function bootstrap. *Canadian Journal of Statistics* **28**, 449–481.

LeDuc, P. R., Messner, W. C., and Wikswo, J. P. (2011). How do control-based approaches enter into biology? *Annual Review of Biomedical Engineering* **13**, 369–396.

López-Fidalgo, J., Tomassi, C., and Trandafir, P. C. (2007). An optimal experimental design criterion for discriminating between non-normal models. *Journal of the Royal Statistical Society, Series B* **69**, 231–242.

Maritz, J. S. and Jarrett, R. G. (1978). A note on estimating the variance of the sample median. *Journal of the American Statistical Association* **73**, 194–196.

May, R. M. (2004). Uses and abuses of mathematics in biology. *Science* **303**, 790–793.

Nobre, J. and Singer, J. (2007). Residual analysis for linear mixed models. *Biometrical Journal* **49**, 863–875.

Snider, R. M., McKenzie, J. R., Kraft, L., Kozlov, E., Wikswo, J. P., and Cliffel, D. E. (2010). The effects of cholera toxin on cellular energy metabolism. *Toxins* **2**, 632–648.

Sohn, R. A. and Menke, W. (2002). Application of maximum likelihood and bootstrap methods to nonlinear curve-fit problems in geochemistry. *Geochemistry Geophysics Geosystems* **3**, 1525–2027.

Wegman, E. J. and Wright, I. W. (1983). Splines in statistics. *Journal of the American Statistical Association* **78**, 351–365.

Wikswo, J. P., Lin, S. F., and Abbas, R. A. (1995). Virtual electrodes in cardiac tissue: A common mechanism for anodal and cathodal stimulation. *Biophysical Journal* **69**, 2195–2210.

Wikswo, J. P., Prokop, A., Baudenbacher, F., Cliffel, D., Csukas, B., and Velkovsky, M. (2006). Engineering challenges of BioNEMS: The integration of microfluidics, micro- and nanodevices, models and external control for systems biology. *IEE Proceedings—Nanobiotechnology* **153**, 81–101.

Received October 2012. Revised March 2013.
Accepted April 2013.

Web-based Supplementary Materials for "Mechanistic Analysis of Challenge-Response Experiments"

M. S. Shotwell, K. J. Drake, V. Y. Sidorov, and J. P. Wikswo
Vanderbilt University, Nashville, TN 37232, USA

June 17, 2013

Web Appendices, Tables, and Figures

The differential equations listed in manuscript equation (2) yield analytical solutions for $D(t)$, $E(t)$, and $O(t)$. The starting values (i.e., for times $t \leq t_{a_0}$) for $D(t)$, $O(t)$, and $E(t)$ are 0, 1, and 1, respectively. Web Figure 4 illustrates the solution for $D(t)$, the anoxia start times (t_{a_0} and t_{a_1}), anoxia end times (t_{r_0} and t_{r_1}), and the offset lengths (t_{off_0} and t_{off_1}). The solutions are as follows:

$$D(t) = \begin{cases} 0 & t \leq t_{a_0} \\ k_0(E(t) - O(t)) - \frac{k_1}{2}(t - t_{a_0})^2 & t_{a_0} < t \end{cases}$$

$$O(t) = \begin{cases} 1 & t \leq t_{a_0} \\ O(t_{a_0})e^{-l_0(t-t_{a_0})} & t_{a_0} < t \leq t_{r_0} \\ 1 - (1 - O(t_{r_0}))e^{-l_1(t-t_{r_0})} & t_{r_0} < t \leq t_{a_1} \\ O(t_{a_1})e^{-l_0(t-t_{a_1})} & t_{a_1} < t \leq t_{r_1} \\ 1 - (1 - O(t_{r_1}))e^{-l_1(t-t_{r_1})} & t_{r_1} < t \end{cases} \tag{1}$$

$$E(t) = \begin{cases} 1 & t \leq t_{a_0} + t_{\text{off}_0} \\ O(t_{a_0} + t_{\text{off}_0})e^{-m_0(t-t_{a_0}-t_{\text{off}_0})} & t_{a_0} + t_{\text{off}_0} < t \leq t_{r_0} \\ 1 - (1 - E(t_{r_0}))e^{-m_1(t-t_{r_0})} & t_{r_0} < t \leq t_{a_1} + t_{\text{off}_1} \\ O(t_{a_1} + t_{\text{off}_1})e^{-m_0(t-t_{a_1}-t_{\text{off}_1})} & t_{a_1} + t_{\text{off}_1} < t \leq t_{r_1} \\ 1 - (1 - E(t_{r_1}))e^{-m_1(t-t_{r_1})} & t_{r_1} < t \end{cases} .$$

Web Table 1: Estimates and 95% confidence intervals for each model parameter, using each statistical inference mechanism (Bootstrap OLS, Bootstrap MLE, and Asymptotic MLE). For the parameters that varied by perfusion media type (k_1, m_0, m_1), and the offset lengths, an estimate and confidence interval are given for their difference. Estimates were computed using APD measured in milliseconds, observation time measured in minutes, and oxygen and metabolic resources measured in arbitrary units. Hence, the unit of measurement for each estimate is a derivative of milliseconds, minutes, units of oxygen, or units of metabolic resource. For example, k_1 is measured in milliseconds per minute per minute. However, these estimates were converted to SI units (*e.g.*, $\mathrm{ms} \cdot \mathrm{s}^{-2}$) for presentation within the manuscript body.

Parameter	Bootstrap OLS	Bootstrap MLE	Asymptotic MLE
k_0	1.8E+2 (1.0E+2, 3.0E+2)	2.4E+2 (1.3E+2, 5.8E+2)	2.3E+2 (7.8E+1, 3.8E+2)
k_{1N}	1.7E−2 (1.0E−2, 2.7E−2)	1.8E−2 (1.0E−2, 2.8E−2)	1.8E−2 (1.3E−2, 2.3E−2)
k_{1E}	5.8E−3 (5.3E−4, 1.2E−2)	7.1E−3 (2.0E−3, 1.3E−2)	7.2E−3 (2.1E−3, 1.2E−2)
$k_{1N} - k_{1E}$	1.2E−2 (2.6E−3, 2.2E−2)	1.1E−2 (1.3E−3, 2.2E−2)	1.1E−2 (3.9E−3, 1.8E−2)
l_0	4.8E−2 (2.9E−2, 6.7E−2)	3.6E−2 (1.8E−2, 5.7E−2)	3.5E−2 (1.1E−2, 5.9E−2)
l_1	1.6E+0 (1.0E+0, 2.7E+0)	1.8E+0 (9.9E−1, 3.8E+0)	1.5E+0 (9.5E−1, 2.0E+0)
m_{0N}	1.7E−1 (7.5E−2, 3.0E−1)	1.2E−1 (4.5E−2, 2.7E−1)	1.1E−1 (2.6E−2, 1.9E−1)
m_{0E}	1.5E−1 (7.6E−2, 2.4E−1)	1.1E−1 (3.0E−2, 1.8E−1)	1.0E−1 (2.6E−2, 1.7E−1)
$m_{0N} - m_{0E}$	1.9E−2 (−6.7E−2, 1.5E−1)	1.1E−2 (−5.2E−2, 1.6E−1)	7.4E−3 (−1.0E−2, 2.5E−2)
m_{1N}	5.8E−1 (3.9E−1, 7.4E−1)	5.8E−1 (4.1E−1, 7.4E−1)	5.9E−1 (4.9E−1, 7.0E−1)
m_{1E}	6.5E−1 (5.6E−1, 8.0E−1)	6.2E−1 (5.1E−1, 7.6E−1)	6.3E−1 (5.2E−1, 7.4E−1)
$m_{1E} - m_{1N}$	7.6E−2 (−2.9E−2, 2.2E−1)	4.2E−2 (−6.4E−2, 1.8E−1)	3.5E−2 (−6.2E−2, 1.3E−1)
t_{off_0}	1.7E+0 (1.5E+0, 2.3E+0)	1.7E+0 (1.4E+0, 2.0E+0)	1.6E+0 (1.4E+0, 1.8E+0)
t_{off_1}	8.0E−1 (5.2E−1, 1.4E+0)	7.8E−1 (3.0E−1, 1.4E+0)	7.4E−1 (5.5E−1, 9.2E−1)
$t_{\mathrm{off}_0} - t_{\mathrm{off}_1}$	9.2E−1 (6.5E−1, 1.2E+0)	8.8E−1 (3.3E−1, 1.5E+0)	9.1E−1 (6.9E−1, 1.1E+0)
ρ	—	8.1E−1 (7.2E−1, 8.8E−1)	8.1E−1 (7.7E−1, 8.6E−1)
ψ	—	1.5E−1 (9.6E−2, 1.9E−1)	1.5E−1 (1.2E−1, 1.7E−1)
σ	—	8.7E+0 (8.0E+0, 1.1E+1)	9.2E+0 (8.2E+0, 1.0E+1)

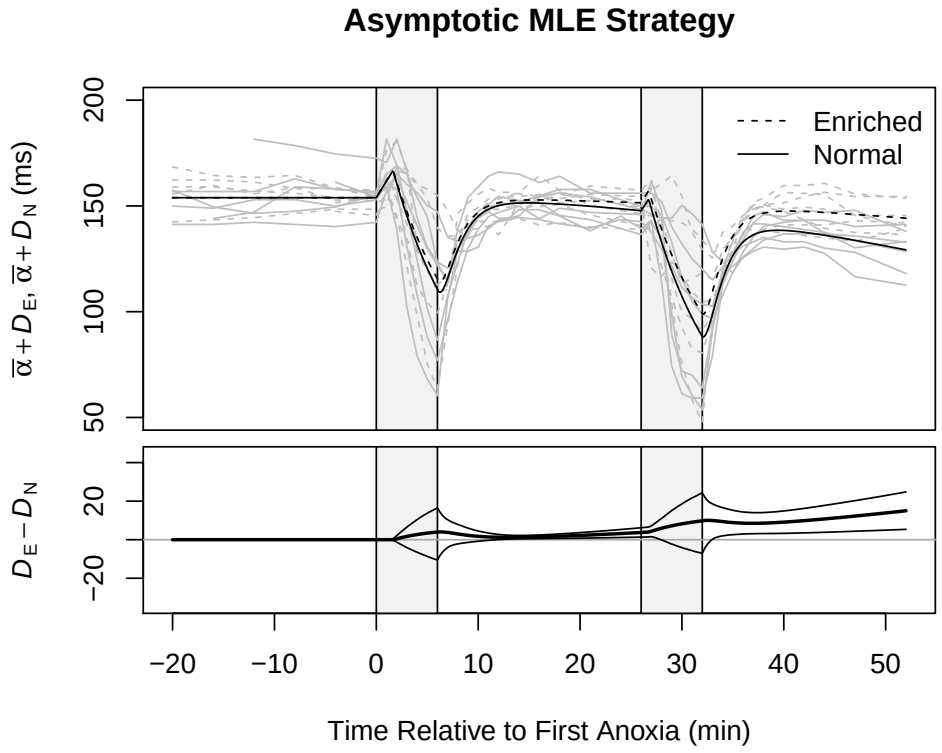

Web Figure 1: Maximum likelihood model fit. The top panel shows raw APD measurements (dotted lines) adjusted vertically by subtracting the corresponding $\hat{\alpha}_j$. Estimated mean APD curves (solid lines) are overlaid. The lower panel shows the estimated difference in mean APD curves for enriched versus normal media groups, with pointwise **asymptotic** 95% confidence band. In either panel, vertical gray bars delineate the periods of anoxia challenge.

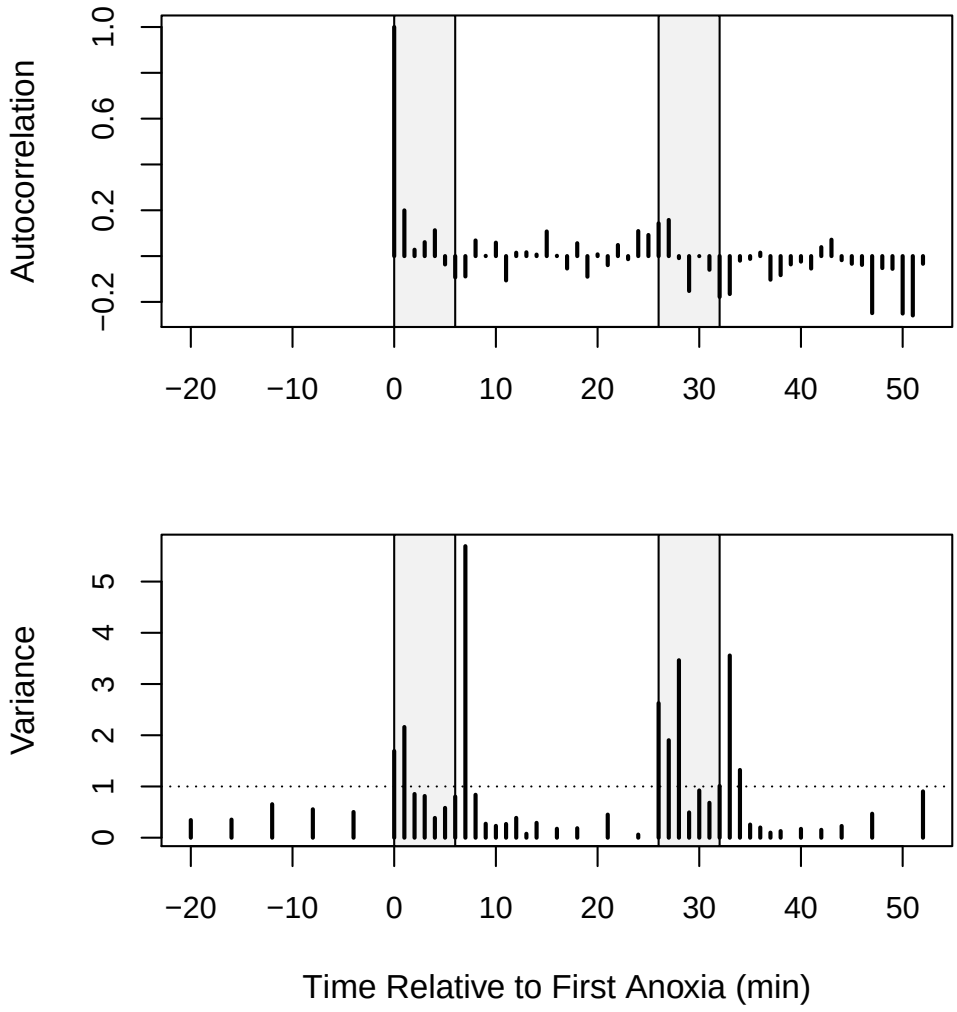

Web Figure 2: Standardized residual analysis of the MLE model fit. Upper panel: estimated residual autocorrelation among time series measurements, in lags up to 52 minutes. Lower panel: estimated residual variance at each time where measurements were collected. The zero-lag time in the upper panel was aligned with time zero in the lower panel to illustrate the effect of repeat anoxia challenge on the estimated autocorrelation. However, note that autocorrelation estimates are increasingly uncertain for higher lag times.

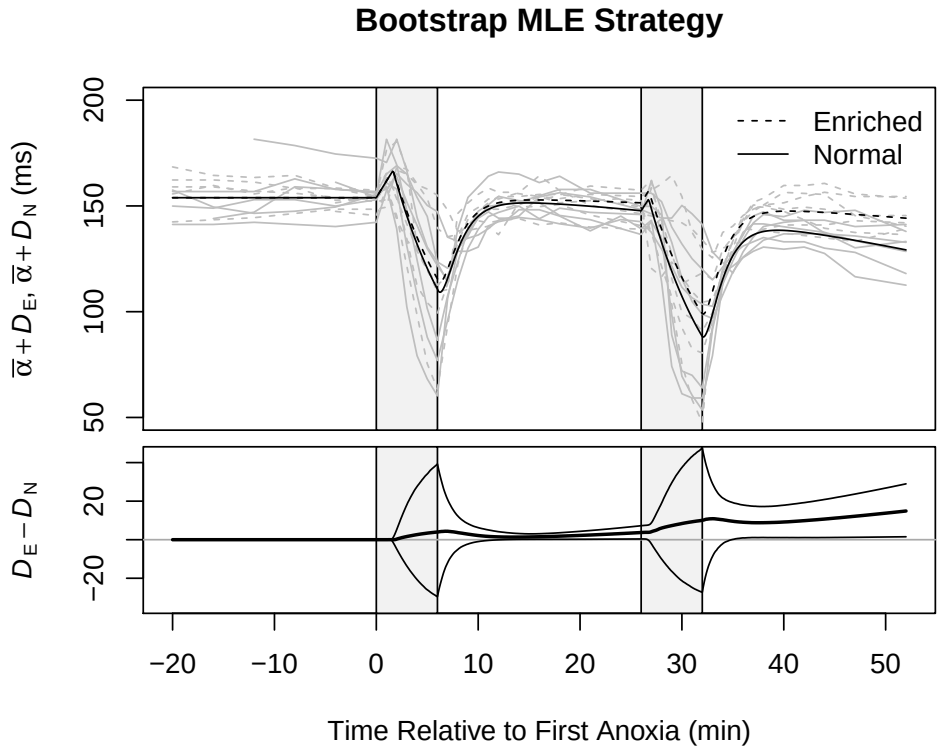

Web Figure 3: Maximum likelihood model fit. The top panel shows raw APD measurements (dotted lines) adjusted vertically by subtracting the corresponding $\hat{\alpha}_j$. Estimated mean APD curves (solid lines) are overlaid. The lower panel shows the estimated difference in mean APD curves for enriched versus normal media groups, with pointwise **bootstrap** 95% confidence band. In either panel, vertical gray bars delineate the periods of anoxia challenge.

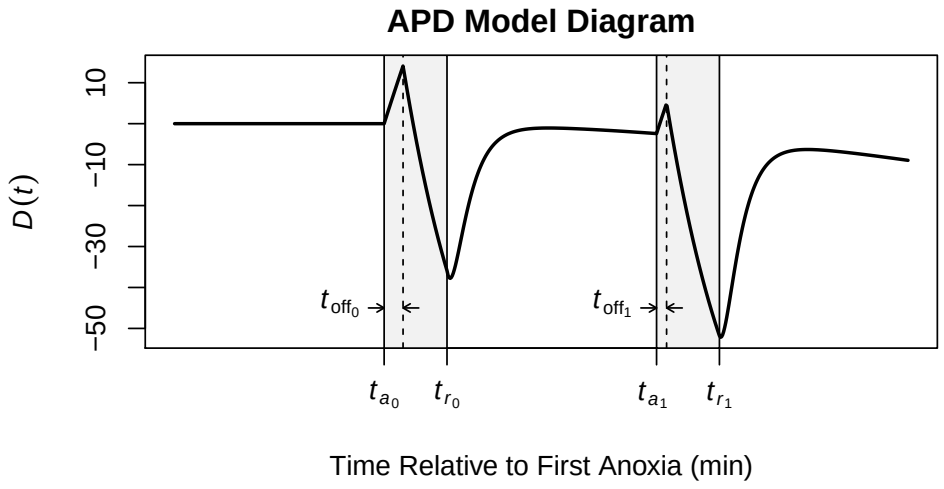

Web Figure 4: Diagram of the solution for $D(t)$. Gray regions represent the two periods of anoxia challenge.

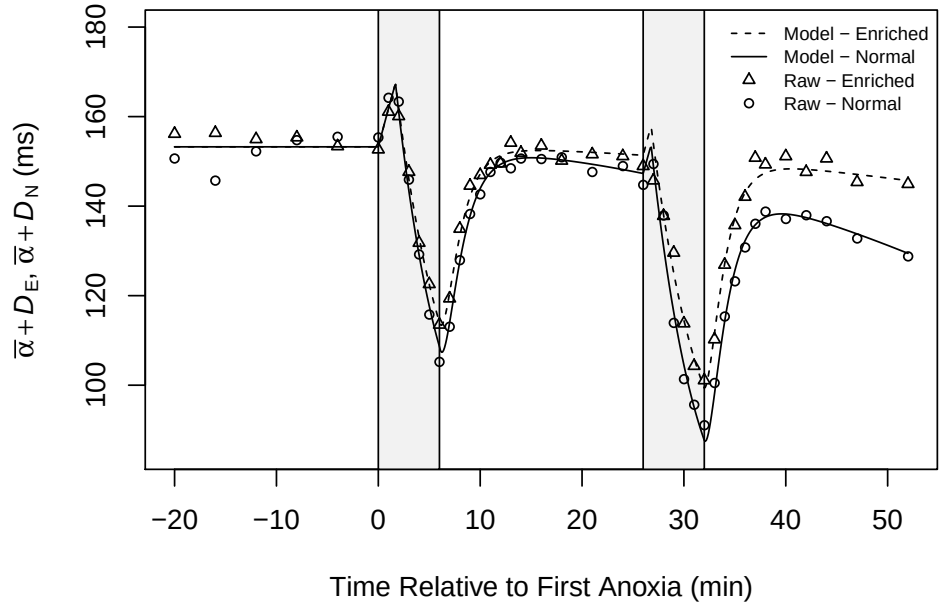

Web Figure 5: Raw APD means plotted against OLS fitted means. Raw APD means are adjusted adjusted vertically by subtracting the corresponding $\hat{\alpha}_j$ from each raw APD measurement. Gray regions represent the two periods of anoxia challenge.

REFERENCES

(1) Drake KJ, Sidorov VY, McGuinness OP, Wasserman DH, Wikswo JP. Amino acids as metabolic substrates during cardiac ischemia. *Exp Biol Med* 2012;237(12):1369-78.

(2) Taegtmeyer H. Energy-Metabolism of the Heart - from Basic Concepts to Clinical-Applications. *Current Problems in Cardiology* 1994;19(2):61-113.

(3) McDonald TF, Macleod DP. Metabolism and Electrical-Activity of Anoxic Ventricular Muscle. *J Physiol Lond* 1973;229(3):559-82.

(4) Nishimura M, Tanaka H, Homma N, Matsuzawa T, Watanabe Y. Ionic mechanisms of the depression of automaticity and conduction in the rabbit atrioventricular node caused by hypoxia or metabolic inhibition and protective action of glucose and valine. *The American Journal of Cardiology* 1989 December 5;64(20):J24-J28.

(5) Morena H, Janse MJ, Fiolet JWT, Krieger WJG, Crijns H, Durrer D. Comparison of the Effects of Regional Ischemia, Hypoxia, Hyperkalemia, and Acidosis on Intracellular and Extracellular Potentials and Metabolism in the Isolated Porcine Heart. *Circ Res* 1980;46(5):634-46.

(6) Liedtke AJ. Alterations of Carbohydrate and Lipid-Metabolism in the Acutely Ischemic Heart. *Prog Cardiovas Dis* 1981;23(5):321-36.

(7) Weiss JN, Lamp ST. Glycolysis Preferentially Inhibits Atp-Sensitive K+ Channels in Isolated Guinea-Pig Cardiac Myocytes. *Science* 1987;238(4823):67-9.

(8) Elliott AC, Smith GL, Allen DG. Simultaneous measurements of action potential duration and intracellular ATP in isolated ferret hearts exposed to cyanide. *Circ Res* 1989 March 1;64(3):583-91.

(9) Bing RJ, Siegel A, Ungar I, Gilbert M. Metabolism of the human heart II. Studies on fat, ketone and amino acid metabolism. *Am J Med* 1954;16:504-15.

(10) Bing RJ. Cardiac Metabolism. *Physiol Rev* 1965 April 1;45(2):171-213.

(11) Kodde IF, van der Stok J, Smolenski RT, de Jong JW. Metabolic and genetic regulation of cardiac energy substrate preference. *Comp Biochem Phys A-Mol Int* 2007 January;146(1):26-39.

(12) Rennie MJ, Bowtell JL, Bruce M, Khogali SEO. Interaction between glutamine availability and metabolism of glycogen, tricarboxylic acid cycle intermediates and glutathione. *J Nutr* 2001;131(9):2488S-90S.

(13) Sambandam N, Lopaschuk GD, Brownsey RW, Allard MF. Energy metabolism in the hypertrophied heart. *Heart Fail Rev* 2002 April;7(2):161-73.

(14) Taegtmeyer H, Goodwin GW, Doenst T, Frazier OH. Substrate Metabolism as a Determinant for Postischemic Functional Recovery of the Heart. *The American Journal of Cardiology* 1997 August 4;80(3, Supplement 1):3A-10A.

(15) Sorokina N, O'Donnell JM, McKinney RD et al. Recruitment of Compensatory Pathways to Sustain Oxidative Flux With Reduced Carnitine Palmitoyltransferase I Activity Characterizes Inefficiency in Energy Metabolism in Hypertrophied Hearts. *Circulation* 2007 April 17;115(15):2033-41.

(16) Huang Y, Zhou M, Sun H, Wang Y. Branched-chain amino acid metabolism in heart disease: an epiphenomenon or a real culprit? *Cardiovasc Res* 2011;90(2):220-3.

(17) Taetrneyer H, Harinstein ME, Gheorghiade M. More than bricks and mortar: Comments on protein and amino acid metabolism in the heart. *Am J Cardiol* 2008;101, Supp. S(11A):3E-7E.

(18) Wischmeyer PE, Jayakar D, Williams U et al. Single dose of glutamine enhances myocardial tissue metabolism, glutathione content, and improves myocardial function after ischemia-reperfusion injury. *JPEN* 2003 November 1;27(6):396-403.

(19) Bolotin G, Raman J, Williams U, Bacha E, Kocherginsky M, Jeevanandam V. Glutamine Improves Myocardial Function Following Ischemia-Reperfusion Injury. *Asian Cardiovasc Thorac Ann* 2007 December 1;15(6):463-7.

(20) Støttrup NB, Kristiansen SB, Løfgren Bo et al. L-Glutamate And Glutamine Improve Haemodynamic Function And Restore Myocardial Glycogen Content During Postischaemic Reperfusion: A Radioactive Tracer Study In The Rat Isolated Heart. *Clin Exp Pharmacol P* 2006;33(11):1099-103.

(21) Liu J, Marchase RB, Chatham JC. Glutamine-induced protection of isolated rat heart from ischemia/reperfusion injury is mediated via the hexosamine biosynthesis pathway and increased protein O-GlcNAc levels. *J Mol Cell Cardiol* 2007 January;42(1):177-85.

(22) Mudge GH, Mills RM, Taegtmeyer H, Gorlin R, Lesch M. Alterations of Myocardial Amino-Acid Metabolism in Chronic Ischemic Heart-Disease. *J Clin Invest* 1976;58(5):1185-92.

(23) Schwartz RG, Barrett EJ, Francis CK, Jacob R, Zaret BL. Regulation of Myocardial Amino-Acid Balance in the Conscious Dog. *J Clin Invest* 1985;75(4):1204-11.

(24) Taegtmeyer H, Peterson MB, Ragavan VV, Ferguson AG, Lesch M. De novo alanine synthesis in isolated oxygen-deprived rabbit myocardium. *J Biol Chem* 1977 July 25;252(14):5010-8.

(25) Peuhkurinen KJ, Takala TES, Nuutinen EM, Hassinen IE. Tricarboxylic-Acid Cycle Metabolites During Ischemia in Isolated Perfused Rat-Heart. *Am J Physiol* 1983;244(2):H281-H288.

(26) Williams IH, Sugden PH, Morgan HE. Use of aromatic amino acids as monitors of protein turnover. *Am J Physiol Endocrinol Metab* 1981 June 1;240(6):E677-E681.

(27) Morgan HE, Earl DCN, Broadus A, Wolpert EB, Giger KE, Jefferson LS. Regulation of Protein Synthesis in Heart Muscle. I. Effect of amino acid levels on protein synthesis. *J Biol Chem* 1971 April 10;246(7):2152-62.

(28) Lomivorotov VV, Efremov SM, Shmirev VA, Ponomarev DN, Lomivorotov VN, Karaskov AM. Glutamine Is Cardioprotective in Patients with Ischemic Heart Disease following Cardiopulmonary Bypass. *Heart Surgery Forum* 2011;14(6):E384-E388.

(29) Cohen DM, Guthrie PH, Gao XL, Sakai R, Taegtmeyer H. Glutamine cycling in isolated working rat heart. *Am J Physiol -Endoc M* 2003;285(6):E1312-E1316.

(30) Julia P, Young HH, Buckberg GD, Kofsky ER, Bugyi HI. Studies of myocardial protection in the immature heart. II. Evidence for importance of amino acid metabolism in tolerance to ischemia. *J Thorac Cardiovasc Surg* 1990;100(6):888-95.

(31) Opie LH. Metabolic-Regulation in Ischemia and Hypoxia - Effects of Anoxia and Regional Ischemia on Metabolism of Glucose and Fatty-Acids. *Cardiovasc Res* 1976;38(5):52-74.

(32) Neely JR, Morgan HE. Relationship Between Carbohydrate and Lipid-Metabolism and Energy-Balance of Heart-Muscle. *Annu Rev Physiol* 1974;36:413-59.

(33) Rupert BE, Segar JL, Schutte BC, Scholz TD. Metabolic adaptation of the hypertrophied heart: Role of the malate/aspartate and alpha-glycerophosphate shuttles. *J Mol Cell Cardiol* 2000;32(12):2287-97.

(34) Stanley WC, Recchia FA, Lopaschuk GD. Myocardial Substrate Metabolism in the Normal and Failing Heart. *Physiol Rev* 2005 July 1;85(3):1093-129.

(35) Opie LH. Cardiac Metabolism - Emergence, Decline, and Resurgence .2. *Cardiovasc Res* 1992;26(9):817-30.

(36) Suleiman MS, Dihmis WC, Caputo M, Angelini GD, Bryan AJ. Changes in myocardial concentration of glutamate and aspartate during coronary artery surgery. *Am J Physiol Heart Circ Physiol* 1997 March 1;272(3):H1063-H1069.

(37) Williams H, King N, Griffiths EJ, Suleiman MS. Glutamate-loading stimulates metabolic flux and improves cell recovery following chemical hypoxia in isolated cardiomyocytes. *J Mol Cell Cardiol* 2001;33(12):2109-19.

(38) Todorova V, Vanderpool D, Blossom S et al. Oral glutamine protects against cyclophosphamide-induced cardiotoxicity in experimental rats through increase of cardiac glutathione. *Nutrition* 2009;25(7-8):812-7.

(39) Engel JM, Muhling J, Kwapisz M, Heidt M. Glutamine administration in patients undergoing cardiac surgery and the influence on blood glutathione levels. *Acta Anaesthesiol Scand* 2009;53(10):1317-23.

(40) McGuinness J, Neilan TG, Cummins R, Sharkasi A, Bouchier-Hayes D, Redmond JM. Intravenous Glutamine Enhances COX-2 Activity Giving Cardioprotection. *J Surg Res* 2009;152(1):140-7.

(41) Hissa MN, Vasconcelos RCd, Guimaraes SB, Silva RP, Garcia JHP, Vasconcelos PRLd. Preoperative glutamine infusion improves glycemia in heart surgery patients. *Acta Cir Bras* 2011;26:77-81.

(42) Dinkelborg LM, Kinne RKH, Grieshaber MK. Transport and metabolism of L-glutamate during oxygenation, anoxia, and reoxygenation of rat cardiac myocytes. *Am J Physiol Heart* 1996;39(5):H1825-H1832.

(43) Malandro MS, Kilberg MS. Molecular biology of mammalian amino acid transporters. *Annu Rev Biochem* 1996;65:305-36.

(44) Razeghi P, Sharma S, Ying J et al. Atrophic remodeling of the heart in vivo simultaneously activates pathways of protein synthesis and degradation. *Circulation* 2003;108(20):2536-41.

(45) Schelbert HR, Phelps ME, Huang SC, Macdonald NS, Hansen H, Kuhl DE. N-13 Ammonia As An Indicator of Myocardial Blood-Flow. *Circulation* 1981;63(6):1259-72.

(46) Stottrup NB, Kristiansen SB, Lofgren B et al. L-glutamate and glutamine improve haemodynamic function and restore myocardial glycogen content during postischaemic reperfusion: A radioactive tracer study in the rat isolated heart. *Clin Exp Pharmacol P* 2006;33(11):1099-103.

(47) Burgess SC, Babcock EE, Jeffrey FMH, Sherry AD, Malloy CR. NMR indirect detection of glutamate to measure citric acid cycle flux in the isolated perfused mouse heart. *FEBS Lett* 2001;505(1):163-7.

(48) Noguchi Y, Young JD, Aleman JO, Hansen ME, Kelleher JK, Stephanopoulos G. Effect of anaplerotic fluxes and amino acid availability on hepatic lipoapoptosis. *Journal of Biological Chemistry* 2009;284(48):33425-36.

(49) Enders JR, Goodwin CR, Marasco CC, Seale KT, Wikswo JP, McLean JA. Advanced structural Mass Spectrometry for Systems biology: Pulling the Needles from Haystacks. *Spectroscopy Supp Curr Trends Mass Spectrometry* 2011;July:18-23.

(50) Enders JR, Kliman M, Sundarapandian S, McLean JA. Peptide and protein analysis using ion mobility-mass spectrometry. In: Gross ML, Chen G, Pramanik B, editors. *Peptide and Protein Mass Spectrometry in Drug Discovery*. J. Wiley & Sons; 2011. p. 139-74.

(51) Enders JR, Marasco CC, Kole A et al. Towards monitoring real-time cellular response using an integrated microfluidics-MALDI/NESI-ion mobility-mass spectrometry platform. *IET Syst Biol* 2010;4(6):416-27.

(52) Goodwin CR, Fenn LS, Derewacz DK, Bachmann BO, McLean JA. Structural Mass Spectrometry: Rapid Methods for Separation and Analysis of Peptide Natural Products. *J Nat Prod* 2012 January 4;75:48-53.

(53) Kerr TJ, McLean JA. Peptide quantitation using primary amine selective metal chelation labels for mass spectrometry. *Chem Commun* 2010;46(30):5479-81.

(54) Marzilli M, Affinito S. Evidence of efficacy of metabolic agents. *Heart and Metabolism* 2005;27:21-3.

(55) Marzilli M. Trimetazidine: a metabolic agent for the treatment of stable angina. *Eur Heart J Suppl* 2001 November 1;3(suppl_O):O12-O15.

(56) Lee J, Niederer S, Nordsletten D et al. Coupling contraction, excitation, ventricular and coronary blood flow across scale and physics in the heart.

Philosophical Transactions of the Royal Society of London, Series A 2009;367(1896):2311-31.

(57) Niederer SA, Fink M, Noble D, Smith NP. A meta-analysis of cardiac electrophysiology computational models. *Experimental Physiology* 2009;94(5):486-95.

(58) Fink M, Niederer SA, Cherry EM et al. Cardiac cell modelling: Observations from the heart of the cardiac physiome project. *Progress in Biophysics and Molecular Biology* 2011 January;104(1-3):2-21.

(59) Franz MR. Method and theory of monophasic action potential recording. *Prog Cardiovasc Dis* 1991 May;33(6):347-68.

(60) Franz MR. Current status of monophasic action potential recording: theories, measurements and interpretations. *Cardiovasc Res* 1999 January;41(1):25-40.

(61) Banville I, Gray RA. Effect of action potential duration and conduction velocity restitution and their spatial dispersion on alternans and the stability of arrhythmias. *J Cardiovasc Electrophysiol* 2002 November;13(11):1141-9.

(62) Knollmann BC, Schober T, Petersen AO, Sirenko SG, Franz MR. Action potential characterization in intact mouse heart: steady-state cycle length dependence and electrical restitution. *Am J Physiol Heart Circ Physiol* 2007 January;292(1):H614-H621.

(63) Sidorov VY, Uzelac I, Wikswo JP. Effects of $[K^+]_o$ heterogeneity on reentry induction and arrhythmia dynamics. *In preparation* 2008.

(64) Sidorov VY, Holcomb MR, Woods MC, Gray RA, Wikswo JP. Effects of unipolar stimulation on voltage and calcium distributions in the isolated rabbit heart. *Basic Res Cardiol* 2008;103(6):537-51.

(65) Shotwell MS, Drake KJ, Sidorov VY, Wikswo JP. Mechanistic analysis of challenge-response experiments. *Biometrics* 2013 September;69(3):741-7.

(66) Pinheiro JC, Bates DM. *Mixed-effects models in S and S-PLUS*. New York: Springer, 2000.

(67) Drake KJ, Shotwell MS, Wikswo JP, Sidorov VY. Glutamine and Glutamate Limit the Shortening of Action Potential Duration in Anoxia-Challenged Rabbit Hearts. *Physiological Reports* 2015;3(9):Article e12535.

(68) Taegtmeyer H, Goodwin GW, Doenst T, Frazier OH. Substrate metabolism as a determinant for postischemic functional recovery of the heart. *Am J Cardiol* 1997 August 4;80(3A):3A-10A.

(69) Drake KJ, Sidorov VY, McGuinness OP, Wasserman DH, Wikswo JP. Amino acids as metabolic substrates during cardiac ischemia. *Exp Biol Med (Maywood)* 2012 December;237(12):1369-78.

(70) Cohen DM, Guthrie PH, Gao XL, Sakai R, Taegtmeyer H. Glutamine cycling in isolated working rat heart. *American Journal of Physiology-Endocrinology and Metabolism* 2003;285(6):E1312-E1316.

(71) Stottrup NB, Kristiansen SB, Lofgren B et al. L-glutamate and glutamine improve haemodynamic function and restore myocardial glycogen content during postischaemic reperfusion: A radioactive tracer study in the rat isolated heart. *Clinical and Experimental Pharmacology and Physiology* 2006;33(11):1099-103.

(72) Wischmeyer PE, Jayakar D, Williams U et al. Single dose of glutamine enhances myocardial tissue metabolism, glutathione content, and improves myocardial function after ischemia-reperfusion injury. *Journal of Parenteral and Enteral Nutrition* 2003 November 1;27(6):396-403.

(73) Bolotin G, Raman J, Williams U, Bacha E, Kocherginsky M, Jeevanandam V. Glutamine Improves Myocardial Function Following Ischemia-Reperfusion Injury. *Asian Cardiovascular Thoracic Annals* 2007 December 1;15(6):463-7.

(74) Lomivorotov VV, Efremov SM, Shmirev VA, Ponomarev DN, Lomivorotov VN, Karaskov AM. Glutamine Is Cardioprotective in Patients with Ischemic Heart Disease following Cardiopulmonary Bypass. *Heart Surgery Forum* 2011;14(6):E384-E388.

(75) Greco FA. Plasma amino acids. 2011 May 12;Available at: URL: http://www.nlm.nih.gov/medlineplus/ency/article/003361.htm. AccessedFebruary 22, 2013.

(76) Peuhkurinen KJ, Takala TES, Nuutinen EM, Hassinen IE. Tricarboxylic-Acid Cycle Metabolites During Ischemia in Isolated Perfused Rat-Heart. *American Journal of Physiology* 1983;244(2):H281-H288.

(77) Suleiman MS, Dihmis WC, Caputo M, Angelini GD, Bryan AJ. Changes in myocardial concentration of glutamate and aspartate during coronary artery surgery. *AJP - Heart and Circulatory Physiology* 1997 March 1;272(3):H1063-H1069.

(78) Dinkelborg LM, Kinne RKH, Grieshaber MK. Transport and metabolism of L-glutamate during oxygenation, anoxia, and reoxygenation of rat cardiac

myocytes. *American Journal Of Physiology-Heart And Circulatory Physiology* 1996;39(5):H1825-H1832.

(79) Williams H, King N, Griffiths EJ, Suleiman MS. Glutamate-loading stimulates metabolic flux and improves cell recovery following chemical hypoxia in isolated cardiomyocytes. *Journal of Molecular and Cellular Cardiology* 2001;33(12):2109-19.

(80) Graham TE, Sgro V, Friars D, Gibala MJ. Glutamate ingestion: the plasma and muscle free amino acid pools of resting humans. *Am J Physiol -Endoc M* 2000;278(1):E83-E89.

(81) Todorova V, Vanderpool D, Blossom S et al. Oral glutamine protects against cyclophosphamide-induced cardiotoxicity in experimental rats through increase of cardiac glutathione. *Nutrition* 2009;25(7-8):812-7.

(82) Engel JM, Muhling J, Kwapisz M, Heidt M. Glutamine administration in patients undergoing cardiac surgery and the influence on blood glutathione levels. *Acta Anaesthesiologica Scandinavica* 2009;53(10):1317-23.

(83) Carmeliet E, Boulpaep E. Effect of 2,4-dinitrophenol on the duration of action potential of the ventricular muscle in frog. *C R Seances Soc Biol Fil* 1957;151(12):2226-8.

(84) Carmeliet E. Cardiac transmembrane potentials and metabolism. *Circ Res* 1978 May;42(5):577-87.

(85) Isenberg G, Vereecke J, van der Heyden G, Carmeliet E. The shortening of the action potential by DNP in guinea-pig ventricular myocytes is mediated by an increase of a time-independent K conductance. *Pflugers Arch* 1983 June 1;397(4):251-9.

(86) Verkerk AO, Veldkamp MW, van Ginneken AC, Bouman LN. Biphasic response of action potential duration to metabolic inhibition in rabbit and human ventricular myocytes: role of transient outward current and ATP-regulated potassium current. *J Mol Cell Cardiol* 1996 December;28(12):2443-56.

(87) Freedberg AS, Papp JG, Williams EM. The effect of altered thyroid state on atrial intracellular potentials. *J Physiol* 1970 April;207(2):357-69.

(88) Ostadal B, Prochazka J, Pelouch V, Urbanova D, Widimsky J. Comparison of cardiopulmonary responses of male and female rats to intermittent high altitude hypoxia. *Physiol Bohemoslov* 1984;33(2):129-38.

(89) Hearse DJ. Myocardial protection during ischemia and reperfusion. *Mol Cell Biochem* 1998 September;186(1-2):177-84.

(90) Fazio S, Palmieri EA, Lombardi G, Biondi B. Effects of thyroid hormone on the cardiovascular system. *Recent Prog Horm Res* 2004;59:31-50.

(91) Shotwell MS, Drake KJ, Sidorov VY, Wikswo JP. Mechanistic analysis of challenge-response experiments. *Biometrics* 2013;69(3):741-7.

(92) Godfrey K. *Compartmental models and their application*. New York: Academic Press, 1983.

(93) Roger VL, Go AS, Lloyd-Jones DM et al. Heart Disease and Stroke Statistics-2011 Update A Report From the American Heart Association. *Circulation* 2011;123(4):E18-E209.

(94) Lopaschuk GD, Stanley WA, Lopaschuk CC. Metabolic approach in heart failure: the rationale for metabolic interventions. *Heart and Metabolism* 2005;27:5-10.

(95) Stanley WC, Chandler MP. Energy metabolism in the normal and failing heart: potential for therapeutic interventions. *Heart Fail Rev* 2002 April;7(2):115-30.

(96) Barr RL, Lopaschuk GD. Direct measurement of energy metabolism in the isolated working rat heart. *J Pharmacol Toxicol Methods* 1997;38(1):11-7.

(97) Sutherland FJ, Hearse DJ. The isolated blood and perfusion fluid perfused heart. *Pharmacol Res* 2000;41(6):613-27.

(98) Loiselle DS, Crampin EJ, Niederer SA, Smith NP, Barclay CJ. Energetic consequences of mechanical loads. *Progr Biophys Mol Biol* 2008;97(2-3):348-66.

(99) Eckle T, Kohler D, Lehmann R, El Kasmi KC, Eltzschig HK. Hypoxia-inducible factor-1 is central to cardioprotection - A new paradigm for ischemic preconditioning. *Circulation* 2008;118(2):166-75.

(100) Loor G, Schumacker PT. Role of hypoxia-inducible factor in cell survival during myocardial ischemia-reperfusion. *Cell Death Differ* 2008;15(4):686-90.

(101) Kido M, Du LL, Sullivan CC et al. Hypoxia-inducible factor 1-alpha reduces infarction and attenuates progression of cardiac dysfunction after myocardial infarction in the mouse. *J Am Coll Cardiol* 2005;46(11):2116-24.

(102) Rodriguez B, Ferrero JM, Jr., Trenor B. Mechanistic investigation of extracellular K^+ accumulation during acute myocardial ischemia: a simulation study. *Am J Physiol Heart* 2002 August 1;283(2):H490-H500.

(103) Rodriguez B, Trayanova N, Noble D. Modeling Cardiac Ischemia. *Ann New York Acad Sci* 2006 October 1;1080(1):395-414.

(104) Aon MA, Cortassa S, Marban E, O'Rourke B. Synchronized Whole Cell Oscillations in Mitochondrial Metabolism Triggered by a Local Release of Reactive Oxygen Species in Cardiac Myocytes. *J Biol Chem* 2003 November 7;278(45):44735-44.

(105) Cortassa S, Aon MA, Winslow RL, O'Rourke B. A mitochondrial oscillator dependent on reactive oxygen species. *Biophys J* 2004;87(3):2060-73.

(106) Cortassa S, Aon MA, Marban E, Winslow RL, O'Rourke B. An integrated model of cardiac mitochondrial energy metabolism and calcium dynamics. *Biophys J* 2003;84(4):2734-55.

(107) Cortassa S, Aon MA, O'Rourke B et al. A Computational Model Integrating Electrophysiology, Contraction, and Mitochondrial Bioenergetics in the Ventricular Myocyte. *Biophys J* 2006 August 15;91(4):1564-89.

(108) Winslow RL, Cortassa S, O'Rourke B, Hashambhoy Y, Rice JJ, Greenstein JL. Integrative Modeling of the Cardiac Ventricular Myocyte. Wiley Interdiscip Rev Syst Biol Med 3[4], 392-413. 2011.

(109) Cortassa S, O'Rourke B, Winslow RL, Aon MA. Control and Regulation of Mitochondrial Energetics in an Integrated Model of Cardiomyocyte Function. Biophysical Journal 96[6], 2466-2478. 3-18-0009.